Section 1

Fission Product Release From Reactor Core Material

Fission product release from core material during accidents involving meltdown would probably occur more or less continuously until the system finally cools. During this period, release rates should vary over wide limits depending on fission product properties, system temperatures, and the surface to volume ratio of the molten material. However, it is possible to identify four conditions or times at which major driving forces for release exist. These periods of high rates should account for most of the total release. The four major release components are:

a. Gap release - fission product release which occurs when the claddings experience initial rupture. It consists mostly of activity that was released to void spaces within the fuel rods during normal reactor operation and rapid depressurization of contained gases provides the driving force for escape.

b. Meltdown release - fission product release which occurs from the fuel while it first heats to melting and becomes molten. High gas flows in the core during this period sweep the activity out of the core region.

c. Vaporization release - fission product release which occurs after large amounts of molten core material fall into the reactor cavity from the pressure vessel. Turbulence caused by internal convection and melt sparging by gaseous decomposition products of concrete produce the driving forces for escape.

d. Oxidation release - fission product release which occurs just after and is a result of a steam explosion event. Finely divided fuel material is scattered into an oxygen atmosphere and undergoes extensive oxidation which liberates specific fission products.

By concentrating on the processes and factors which will control these four components, it was decided that release terms for representative accident sequences could be developed. Each one pertains to a specific, identifiable time period in the core meltdown scenario of either water reactor type. Therefore, PWR and BWR analyses both can utilize the same set of release components but the particular number of components and the timing of the releases will depend on the reactor type and the particular accident sequence being examined. The subsections which follow describe each component in more detail and present the release values that were arrived at on the basis of the current interpretations of fission product behavior that are contained in appendices to this report. The relevant appendices are cited within the text.

1.1 GAP RELEASE COMPONENT

For the purposes of this work, gap release is defined as the fission product inventory that is free to escape in gaseous or vapor form from core fuel rods if the cladding ruptures. The number of core fuel rod claddings that will rupture depends on the effectiveness of the emergency core cooling systems. For highly effective emergency cooling no claddings may rupture, while for degraded cooling conditions, leading to fuel rod melting, essentially all claddings will rupture during the temperature rise to melting. Between these two extremes there exist a large series of core cooling temperature conditions which can lead to various percentages of cladding ruptures.

Cladding rupture temperatures depend upon several factors; rate of temperature rise, internal gas pressure, and cladding physical and mechanical properties. However, rupture temperatures are likely to range from about 1400 to 2000 F. Fission products which have migrated to the surface of the fuel pellets or to the interior surface of the cladding during normal reactor operation can potentially be released. The driving force for escape comes from the rapid release of inert gases (helium and fission gas) stored in the plenum and gas gap spaces of the fuel rods. Internal gas pressures ranging from a few hundred psia to 2000 psia can exist.

Only fission product material which exists in vapor form should escape during the rod depressurization. Therefore, if vaporization from condensed phases or reaction layers within the fuel rod is incomplete when depressuri-

zation takes place, the potential release would not be realized. After the depressurization, very little driving force exists to carry fission product vapors along the narrow annulus to the rupture location in the cladding. Consequently, in this work the gap release component will be confined to an estimate of the release that occurs at the time of cladding rupture only. For accident conditions which are less severe than core meltdown, the gap release component values developed here may be reduced according to the percentage of the fuel rod claddings that are expected to experience rupture.

Two fractions make up the gap release component: (1) the release fraction, and (2) the escape fraction. The release fraction defines the potential for release from UO_2 fuel and is the result obtained from most fission product release models. The escape fraction represents an estimate of the degree of volatility of the fission product at fuel rod cladding rupture. The processes and reactions that need to be considered in estimating the escape fraction include physical condensation and reactions with fuel material, cladding, other fission products and gaseous impurities in the rods.

1.1.1 THE RELEASE FRACTION

The three sets of gap release calculations which are reported in Appendices A, B, and C produced the release fraction estimates shown in Table VII 1-1. These results are based on PWR core properties but results for a BWR are so similar that Table VII 1-1 values will be used for both reactor types. The values in Table VII 1-1 also represent best estimate releases for the several species and these contain different uncertainties depending upon the release models used, variations in basic parameters, or differences in methods to compute temperature profiles in operating fuel. Inspection of results given in Appendices A, B, and C show that uncertainties range from factors of ± 2 for some species to factors ± 10 or more for others. As a rule, the magnitude of the uncertainty tends to decrease as the decay half-life increases.

The ultimate use of these release fractions in total accident release calculations demands that a single value be assigned for each chemical group; that is, isotopic dependent release behavior must be ignored. Consequently, in the last column of Table VII 1-1, average release values are listed which will be used for all isotopes of each of the applicable chemical elements. The average values in each case are the simple arithmetic means of the three calculated releases for the particular isotope. This isotope was selected on the basis that it represents the radiologically important one for the element. Note that no direct calculations of tellurium releases were made. Results of out-of-pile experiments (Ref. 2) indicate that its release should be similar to iodine and cesium, and on this basis the value of 0.10 for the principal isotope, Te-132, was selected. Since the isotopes that were selected to represent each chemical group have relatively long half lives, the uncertainties in the average release fractions should be nearer the lower end of the uncertainty range as noted above. This was the basis for the uncertainty factors that are specified in Table VII 1-1.

The data in Table VII 1-1 represent the best effort that can be made with current mathematical models in calculating fission product releases during reactor operation. Due to lack of basic information for some species or parameters, simplifying assumptions are often made which tend to overestimate rather than underestimate releases. Therefore, the results should be interpreted as current state-of-the-art and not as absolute values. Future experimental and theoretical study may indicate lower releases, and when this occurs the models and results used here can be modified.

1.1.2 THE ESCAPE FRACTION

The rationale used to select escape fraction values will be discussed on an element by element basis.

1.1.2.1 Noble Gases.

The noble gases are gaseous at room temperature and are known to be very unreactive chemically. At cladding rupture the only mechanism which could retard their escape would be flow restrictions along the gas gap to the hole or split in the cladding. Since this constitutes only a delay process, which depends on very specific details of fuel rod structure, no retention of released noble gases in the fuel rod gas space can be claimed.

1.1.2.2 Halogens.

Elemental iodine would be entirely gaseous at normal reactor fuel rod operating temperatures and particularly at the cladding rupture temperatures. However, iodine readily reacts with

metals to form iodides which have different volatilities. Possibilities include zirconium iodides (reaction with cladding), cesium iodine (reaction with fission-product cesium), and hydrogen iodide (reaction with trace hydrogen or water vapor).

Experimental work by Feuerstein (Ref. 3) has shown that a series of zirconium iodides can form when iodine in Zircaloy capsules is heated, and several minutes is required to volatilize appreciable fractions of the reaction product at a temperature of 800 C (1472 F). Indirect evidence of iodine reaction with Zircaloy in operating fuel rods has been obtained by Weidenbaum (Ref. 4). Collins, et al (Ref. 5) performed puncture tests with irradiated Zircaloy-2 clad UO_2 in steam at about 1000 C (1832 F) from which it was concluded that only 10 percent of the iodine that was expected to be free within the cans escaped through the puncture hole. Lorenz and Parker (Ref. 6) have conducted a pair of in-reactor fuel rod failure transient tests with pressurized Zircaloy-2 clad fuel rods. The fission product release data for the two experiments indicated 25 percent and 100 percent escape of the free iodine relative to free noble gases. These limited studies suggest that iodine retention by Zircaloy cladding could limit the escape of iodine from the gas spaces of fuel rods during rupture. The escape fraction value cannot be specified very accurately but would be expected to fall within the range 0.1 to 1.

Contrary to the cladding reaction mechanism, thermodynamic analyses of the fuel-cladding fission product system consistently predict that CsI would be the most stable chemical form for iodine at elevated temperatures (see Appendix E). Since the fission yield for cesium isotopes is more than ten times that for iodine isotopes, there is sufficient cesium for complete conversion of the iodine. If CsI is the dominant iodine species in fuel rods then iodine would exhibit a significantly lower volatility at cladding rupture temperature i.e., a vapor fraction in the range of 0.01 to 0.1 would be expected. As shown above, experimental escape data do not coincide with these low values. In addition there is limited evidence that cesium may undergo compound formation with UO_2* and thus prevent formation of CsI (Refs. 7,8). Thermodynamic analyses have not considered this reaction. Finally, there appears to be no experimental confirmation of the presence of CsI in irradiated fuel rods. Therefore, the possibility of CsI being a major chemical form is not sufficiently established to justify consideration in this work. However, additional experimental work in this area would be useful.

The formation of hydrogen iodide, which might be significant at high temperatures, also has not been verified by experimental work on irradiated fuel rods. The existence of HI as a major species would not alter iodine volatility at cladding rupture temperatures appreciably. Therefore HI will not be considered an important iodine form in this analysis.

In summary the escape fraction for iodine gap release should be based on available experimental evidence that indicates at least partial retention by Zircaloy cladding. On the basis of the range indicated a best estimate value of 1/3 with an uncertainty factor ± 3 is appropriate.

1.1.2.3 Alkali Metals.

The normal boiling point of cesium metal is about 960 K (1270 F) and if the fission product exists in this elemental form, the gap release fraction could be completely vaporized at cladding rupture temperatures. On the other hand the thermal transient may be too rapid and incomplete vaporization would have occurred at this point. Also, compound formation with the fuel (noted above) or with the cladding (possibly with corrosion products) could result in significantly reduced volatility. There is almost no experimental data related to escape of fission product cesium under these conditions. The in-pile transient tests of Lorenz and Parker (Ref. 6) provide the only known experimental estimate. The results of two tests indicate an escape fraction value of about 2/3. Because of the approximate nature of these measurements, it was decided to use the same escape fraction for cesium that is used for iodine; i.e., 1/3 with an uncertainty factor of ± 3.

1.1.2.4 Alkaline Earths.

Depending upon the oxygen activity in the system, fission product strontium would predominately exist as either the metal or the monoxide. However, neither condensed phase has appreciable volatility at clad rupture temperatures. The metal which exhibits the higher vapor pressure should limit vapor fractions to less than 10^{-4} of the total strontium. The ANC fission product release model calculation for strontium, which considers thermodynamic equilibrium in the

* formation of Cs_2UO_4 - see chap 4 NUREG 0772

fuel body, obtained a maximum release fraction of 4×10^{-6} (Appendix B). The in-pile transient test data of Lorenz and Parker (Ref. 6), while quite crude for strontium, indicate escape fractions ranging from about 10^{-2} to 10^{-6}. On the basis of this evidence, it appears that in conjunction with a release fraction of 0.01, a best estimate value for the escape fraction would be 10^{-4} with an uncertainty factor of ± 100.

1.1.2.5 Tellurium.

Thermodynamic calculations indicate that tellurium can exist as either the element or an oxide in the fuel. The stable vapor form at cladding rupture temperatures is probably Te_2, but several experimental studies indicate that tellurium will react with Zircaloy. Genco, et al. (Ref. 9) demonstrated extensive reaction of tellurium vapor with zirconium at temperatures above 400 C (752 F). The in-pile transient tests of Lorenz and Parker (Ref. 6) while very limited indicate an escape fraction for tellurium of between 10^{-1} and 10^{-5}. A complex kinetic situation involving competition among vaporization, reaction with cladding, and escape in the gaseous puff probably determines the escape fraction. Therefore, the value was set at 10^{-3} with an uncertainty factor of ± 100.

1.1.2.6 Other Species.

The volatilities of other fission product species, besides those which are chemical analogs of the elements discussed above, are expected to be so low that their escape at cladding rupture can be considered negligible. Therefore, the results of all the gap release component analysis can now be summarized. Table VII 1-2 presents such a summary showing the gap release fractions, the escape fractions, and the product of these two - the gap release component. The release and escape fractions listed here may be somewhat different from values obtained or recommended by the individual laboratories that contributed to the analyses. This is because current knowledge does not clearly show one analytical approach is superior to the others.

1.2 MELTDOWN RELEASE COMPONENT

The conditions pertaining to this release period begin with rapid boiloff of the water coolant which uncovers the reactor core. Steam, flowing up through the heating core, initiates Zr-H_2O reaction and this accelerates the rate of temperature rise. The cladding begins to melt within one minute and in a few more minutes fuel-melting temperatures are approached in the hotter regions. The process spreads throughout the core and within 30 minutes to 2 hours (Ref. 1) nearly the whole core is molten at temperatures ranging from roughly 2000 to 3000 C. During the later stages of this process molten core material can run through or melt through the grid plate and fall into the bottom of the pressure vessel. If a steam explosion does not occur when residual water is contacted in the lower portion of the pressure vessel, partial quenching and temporary solidification of portions of the molten mass can take place. However, the internal heat generation causes remelting and the inevitable downward migration continues until the pressure vessel fails, probably by meltthrough. Pressure vessel failure is expected to require about 1 hour after most of the core has melted (Ref. 1). Prior to this the high internal temperatures have caused melting of some of the pressure vessel steel and interior structural components. The molten iron is not miscible with the core material (oxide phase) although partial conversion to iron oxides could produce some dissolution in and dilution of the core material. Nevertheless some fission products (i.e., the noble metals) would tend to distribute to the metallic iron phase.

Initial fuel melting is expected to occur in only the center regions of the rods on almost a pellet by pellet scale. Thus the melting fuel will offer a relatively high surface area for release of fission products. As the melting front moves outward, the melting of the individual pellets may continue, but it is also conceivable that larger sections of fuel may collapse into the molten mass. If this fuel melts within the mass rather than at the edge, then fission product release could be inhibited by the time required for transport to a free surface. On the other hand, gaseous fission products, present as bubbles in the UO_2 could rise quickly to the surface of the molten mass and escape. It appears that most of the fission product release that does occur will take place early in the melting period at each core location. Then as the melted fuel mixes with the rest of the molten mass and the mass increases in size, fission product release rates will become much slower. The melting of structural steel in the pressure vessel during this later period is expected to produce a layer of molten iron above the molten core material which would offer a further barrier to

fission product release. Other factors which can inhibit release during meltdown in the pressure vessel include the possibility of crust formation at the melt surface and partial quenching when melt runs or falls into water that may be left in the bottom of the vessel.

The atmosphere in the core region and pressure vessel during meltdown is expected to be a steam-hydrogen mixture with small concentrations of fission product and core material vapors and aerosols. This may be classified a nonoxidizing atmosphere for most fission products, and it, of course, results from partial consumption of steam by metal-water reaction, yielding H_2 in the core region. Although the metal-water reaction that does occur is steam supply limited, some steam flow passes through cooler portions of the core region without complete reaction. It is estimated that during the meltdown phase only about half the Zircaloy is reacted and other metal-water reaction produces only about 50 percent more H_2. Thus total metal-water reaction is only the equivalent of 75 percent Zr-H_2O reaction.

Thermal analyses of core meltdown provide only generalized data on core temperature profiles, geometry changes, and melt behavior versus time. This, combined with the uncertainties which exist in fission product properties at very high temperatures, argue against construction of a highly mechanistic model to calculate fission product release during the meltdown phase. Therefore, in this work, fission product release is treated as being simply proportional to the fraction of core melted.

Mathematically,

$$RCFx(t) = [RFx] \cdot [FCM(t)]$$

where RCFx(t) = Core release fraction for fission product x as a function of time (t):

RFx = Release fraction of fission product x from melted fuel

FCM(t) = Fraction of core melted as a function of time (t)

It is important to note that this approach assigns all release, which is expected to occur during the time core material remains in the pressure vessel, to the early period of first melting. This is consistent with two key observations; (1) the highest steam flows and (2) the highest fuel surface areas are expected during the early period. Thus this should be the period of maximum driving force for fission product escape from the core region. The release fractions (RFx) for the various fission products were estimated by considering:

a. The limited data that are available from small-scale experiments with UO_2 (Appendix D), and

b. The predictions of limited thermodynamic analyses of fuel-cladding-fission product system at high temperature (Appendix E)

The results are summarized in Table VII 1-3 and a short description of the rationale connected with each value is given in the following paragraphs.

a. Noble Gases (Xe, Kr) - Experimental work shows that nearly total release of these essentially chemically inert gases would be expected during the meltdown period if the surface-to-volume ratio of melting material remains high. Although this seems likely and considerable release should occur even before the fuel melts, some gases could become trapped as the molten mass enlarges during the later stages of meltdown. Accordingly, a range of 50 to 100 percent release is considered reasonable but 90 percent should be assumed probable.

b. Halogens (I, Br) - Again nearly total release is expected due to the high volatility, but the rate of release could be limited by transport in the melt to an external surface. Therefore, the same range (50-100 percent release) should apply and 90 percent is considered the probable value.

c. Alkali Metals (Cs, Rb) - Nearly total release would be expected but experimental data on cesium release from molten UO_2 and thermodynamic studies show that the alkali metals are not so highly volatile as the noble gases or halogens. Therefore, the release rate could be somewhat affected by internal transport in the melt or by the possible tendency toward compound formation. Experimental evidence indicates a range of 40 to 90 percent with a probable value of 80 percent.

d. Tellurium - Simple thermodynamics indicate that Te should volatilize almost completely from melting core material in the elemental form. However, experimental data indicate

extensive reaction with unoxidized Zircaloy cladding would tend to hold tellurium in the melt, even though much of the cladding may oxidize during the meltdown period. The tellurium apparently migrates farther into the cladding to react with remaining free metal rather than diffuse out through the oxide layer. Release of the tellurium from a particular core region will occur when nearly all or all of the cladding has been oxidized. Since an average of 50 percent of the core cladding is expected to become oxidized during meltdown, this represents an upper limit for release. However, the oxidation is spread unevenly over the core and a smaller amount of cladding undergoes complete reaction. On this basis tellurium release is estimated to range from 5 to 25 percent.

e. Alkaline Earths (Sr, Ba) - The chemical form and the volatility of these two fission products are very sensitive to the oxygen partial pressure in the system. Strontium metal is more volatile than barium metal but barium oxide is more volatile than strontium oxide. Thermodynamic analyses produce conflicting estimates of volatility and chemical form due to variations in oxygen activities. Experimental data on release from molten fuel material indicate that the two elements would experience about the same release. Data obtained with zirconium clad UO_2 showed up to 20 percent release of strontium and barium over several minutes in a neutral atmosphere, while only a few percent loss was found for bare or stainless steel clad UO_2. The lower volatility of these elements and the probable existence of unoxidized cladding suggest that releases in the range of 2 to 20 percent would occur. Since incomplete cladding oxidation is expected, the probable release value should lie above the geometric mean for this range. Hence, 10 percent is used as the probable value.

f. Noble Metals (Ru, Rh, Pd, Mo, Tc) - Although these elements probably volatilize as the oxides, thermodynamic calculations suggest that the volatile oxide forms are not very stable at the high temperatures and the lower oxygen partial pressure that are expected to be associated with the core meltdown. The first three elements probably exist in the metallic form in the fuel, while the latter two are probably in the form of lower oxides. The metallic species could partially distribute to the molten iron phase and be retained. Experimental data on ruthenium release from molten UO_2 in an oxygen-deficient atmosphere indicate low release. Releases in the range of 1 to 10 percent are considered possible, and 3 percent (the approximate geometric mean) is used as the probable value.

g. Rare Earths (including Y and Np, Pu) - The rare earth elements will generally exist in the fuel as the sesquioxides (M_2O_3) while the actinides, neptunium and plutonium, should form the dioxides (MO_2). The oxides characteristically exhibit low volatility but an estimate of the release fraction is difficult to make. Experimental data for cerium release from small specimens of molten UO_2 indicate losses of several tenths of a percent over a few minutes, or about the same as the UO_2 vaporization loss. In Appendix H, estimates of fuel vaporization rates indicate losses in the range of 0.01 to 1 percent. This range can also be used for the rare earth species but the probable value, 0.3 percent, reflects caution in selecting a characteristic release when the estimate is so approximate.

h. Refractory Oxides (Zr, Nb) - The oxides of these elements are so stable and of such low volatility that they probably would experience less release than the rare earths. However, for simplicity the same release definitions are used here as for the rare earths.

1.3 VAPORIZATION RELEASE COMPONENT

When the molten core and iron penetrate the pressure vessel and fall (or run) into the reactor cavity, the material will be exposed to oxygen from the containment atmosphere, steam from contact with water or vaporized from concrete, and carbon dioxide from thermal decomposition of the limestone aggregate in the concrete. Passage of steam and carbon dioxide through the molten mass will produce a gas sparging effect. In addition these gases or their dissociation products will create highly oxidizing conditions. One can speculate that the iron phase would be (at least partially) converted to oxide which could then dissolve in the core melt. The melt should also contain products of the concrete decomposition; silica, calcium

silicates, or calcium oxide. The products would eventually reduce the density of the oxide phase and the then heavier iron phase might sink to the bottom of the mass (Ref. 10). Conversely, incomplete dissolution could leave a relatively pure UO_2 phase which would continue penetrating downwards (Ref. 11). Lower melting mixed oxide phases forming ahead of the UO_2 would tend to rise and cover the UO_2. Thus, development of several immiscible or partially miscible phases is conceivable. Internal convection would promote mixing within and exchange between phases. Depending upon their solute properties, fission product oxides could distribute to these phases thereby altering the heat source distribution and the temperature profile in the melt system (Ref. 10). Vaporization of fuel and structural materials from the upper surface of the molten mass should produce dense aerosol clouds (smokes) above the melt and buildup of condensation products on nearby surfaces. Agglomeration and growth of smoke particles is expected to cause some vaporized material to settle back. Thus much of the vaporized material should be retained in the reactor vessel cavity. Vaporized fission products, mixed with the much larger quantities of structural material vapors and smoke, should generally follow the distribution of the bulk material. Exceptions to this would be the high volatility species which could escape into the upper part of the containment.

Only highly simplified analyses of the physical situation just outlined have been performed (Refs. 10,11,12). There are many unknown details concerning most of the chemical, physical, thermal, mechanical, and metallurgical properties of the complex system. Analytical results are dependent on basic assumptions which differ among models. No large-scale experimental work on the relevant system has been performed to guide modeling. Concrete penetration rates cannot be estimated accurately because of uncertainties in heat transfer mechanism, melt interaction effects, and/or boundary limit definitions. Release calculations can and have been performed, but the assumptions and data extrapolations needed, lead to estimates that are usually upper limit values (Ref. 11) (See Appendices E and G). The release models are useful in identifying key release processes and species that have a high potential for release by one or more of these processes.

To a first approximation, the extent of release will depend upon species volatility and the rate of transport in the molten mass to an external surface. For the large molten masses that result from core meltdown, the latter process should control release for all except the very low volatility species. For example, estimates have shown that pure diffusion transport would require several hundred hours to achieve significant release fractions, regardless of volatility (Ref. 13). However, additional estimates indicated that thermally induced internal convection currents might increase mass transfer rates such that corresponding releases would occur within several hours (Ref. 13). Very recent approximations based on gas sparging assumptions suggest total release for volatile species in fractions of an hour (Appendix G). The release rates that would actually occur would probably be some mixture between the latter two processes. Also, gross vaporization of the melt could assist the release by creating a receding surface. The uncertainties of the problem require that a simple approach be used to specify fission product releases for this portion of the accident.

1.3.1 VOLATILE FISSION PRODUCTS

The very volatile fission products will escape the melt if they can reach an external surface. The gas sparging process offers a mechanism for inducing mixing and creating a large effective external surface area. The convective mass transfer process offers an alternative and usually slower rate for transport to surfaces where vaporization can occur. Both processes would result in an exponential decrease in the volatile fission product inventory with time. In each case the half-time for release might range from less than one hour to many hours, depending on the gas flow or mass transfer conditions.

Other work on the Reactor Safety Study has resulted in an estimated time for core penetration of the concrete base of about 18 hours (Ref. 1). The analyses also indicate that considerable spalling and decomposition of the concrete would occur within the first half-hour of contact. This would be a period of rapid gas (steam and carbon dioxide) generation during which the sparging process could be a dominant driving force for escape of volatile fission products. Subsequently, lower rates of release would be expected as gas flows decrease but sparging could still efficiently deplete the melt of volatile species (See Appendix G). Thermally induced internal convection and also surface evaporation might assist in the release.

The potential importance of gas sparging to the release of volatiles from the massive melt dictated that treatment of the vaporization release component should be based on this process. Accordingly, a pseudo-exponential rate expression was designed which required only a single input parameter, the characteristic release half-time. Mathematically,

$$VLF(t) = 1 - \exp[-0.693t/\tau]$$

where

VLF(t) = The vaporization loss fraction after time (t)

τ = The characteristic release half-time

In order to avoid excessive calculations during actual accident sequence analyses, a cut-off time for the expression, equivalent to four half-time intervals, was selected. In practice the rate expression was used exactly as written for the first three half-time internvals, but then complete escape of the remaining activity was compressed into the fourth interval. Since this last step involves only 12.5% of the total vaporization release, the approximation should produce only slight perturbations in results.

The value of the characteristic release half-time would be a function of the fission product volatility, the gas sparging rate, and other kinetic factors. In a rigorous sense, there would be a unique value for each fission product species which would vary continuously with the sparging conditions. This complexity is not warranted here and so the half-time value was assigned only to roughly match the period of high sparge gas flow. This period, as noted earlier, has been estimated to last on the order of one-half hour. Thus the best estimate half-time value is considered to be 30 minutes. Use of this uniform value for all fission products probably produces underestimates of the rate of release for the most volatile species and overestimates of the rate of release for species of lesser volatility. Also, the sparging process may not be fully effective in sweeping volatile fission products from the melt either because some sections of the melt are not exposed to sparge gas or because mass transfer limitations inhibit vapor saturation of sparge gas bubbles. Due to uncertainties such as these the 30 minute half-time value which is used in calculations should be considered uncertain by at least an order of magnitude.

The fission products that are sufficiently volatile to experience total loss during this vaporization phase are Xe, Kr, I, Br, Cs, Rb, Te, Se, and Sb. The meltdown release of the first six of these is expected to be quite large, because of their high volatilities, and so little will be left to contribute to the vaporization release component. This is not true for the tellurium group elements, whose meltdown release is considered inhibited by compound formation with Zircaloy cladding. However, by the time the vaporization release begins most of the free zirconium, which exists during core meltdown, should be oxidized (probably from reaction with UO_2). If not, then the oxidizing sparge gases (steam and CO_2) should quickly eliminate free zirconium so that tellurium and its chemical analogues, selenium and antimony, will become very volatile and also experience total release.

1.3.2 LOW VOLATILITY FISSION PRODUCTS

Essentially all the remaining important fission product species must be considered low volatility components. Thus total release of these species should not occur. With one exception this group of elements should be present as oxides in the oxide phase. The noble metals (Ru, Rh, Pd) and to a lesser extent Mo and Tc probably exist as the metals and would be expected to partition into the metallic iron phase of the molten system (Ref. 14). Low release (less than 1 percent) of these species is expected unless complete oxidation of the iron should occur (Appendix G). Although this is not considered likely, localized oxidation could lead to some release and a value of 5 percent is considered to be a realistic estimate. This is probably uncertain by a factor of $\pm$ 5. The other fission products (alkaline earth oxides and rare earth oxides) should be dissolved in the oxide phase of the melt (Ref. 14). Under the generally oxidizing conditions which persist over this period these species are less volatile than UO_2 (Appendix E). The vaporization of UO_2 and of other oxide materials in the melt is very difficult to estimate owing to uncertainties in composition and temperature. High vaporization rates (high temperatures and oxygen pressures) should produce dense aerosol clouds above the melt which would tend to settle out, carrying condensable fission products back down. Low vaporization rates (lower temperatures) would also indicate low losses for these fission products. Considering these limiting processes it is doubtful that more

than 1 percent of these fission product species could be distributed to the atmosphere in the containment over the course of the reactor melt-through period. This estimate is also probably uncertain by a factor of ±5.

The rate of release of the low volatility fission products, for lack of better definition, is assumed here to follow the same exponential function that is used to describe the release rate of the volatile species. On this basis the percentage release values given in Table VII 1-4 indicate the amount of each fission product, remaining in the core material after gap release and melt-down release have occurred, that will escape to the containment atmosphere during the vaporization period.

1.4 OXIDATION RELEASE COMPONENT

A steam explosion event will result in the scattering of finely divided UO_2 (containing fission products) into the atmosphere outside the containment or into the air-steam atmosphere inside containment. In either case, the UO_2 particles will cool and undergo reaction with oxygen to form U_3O_8 at temperatures below about 1500 C (Ref. 15). The reaction is exothermic and is accompanied by release of fission products that are volatile under these conditions. Oak Ridge work on measurement of fission product release during fuel oxidation by air at elevated temperatures is directly applicable (Ref. 16). These data summarized and discussed in Appendix F show large releases of rare gases, iodine, tellurium, and ruthenium during 10 to 15 minute exposures to air at temperatures of 1100 and 1200 C. Since the data indicate positive temperature coefficients for each species, comparable releases should occur in much shorter times at higher temperatures. On this basis the release percentage given in Table VII 1-5 may be treated as essentially instantaneous values. Note, however, that the releases apply only to the fraction of the UO_2 fuel that is expected to be dispersed into an air (oxygen)-containing atmosphere.

1.5 USE OF RELEASE COMPONENT VALUES

The four release components described above would occur more or less sequentially during a reactor meltdown accident. In all cases, the gap component would occur first, followed by the meltdown component, and then by the vaporization component. However, steam explosions could potentially occur any time after appreciable amounts of the core have melted. Thus, the oxidation component is somewhat randomly time oriented.

In using the release component values from Tables VII 1-2 through VII 1-5 to specify release source terms for a particular accident sequence, it should be obvious that proper inventory balances for each fission product must be maintained. For example, the fraction of the total inventory that experiences gap release is then not available for release by any of the other three processes. Consequently, care must be exercised in setting up release source terms. To illustrate this point, a basic release source summary is provided in Table VII 1-6. Here individual core release fractions are given for each component and fission product assuming that, except for the steam explosion fraction, the total core is involved in the release processes. That is, all fuel rod claddings rupture to give the gap release fraction, total core melting occurs, and all of the core melt contributes to the vaporization release fraction (unless preceded by a steam explosion). It is also implicitly assumed that a steam explosion will not precede total meltdown release.

It is emphasized that the single values listed in Table VII 1-6 are based on the best estimate values taken from Tables VII 1-2 through 1-5. Each of the values contains uncertainties as noted in those Tables and should, therefore, not be considered absolute release fractions.

References

1. Carbiener, W. A., et al "Physical Processes in Reactor Meltdown Accidents", WASH-1400, Appendix VIII, October, 1975.

2. Parker, G. W., et al., "Out-of-Pile Studies of Fission Product Release from Overheated Reactor Fuels at ORNL, 1955-1965", ORNL-3981, p 81 (July, 1967).

3. Feuerstein, H., "Behavior of Iodine in Zircaloy Capsules", ORNL-4543 (August, 1970).

4. Weidenbaum, B., et al., "Release of Fission Products from UO_2 Operating at High Power Rating", CONF-650407, Vol. 2, p 885-904, USAEC (1965).

5. Collins, R. D., et al., "Air Cleaning for Reactors with Vented Containments", CONF-660904, Vol. 1, p 419-452 (1967).

6. Lorenz, R. A., and G. W. Parker, "Final Report on the Second Fuel Rod Failure Transient Test of a Zircaloy-Clad Fuel Rod Cluster in TREAT", ORNL-4710 (January, 1972).

7. Chen, H., and P. E. Blackburn, "ANL Reactor Development Program Progress Report for September, 1969", ANL-7618, p 117 (October, 1969).

8. Crouthamel, C. E. and I. Johnson, "ANL Reactor Development Program Progress Report for July, 1971", ANL-7845, p 522 (August, 1971).

9. Genco, J. M., et al., "Fission-Product Deposition and Its Enhancement Under Reactor Accident Conditions: Deposition on Primary System Surfaces", BMI-1863, p 38 (March, 1969).

10. Jansen, G. and D. D. Stepnewski, "Fast Reactor Fuel Interactions with Floor Material After a Hypothetical Core Meltdown", Nucl. Tech. 17, 85-95 (1973).

11. Morrison, D. L., et al., "An Evaluation of the Applicability of Existing Data to the Analytical Description of a Nuclear Reactor Accident-Core Meltdown Evaluation", BMI-1910, Appendix B (July, 1971).

12. Ergen, W. K., et al., "Emergency Core Cooling: Report of Advisory Task Force on Power Reactor Emergency Cooling (USAEC).

13. Fontana, M. H., "An Estimate of the Enhancement of Fission Product Release from Molten Fuel by Thermally Induced Internal Circulation", Nucl Appl, 9, 364-375 (1970).

14. Fischer, J., J. D. Schilb, and M. G. Chasonov, "Investigation of the Distribution of Fission Products Among Molten Fuel and Reactor Phases. Part I - The Distribution of Fission Products Between Molten Iron and Molten Uranium Dioxide", ANL-7864 (October, 1971).

15. Parker, G. W., et al., "Out-of-Pile Studies of Fission Product Release from Overheated Reactor Fuels at ORNL, 1955-1965", ORNL-3981, p 4 (July, 1967).

16. Parker, G. W., et al., "Out-of-Pile Studies of Fission Product Release from Overheated Reactor Fuels at ORNL, 1955-1965", ORNL-3981, p 85 (July, 1967).

TABLE VII 1-1 FRACTIONS RELEASED TO GAP (TOTAL CORE)

Fission Product (decay half-life)	Calculated Fractions ANC[a]	BCL[b]	ORNL[c]	Chemical Groups	Average Release Fraction
Xe, Kr (long lived)	0.06	0.10	0.08		
Xe-133 (5.27 day)	0.04	0.02	0.02	Noble Gases	0.03[d]
Xe-135 (9.2 hour)	0.0002	0.004	0.004		
I, Br (long lived)	0.06	0.10	0.14		
I-131 (8.06 day)	0.06	0.03	0.05	Halogens	0.05[d]
I-132 (2.3 hour)	0.0007	0.005	0.006		
I-133 (20.8 hour)	0.007	0.01	0.02		
Cs, Rb (long lived)	0.20	0.05	0.21		0.15[e]
Cs-138 (32 minutes)	0.00001	0.0005	0.005	Alkali Metals	
Sr, Ba (long lived)	0.000004[f]	0.02	0.02		0.01[d]
Sr-89 (51 day)	-	0.01	0.015		
Sr-91 (9.7 hour)	-	0.002	0.01	Alkaline Earths	
Te-132 (78 hour)	(estimated value)			Tellurium	0.10[d]

(a) See Appendix B

(b) See Appendix A

(c) See Appendix C

(d) Values can be higher or lower by a factor of 4

(e) Value can be higher by a factor of 2 or lower by a factor of 4

(f) This value results from thermodynamic restrictions not considered in the other two models. See discussion of the escape fraction for this species.

TABLE VII 1-2 GAP RELEASE COMPONENT VALUES

Fission Product Species	Gap Release Fraction	Gap Escape Fraction	Total Gap Release Value
Xe, Kr	0.03[a]	1	0.03
I-Br	0.05[a]	1/3[c]	0.017
Cs, Rb	0.15[b]	1/3[c]	0.05
Sr, Ba	0.01[a]	10^{-4}[d]	0.000001
Te, Se, Sb	0.10[a]	10^{-3}[d]	0.0001
Others	-	-	Negligible[e]

(a) Values can be higher or lower by a factor of 4

(b) Value can be higher by a factor of 2 or lower by a factor of 4

(c) Values can be higher or lower by a factor of 3

(d) Values can be higher or lower by a factor of 100

(e) While no numerical value was developed for these various species, the number should not exceed that used for strontium-barium.

TABLE VII 1-3 MELTDOWN RELEASE COMPONENT VALUES

Elements	Release Range (percent)	Best Estimate (percent)
Xe, Kr	50-100	90
I, Br	50-100	90
Cs, Rb	40-90	80
Te[a]	5-25	15
Ba, Sr	2-20	10
Noble Metals[b]	1-10	3
Rare Earths[c]	.01-1	0.3
Zr, Nb	.01-1	0.3

(a) Includes Se, Sb
(b) Includes Ru, Rh, Pd, Mo, Tc
(c) Includes Y, La, Ce, Pr, Nd, Pm, Sm, Eu, Np, Pu

TABLE VII 1-4 VAPORIZATION RELEASE COMPONENT VALUES[a]

Fission Product	Release, Percent
Xe, Kr	100
I, Br	100
Cs, Rb	100
Te, Se, Sb	100
Ru, Rh, Pd, Mo, Tc	5[c]
Refractory Oxides[b]	1[c]

(a) Releases for the amount that remains after the gap and meltdown releases have occurred. The rate is approximated by an exponential function with a half-time of 30 min although this value is considered uncertain by an order of magnitude.

(b) Includes Sr, Ba, Y, La, Ce, Nd, Pr, Eu, Pm, Sm, Np, Pu.

(c) Values can be higher or lower by a factor of 5.

TABLE VII 1-5 FISSION PRODUCT RELEASES DURING STEAM EXPLOSIONS

Fission Product	Release From Oxidation, Percent	
	Range	Best Value
Xe, Kr	80-100	90
I, Br	80-100	90
Te, Se (Sb)	40-80	60
Ru (Mo, Tc, Pd, Rh)	80-100	90

TABLE VII 1-6 FISSION PRODUCT RELEASE SOURCE SUMMARY-BEST ESTIMATE TOTAL CORE RELEASE FRACTIONS

Fission Product	Gap Release Fraction	Meltdown Release Fraction	Vaporization Release Fraction[d]	Steam Explosion Fraction[e]
Xe, Kr	0.030	0.870	0.100	(X)(Y) 0.90
I, Br	0.017	0.883	0.100	(X)(Y) 0.90
Cs, Rb	0.050	0.760	0.190	--
Te[a]	0.0001	0.150	0.850	(X)(Y) (0.60)
Sr, Ba	0.000001	0.100	0.010	--
Ru[b]	--	0.030	0.050	(X)(Y) (0.90)
La[c]	--	0.003	0.010	--

(a) Includes Se, Sb

(b) Includes Mo, Pd, Rh, Tc

(c) Includes Nd, Eu, Y, Ce, Pr, Pm, Sm, Np, Pu, Zr, Nb

(d) Exponential loss over 2 hours with halftime of 30 minutes. If a steam explosion occurs prior to this, only the core fraction not involved in the steam explosion can experience vaporization.

(e) X = Fraction of core involved in the steam explosion. Y = Fraction of inventory remaining for release by oxidation.

Section 2

Fission Product Release From The Primary Coolant System

Once fission products escape the core region, transport through portions of the primary coolant system is required to reach the containment atmosphere. Plateout or deposition on internal surfaces in the primary system could potentially limit the amount of activity that leaves the system. The retention of fission products would depend upon bulk gas flow rates (mass transfer rates), temperatures, materials properties (fission products and structural materials), and geometry, all of which vary with time and position in the system. Comprehensive analysis of this problem, if all the needed data were available, would require a complex mathematical model and would generate involved sets of fission product primary system release rates as a function of time. It was determined that such an approach was not feasible for this study. Instead, it was decided to use generalized bounding calculations of fission product behavior to develop simple retention factors for the primary system transport step. These factors are analogous to the gap escape fractions described earlier and can be termed primary system escape fractions.

General calculations relating to fission product retention in the primary system are described in Appendix I for iodine and in Appendix H for the solid fission products. These analyses concentrate on the upper region of the pressure vessel and on bulk steam flow conditions which would be characteristic of water boiloff during core meltdown. Therefore, the results are applicable to all PWR and some BWR accident sequences. Conclusions reached from the analyses regarding primary system escape fractions are summarized and discussed in the next subsection. This is then followed by an assessment of several special cases which can be encountered in some accident sequences where the analyses in Appendices H and I are not applicable.

2.1 GENERAL PRIMARY SYSTEM ESCAPE FRACTIONS

2.1.1 NOBLE GASES

Xenon and krypton are gases at room temperature and essentially inert chemically. These fission products would be carried directly out of the primary system by the bulk gas flow. Therefore, an escape fraction of unity should be used.

2.1.2 IODINE

The analysis presented in Appendix I utilizes experimental deposition data. It indicates that very limited deposition (at most a few percent) would occur in the upper region of either a PWR or a BWR pressure vessel, whether the iodine is assumed to be elemental or HI. This amount of retention is insignificant compared to that which would be carried out by the bulk gas flow so an escape fraction of unity should be used.

2.1.3 SOLID FISSION PRODUCTS

The bounding calculations described in Appendix H indicate that fission products, having normal boiling points below roughly 1500 F, should experience only temporary retention on internal pressure vessel surfaces during a reactor core meltdown. The slight time delay in transport out of the vessel is expected to have no appreciable effect on the subsequent fate of these species in the containment volume. The fission products that would generally exhibit this behavior include the alkali metals (cesium and rubidium) the tellurium group (tellurium, selenium, and probably antimony), and the alkaline earths (strontium and barium). Therefore, an escape fraction of one should be used for these species.

Conclusions formulated in Appendix H also indicate that an escape fraction of one should be used for the noble metals (ruthenium) and rare earth group (yttrium) because of the potential for particle formation. If ruthenium released from the core region should convert to the volatile oxide during transport in the pressure vessel, then an escape fraction of unity is even more certain.

It is important to note that the core meltdown release values given in Table VII 1-3 being used for the solid fission products are based to a large extent on experimental melting studies. The experimental data are usually indicative of release from a high temperature region of the apparatus rather than from the peak (melting) temperature location. Since the pressure vessel should reach comparable temperatures during and fol-

lowing core meltdown, one would, by analogy, expect complete escape of the meltdown release fractions. The calculations pertaining to plateout in Appendix H tend to support this conclusion and offer some insight concerning the reasons and processes that could be involved.

2.2 SPECIAL CASES OF PRIMARY SYSTEM RETENTION OF FISSION PRODUCTS

Three special situations were identified in which the use of unit escape fractions for released fission products in the primary coolant system should perhaps be modified. Modifications were made in two of these cases but not in the third.

2.2.1 PWR COLD LEG PIPE BREAK

For a cold leg break in a PWR, steam or steam-hydrogen flow from the core region will pass through the upper plenum of the pressure vessel just as for a hot leg break. However, instead of exiting directly to the containment vessel, the gas and fission product vapors must then travel through the steam generator section in order to reach the containment. The large surface area of the steam generator tubes and the relatively low temperatures (initially about 500 F) would present favorable conditions for plateout of condensable species. No retention of the noble gases would occur and the analysis in Appendix I indicates that very limited deposition of fission product iodine would be expected. Therefore, an escape fraction of unity for these two species is still valid.

The solid fission products should experience high retention during the early phases of core meltdown. Exceptions could result from penetration of particulates containing low volatility fission products. Otherwise, plateout would be expected to occur at the head end of the steam generator tubes. The plateout area would heat-up due to heat transfer from the incoming bulk gas and absorption of decay energy from the condensed fission products. Fission product vaporization followed by re-condensation farther along the tubes could occur repetitively and smear the activity out. The eventual loss of bulk gas flow might leave this fission product material deposited in the steam generator. On the other hand, steam generator tube temperatures may rise sufficiently to cause significant fission product escape before loss of bulk gas flow.

This complex heat and mass transfer problem was not analyzed. Instead, it was decided to treat both types of pipe breaks identically with respect to primary system solid fission product retention; i.e., unit escape fractions were used regardless of break location. This represents worst conditions for release of radioactvity to the containment space, an assumption which appears valid for hot leg breaks but possibly overpessimistic for cold leg breaks.

2.2.2 BWR CORE MELTDOWN WITH ECC INJECTION

For a BWR loss of coolant accident resulting from a recirculation line break, it is conceivable that a situation develops in which abnormal conditions in the reactor core prevent effective cooling even though normally adequate emergency coolant pump flow is achieved. Thus, core melting and metal-water reaction occurs, but either the affected region is surrounded by ECC water (due to core spray and low pressure injection flow) or the opening in the pressure vessel is submerged under several feet of water (due to flooding to the top of the jet pumps). This presents a unique environment for the fission products that are liberated during fuel melting.

In either condition the released fission products, carried by the bulk steam-hydrogen mixture, must pass through several feet of water in order to escape from the pressure vessel. The steam should be condensed but the remaining hydrogen will provide the driving force for carrying fission product activity out to the primary containment. The amount of fission product activity which does escape will depend on the trapping capability of the water and the degree of deposition on upper vessel structures. Deposition may only delay the escape of activity as vessel temperatures eventually rise, and fission products trapped in the ECC water could circulate within the pressure vessel, sometimes encounter the melting core region, and undergo vaporization again. Consequently, the determination of a primary system retention factor is not as straight-forward as it would first appear.

Recognizing that the core meltdown fission product release fractions defined earlier contain an implied primary system plateout factor, the escape fraction for this flooded meltdown situation should consider only the retention effect of the ECC water. Limited work on fission product cleanup in steam suppression systems (Ref. 1) offers some basis for estimating this effect. The

data indicate decontamination factors (the reciprocal of escape fraction) ranging from about 10^1 to 10^3 for iodine and particle removal from steam-air mixtures passed through a water lute. While the geometry and temperature conditions are different than indicated for the present problem, the fundamental process in both cases is the removal of trace species from a condensable-noncondensable gas mixture during passage through a water column. Because of the more severe conditions, the possibility of ineffective removal must be considered.

Therefore, escape fractions extending from one (no retention) down to 0.001 (high retention) appear feasible. A value of 0.1 should be used for realistic accident calculations.[1]

2.2.3 BWR DRY VESSEL MELTDOWN

A second BWR accident situation that leads to unique conditions for escape of released fission products from the pressure vessel is a dry core heatup starting with the end-of-blowdown conditions. In this accident there is no water in the pressure vessel (no ECC delivery) and consequently no boiloff steam flow occurs to carry fission products out of the vessel. Therefore, the only gas flow driving fission products out of the vessel is due to simple gas expansion as internal temperatures increase from decay heating. (The fission product noble gas inventory, about 4.5 lb-moles, would not contribute significantly to the total gas content of the vessel.)

Thermal analyses (Ref. 2), for dry heatup in a typical BWR indicate steam flow velocities in the steam separators of less than a foot per minute. Thus, fission products escaping from the core should spend at least on the order of half an hour in the steam separator and dryer region of the pressure vessel. As the fission products plate out and decay, much of the fission product decay heat would be absorbed in the structural material above the core during this time period. Table VII 2-1 lists average temperatures of the structural material above the core for different accident times. These temperatures were calculated assuming that all of the decay heat lost from the core due to fission product release is absorbed in the material above the core. The weight of the material was 229,000 lb. The results indicate that the decay heat of the released fission product is insufficient to completely melt all the steel structure above the core at an accident time of one hour. However, since core meltdown has been estimated to require about two hours, it appears that pressure vessel temperatures of about 2800 F would be reached sometime during the latter half of the meltdown period.

Therefore, from the beginning to the end of core melting, the absolute temperature inside the pressure vessel should approximately triple, producing a corresponding expansion of the contained gases. Accordingly, when the meltdown period is completed about two-thirds of the original gas will have expanded out of the vessel. Ignoring retention on internal surfaces because of the high temperatures, this fraction can be used to approximate the escape of fission products released from the core during meltdown. Thus, at the end of core meltdown in accident sequences of this type, 2/3 of the fission product release term is assumed to have escaped the pressure vessel, and the other 1/3 is assumed to remain as vapors inside the vessel.

2.3 SUMMARY OF PRIMARY SYSTEM ESCAPE FRACTIONS

2.3.1 PWR SYSTEMS

An escape fraction of one for all fission products is used in all calculations of PWR accidents regardless of pipe break location.

2.3.2 BWR SYSTEMS

In BWR accident sequences where water boiloff after ECC interruption occurs, an escape fraction of one is used for all fission products.

In BWR accident sequences where ECC flow occurs but with core meltdown, an escape fraction of one is used for noble gas fission products but a value of 0.1 is used for all other fission products.

In BWR accident sequences where no ECC delivery ever occurs, it is assumed that at the end of core meltdown, 2/3 of all fission products that have been released will have escaped the pressure vessel.

---

[1] For noble gases a value of unity should be used.

References

1. Diffey, H. R., C. H. Rummary, M. J. S. Smith and R. A. Stinchcombe, "Iodine Cleanup in a Steam Suppression System", British Report AERE R-4882 (1965).

2. Carbiener, W. A., et al "Physical Processes in Reactor Meltdown Accidents", WASH-1400, Appendix VIII, October, 1975.

TABLE VII 2-1 ESTIMATED AVERAGE TEMPERATURES OF UPPER STRUCTURAL MATERIAL IN A BWR PRESSURE VESSEL DURING DRY MELTDOWN

Accident Time (minutes)	Average Temperature, F
0	550
20	800
40	1200
60	1680
80	2240
95	2750

Section 3

Fission Product Leakage From The Containment System

Analysis of fission product behavior in the reactor containment system is the final step in specifying the accident source term. The amount of radioactive material which escapes this barrier constitutes the source for dispersion in the natural environment. Fission products injected into the containment space by one of the four release processes will undergo removal from the internal atmosphere by a combination of mechanisms. The exact combination would vary among different plant types and accident-sequence conditions, but common to all is the removal that would occur as a result of natural transport and deposition processes. Various engineered safety systems can operate to remove fission products from containment atmospheres; i.e., aqueous spray systems and recirculating filter units in PWR plants, and suppression pool scrubbing and once-through filter units in BWR plants. The size of the fission product source which escapes to the environment critically depends upon how effectively the removal processes within containment compete with leakage from the containment. Analysis of this problem of competing rate processes required development of rate models.

3.1 PWR CONTAINMENT MODELS

Models developed for PWR accident sequence analyses were of two types; (1) a single-volume hand calculation model, and (2) a multicompartment computer coded model. The single volume model was used for preliminary hand calculations of PWR accident sequences using simplified constant rate coefficient values. The multicompartment model was developed and used for all detailed accident sequence calculations, incorporating variable rate coefficients, multivolume capabilities, and time variable fission product input and containment leakage quantities. The two models are described below.

3.1.1 SINGLE VOLUME CONTAINMENT MODEL

The single volume containment model assumes that the vapor phase consists of one well-mixed compartment. This assumption enables one to write the following single differential equation for each fission product species:

$$d\frac{C_i}{dt} = -\left(\sum_j \lambda_{ij}\right) C_i - \alpha_i C_i + R_i(t) \qquad \text{(VII 3-1)}$$

Initial Condition: $C_i = C_i(t')$ at $t = t'$

C_i = airborne moles of component i

λ_{ij} = removal rate constant via mechanism j

α_i = leak rate, fraction of the volume/time

$R_i(t)$ = source term (moles/time).

This equation is easily solved for constant λ_{ij}, α_i and R_i to get

$$C_i = \frac{R_i}{(\Sigma\lambda_{ij} + \alpha_i)} - \left[\frac{R_i}{(\Sigma\lambda_{ij} + \alpha_i)} - C_i(t')\right] \exp -(\Sigma\lambda_{ij} + \alpha_i)(t-t') \qquad \text{(VII 3-2)}$$

The escaped amount during the interval t-t' is the integral

$$Q_i = \int_{t'}^{t} C_i V \alpha_i \, dt,$$

where V is the volume of the vessel. Thus

$$Q_i = \frac{R_i V \alpha_i}{(\Sigma\lambda_{ij} + \alpha_i)}(t-t') - \left[\frac{R_i}{(\Sigma\lambda_{ij} + \alpha_i)} - C_i(t')\right]\left(\frac{\alpha_i V}{\Sigma\lambda_{ij} + \alpha_i}\right) \times 1-\exp\left[-(\Sigma\lambda_{ij} + \alpha_i)(t-t')\right] . \qquad \text{(VII 3-3)}$$

The two equations for $C_i(t)$ and $Q_i(t-t')$ can be used to calculate airborne fractions and leakage fractions for various accident sequences by hand. The values of R_i to be used for various species are

described in earlier sections of this report. The only release of fission products encountered where R_i = constant for some time period is the melt release. This simplifies most of the computations to using an initial condition for a time period where the λ_{ij}'s and α_i's are considered to be constant. If the λ's or α's change at some time, t', a new t' should be considered as the beginning of a new time period of constant new λ's or α's. The bases for the various values of λ_{ij} are discussed in Appendix J and a list of these coefficients is given in Table VII 3-1. Values of α_i must be specified from analyses of containment response for the accident sequence being calculated.

3.1.2 MULTICOMPARTMENT CONTAINMENT MODEL

To better simulate containment geometry and time variable removal rates, a model was developed to analyze the atmospheric source from a set of compartments whose airborne contents are well mixed and are altered by intercompartmental flow in addition to deposition rates, leak rates, spray removal rates, etc. This system is described by a set of equations of the form

$$dC_i^{mr}/dt = \sum_j H_{ij}^{mr} C_j^{mr} \qquad \text{(VII 3-4)}$$

where

C_i^{mr} = airborne fraction of initial release of material m in release type r contained in compartment i

$$H_{ij}^{mr} = \left(\lambda_i^{mr} + \sum_j G_{ki}/V_k\right)\delta_{ij} + (G_{ji}/V_j)\left(1-E_{ji}^{mr}\right)$$

λ_i^{mr} = removal coefficient from compartment i by settling, leak, spray removal, and other processes not involving flow to or from another compartment

G_{ji} = volume flow rate from compartment j to compartment i

E_{ji}^{mr} = filter removal fraction for material m from release r

V_j = volume of compartment j

δ_{ij} = 1 if i = j

δ_{ij} = 0 if i ≠ j

Note that the flow terms assume uniform mixing within each compartment.

For a given release type and material type, the equation set can be written in matrix notation

$$\frac{dC}{dt} = HC \qquad \text{(VII 3-5)}$$

Where C is the column vector of airborne release fractions in the respective compartments and H is the matrix of rate constants governing the evolution. The solution of this differential equation for the column vector C for constant coefficients in the H matrix is given exactly by

$$C(t) = e^{Ht}\, C(o) \qquad \text{(VII 3-6)}$$

or

$$C(t) = C(t_o) + (t-t_o)\, H \left(\frac{e^{(t-t_o)H}-1}{(t-t_o)H}\right) C(t_o). \qquad \text{(VII 3-7)}$$

Fast computer techniques for generating this solution have been developed by B. H. Duane (Ref. 1) and were utilized here. By calling the numerical integration subroutines developed by Duane at each time step after calculating the H matrix, the accuracy limit becomes that imposed by the assumption of constant H matrix elements within the time step. Numerical error in generating the solution to the coupled set of equations with constant coefficients can be made on the order of 10^{-6} percent.

To integrate the amount leaked within the time step, N additional fictitious compartments were defined whose function is to accumulate the leaked material from the N real compartments. The fractions C_{i+N}, i = 1, 2, ···N, are cumulative leaks obtained from the solution of

$$\frac{d}{dr}\left(C_{i+N}\right) = \alpha_i C_i$$

where α_i is one part of H_{ii}. The previously defined N x NH matrix was

augmented to form a 2N x 2N H matrix according to

$$H_{i+N,j} = \alpha_k \delta_{ij}$$

$$H_{i,\ j+N} = 0 \qquad \text{For } i = 1, 2, \cdots, N$$

$$H_{i+N,\ j+N} = 0 \qquad j = 1, 2, \cdots, N$$

If one takes the material quantity in the fictitious compartments to be zero at the start of a time step, the fraction of the initial release material leaked during the time step will be

$$\sum_{i=N}^{2N} c_i.$$

Computer code CORRAL[1] was written to solve the set of equations and at the same time compute each rate parameter as a function of time and/or as a function of vessel conditions (p, T, humidity). A more detailed description of the various models used to compute rate parameters follows.

Nine time dependent parameters are computed from input data at the time of solution of the differential equations. These are:

1. Compartment pressure, p(k), psig
2. Compartment temp, T(k), F
3. Compartment vapor mole fraction, VAP(k)
4. Compartment wall-bulk temperature difference, DELTA T(k), F

5.-6. Leak rates of molecular iodine and particulates from each compartment, ELI2(k), ELP(k), fractions/hr

7. Flow rates between compartments, G(j, k), ft^3/hr

8.-9. Filter decontamination efficiencies for flow between compartments, EFI2(J,K), EFP (j, k), dimensionless.

[1]Containment Of Radionuclides Released After LOCA.

The first four parameters enable one to compute transport coefficients involved in depletion rate coefficient calculations.

The bulk gas viscosities of steam-air mixtures (μ_m) are computed according to the following equations (Ref. 2):

$$\mu_m = \frac{\mu_A}{1 + \frac{y_s}{y_a}\phi_{As}} + \frac{\mu_s}{1 + \frac{y_A}{y_s}\phi_{sA}}, \qquad \text{(VII 3-8)}$$

where

μ_m = viscosity of mixture

$$\mu_A = 0.0414 \left[\frac{T,R}{492}\right]^{0.768}, \text{ lb/ft/hr}$$

$$\mu_s = \frac{0.003339\ (T,\ R)^{1.5}}{(T_R + 1224.2)}$$

y_A = mole fraction of air

y_s = mole fraction of steam

$$\phi_{As} = \frac{\left[1 + \left(\frac{\mu_A}{\mu_s}\right)^{1/2}\left(\frac{\mu_s}{\mu_A}\right)^{1/4}\right]^2}{2\sqrt{2}\left[1 + \left(\frac{\mu_A}{\mu_s}\right)\right]^{1/2}}$$

ϕ_{sA} = above with subscripts reversed.

The diffusivity of I_2 in the steam-air mixtures was found using data and equations from Knudsen (Ref. 2).

$$D_{I_2} = \frac{1}{\frac{y_A}{D_A} + \frac{y_s}{D_s}}, \qquad \text{(VII 3-9)}$$

where

$$D_A = 2.03\ \text{E-05}\ (T, K)^{1.5}/(P, atm)/W_A, \text{ cm}^2/\text{sec}$$

$$D_B = 3.24\ \text{E-05}\ (T, K)^{1.5}/(P, atm)/W_S$$

$$W_A = 0.7075 + 141.73/T, K$$

$$W_S = 0.7075 + 454.72/T, K.$$

The diffusivity of I_2 in water (spray drops) was computed using the standard Wilke-Chang relationship (Ref. 2), where

$$D_\ell = \frac{(7.4 \times 10^{-8})(xM_\ell)^{1/2}\, T(K)}{\mu_L V^{0.6}}, \text{ cm}^2/\text{sec},$$

(VII 3-10)

where

x = degree of solvent association = 2.6 for H_2O

M_ℓ = molecular weight of solvent

μ_L = solvent viscosity, cp

μ_L = $100/\{2.1484\ [(T,(K) - 281.6) + (8078.4 + (T,(K)-281.6)^2)\ 0.5] -120\}$ for H_2O

V = molar volume of diffusing substance = 71.5 cm^3/gmole for I_2.

3.1.2.1 Natural Deposition.

The mechanism of natural deposition of I_2 is governed by diffusion with natural convection generated by temperature differences between bulk gas and the wall (DELTAT(k)). Knudsen and Hilliard (Ref. 3) claim that a mass transfer analogy can be made with correlations predicting natural convective heat transfer coefficients. In similar manner, the model uses expressions for Sherwood numbers for laminar and turbulent flow using a thermal Grasholf number,

$$Gr = \ell^3 \frac{(T_{wall} - T_{bulk})}{(\mu_M/\rho_m)^2\, T_{bulk}}\, g.$$

Thus for laminar flow ($Gr < 10^9$), the Sherwood number is

$$N_{Sh} = \frac{k_c \ell}{D_{I_2}} = 0.59\ (Gr\ Sc)^{1/4},$$

(VII 3-11)

and for turbulent flow ($10^9 < Gr < 10^{12}$),

$$N_{Sh} = \frac{k_c \ell}{D_{I_2}} = 0.13\ (Gr\ Sc)^{1/3},$$

where (VII 3-12)

Sc = Schmidt number = $\mu_M/\rho_M\, D_{I_2}$

ℓ = length of the wall

k_c = mass transfer coefficient.

A combination of the two Sherwood numbers is used to compute the actual Sherwood number. Since the turbulence in most cases occurs around 10 ft from the top of the wall, a weighted average was used.

$$N_{Sh}\ (\text{overall}) = \frac{\ell - 10}{\ell} N_{Sh}\ (\text{turbulent}) + \frac{10}{\ell} N_{Sh}\ (\text{laminar}).$$

To convert the mass transfer coefficient into a deposition lambda (λ_{ij}) is a simple step. Thus,

$$\lambda_{ij}(k) = k_c\ (k)\ A(k)/V(k)$$

where A(k) and V(k) are surface area and volume of compartment k, respectively.

Another natural deposition process of interest is the settling of particulates. This involves a calculation of terminal settling velocities, V_s assuming spherical, unit density particles.

$$d^2\ (\rho_p - \rho_m)\ g/18\ \mu_m = V_s \quad \text{(VII 3-13)}$$

Particle diameters used were considered as functions of time. Hilliard and Coleman (Ref. 4) report that the settling velocities decrease with time after release. In CORRAL it was decided to use their data and assign an early particle diameter (15μ) and a late particle diameter (5μ) ("several hours" later = 4 hours) and linearly interpolate between them. After 4 hours the particle size was kept constant at the late value. To get the natural deposition lambda for particulates use

$$\lambda = V_s \frac{A\ (\text{floor area})}{V\ (\text{compartment volume})}$$

3.1.2.2 Spray Removal.

The spray removal model of I_2 by boric acid and caustic sprays used in CORRAL combines a gas phase mass transfer coefficient, a drop-gas interfacial equilibrium distribution coefficient and a stagnant liquid film mass transfer coef-

ficient. The expression for the spray lambda (s) is given by

$$\lambda = \frac{FH}{V}\left[1 - \exp - \left(6\frac{k_g\, t_e}{d(H + k_g/k_\ell)}\right)\right] \qquad \text{(VII 3-14)}$$

where

F = spray flow rate

H = equilibrium distribution coefficient ($C_g = C_\ell/H_j$ at equil.)

V = spray compartment volume

d = spray drop diameter

t_e = drop residence time - height of fall/terminal velocity

and the gas mass transfer coefficient, k_g, is given by Ranz and Marshall (Ref. 5) as

$$k_g = \frac{D_{I_2}}{d}\left\{2.0 + 0.60\ Re^{1/2}\ Sc^{1/3}\right\}$$

and

$$k_\ell = \frac{2\pi^2 D_\ell}{3d}$$

D_ℓ = I_2 diffusivity in liquid.

The latter is the Griffiths model discussed by Postma (Ref. 6). Incorporating the latter is a more conservative approach when $k_g/k_\ell \geq 5$ H. The terminal velocities of the falling drops are found by matching the velocity independent dimensionless number

$$f_D\ Re^2 = 4\ \rho_M\ (\rho_L - \rho_M)\ d^3\ g/3\mu_M^2$$

with the appropriate range of Reynolds number (Re). For spray drops the range of Re is 10-700. For 10 < Re < 100, $f_D Re^2 = 15.71\ Re^{1.417}$, and for 100 < Re < 700, $f_D Re^2 = 6.477\ Re^{1.609}$ (Ref. 7).

Spray lambdas for removal of particles follow the equation (Ref. 8):

$$\lambda = \frac{3F\ Eh}{2\ V\ d}, \qquad \text{(VII 3-15)}$$

where

F = spray flow rate
h = spray fall height
d = spray diameter
V = compartment volume
E = Spray collection efficiency.

In CORRAL empirical results from CSE data are used to predict E. Apparently the efficiency is a function of a normalized liquid volume sprayed (total volume sprayed/total compartment volume - Ft/V). Figure VII 3-1 shows the CSE data, and the curve in this figure was used to compute drop collection efficiencies in CORRAL. The diffusiophoresis was subtracted from the efficiency and the following expressions were fit to the remaining curve. To make these relationships apply to a spray lambda

Ft/V	E
0 - 0.002	$E = -15.825\ (Ft/V) + .055$
.002 - .0193	$E = .04125 - [.08626 + 42.68\ (Ft/V)]^{1/2}/21.34$
.0193	$E = .0015$

with multiple sprays being used at various times, the quantity Ft/V is now the sum $\Sigma\ F_i\ t_i/V$ for any one release of particles. Each release of particles would have its own spray aging relationship, and at this time no simple means of tying sequential release together into one relationship seems possible. Only when particle size distributions are known throughout a spray aging process can sequential releases be tied together.

It should be noted that in CORRAL, no spray cutoff is used at C(t)/C(0) = .02; spray aging is used in its place.

3.1.2.3 I_2 Equilibrium.

When airborne molecular iodine is depleted by either sprays or natural deposition, the depletion rate becomes independent of the two above mechanisms when the concentration falls below about 1 percent of the initial value (a conservative estimate, i.e., a lower value is less conservative (Ref. 8). At concentrations below this level, an apparent equilibrium situation exists where the concentrations in liquid and gas phases are related by an equilibrium distribu-

tion constant, $H = C_\ell/C_g$. H is a function of time (probably due to slow liquid phase chemical reaction) and has been experimentally determined. In program CORRAL it has been possible to incorporate $H = H(t)$ when equilibrium conditions exist.

To get the equilibrium described quantitatively, an equivalent lambda for depletion of gas phase I_2 had to be developed, since the value of H increases with increasing time, the gas phase is being depleted as time goes on. To get this equivalent lambda, we can write a mass balance for I_2. If C_{go} is the initial airborne concentration, then

$$C_{go}\, V_g = C_\ell\, V_\ell + C_g\, V_g \qquad \text{(VII 3-16)}$$

or

$$\frac{C_g}{C_{go}} = \frac{C_g\, V_g}{C_\ell V_\ell + C_g V_g} = \frac{1}{\frac{C_\ell V_\ell}{C_g V_g} + 1} = \frac{1}{H\frac{V_\ell}{V_g} + 1}. \qquad \text{(VII 3-17)}$$

Then for $H = H(t)$, we can write the removal rate of I_2 by

$$d\,\frac{C_g/C_{go}}{dt} = -\,\frac{1}{\left(H\,\frac{V_\ell}{V_g} + 1\right)^2}\left(\frac{V_\ell}{V_g}\right)\frac{dH}{dt}$$

where the equivalent lambda is

$$\frac{dCg}{Cg} = -\left\{\left(\frac{1}{H\,\frac{V_\ell}{V_g} + 1}\right)\frac{V_\ell}{V_g}\,\frac{dH}{dt}\right\} dt = -\,\lambda dt. \qquad \text{(VII 3-18)}$$

Data show that $H\, V_\ell/V_g >> 1$ for boric acid and caustic solutions in equilibrium with I_2, so that

$$\lambda = \frac{1}{H}\,\frac{dH}{dt}\,. \qquad \text{(VII 3-19)}$$

Typical data for sprays are shown in Tables VII 3-2 and VII 3-3.

3.1.2.4 Intercompartmental Flow Rates.

In two cases intercompartmental flow rates can be calculated. If circulation fans move air throughout the containment vessel or if boil-off occurs with steam evolution into one compartment, one can use these flow rates to provide a basis for estimating intercompartmental flows. In addition, natural convection driven by wall-bulk gas temperature differences can be a major contributor to flow rates. These rates can be estimated but with a high degree of uncertainty. In this study, high flow rates have been used to eliminate mixing as a parameter. Numerically, the high flow rate selected was equivalent to 10 PWR containment volumes per hour.

3.1.2.5 Design of CORRAL for PWR Analyses.

A schematic diagram of the containment geometry used in CORRAL-PWR calculations is given in Fig. VII 3-2. Four internal compartments of a large PWR containment vessel are modeled.

a. The Primary Cubicle - The small internal compartment which houses the piping, steam generator, and pump of one of the primary coolant loops, specifically the loop which experiences the large pipe break.

b. The Main Volume - The large space above the reactor cavity inside the polar crane wall and including the high dome. This volume is sprayed.

c. The Outer Annulus - The annular volume between the polar crane wall and the containment vessel outer wall.

d. The Lower Volume - This corresponds to the basement or the lowest level inside the containment structure.

The gas flow path between the four compartments is indicated on the diagram. The interchange between compartments 1 and 2 (Q_O) is determined by the primary system steam generation rate, while the circulation flow between compartments 2, 3, and 4 (Q_F) is set at a high value (as noted in the previous section) to simulate efficient interchange between these volumes. The PWR contaminant is thus divided into four well-mixed regions having different rates of airborne fission product removal. The removal processes that are included for each compartment are listed below the diagram along with the fission product injection locations. Note that all external leakage from the containment is assumed to occur from the outer annulus. Due to the well-mixed condition that is used, this affects only the amount of deposition that is calculated to occur in this

compartment and not the total inventory that leaks. An exception to this leakage path definition occurs when accident sequence analysis specifies puff releases from containment (i.e., sudden failure by explosion or overpressure). In such cases the same volume percent of the airborne contents of all four compartments is included in the puff loss value.

3.2 BWR MULTICOMPARTMENT MODEL

The multicompartment feature of code CORRAL was essential to estimating atmospheric source calculations from a BWR. A BWR containment system is not a set of openly connected compartments like a PWR, where the whole containment system can be usually considered as "well mixed". The compartments of a BWR are usually closed to one another and flows between them occur in complex ways during postulated accidents.

As many as six compartments are used in some BWR accident sequences. The first five are:

a. The Drywell where natural deposition can occur.

b. The Wetwell where pool scrubbing and natural deposition can occur.

c. The Drywell annular gap where natural deposition can occur.

d. The Reactor Building where natural deposition can occur.

e. The Standby Gas Treatment System (a series of filters).

The sixth compartment used was a fictitious dumping ground for ground level atmospheric sources when elevated (stack) sources occurred simultaneously. The schematic diagram of CORRAL for BWR accidents is shown in Fig. VII 3-3.

Natural deposition is the most common removal mechanism for fission products, although it is not necessarily the most effective mechanism. Natural deposition of particulates occurs on horizontal surfaces in all large compartments just as in a PWR. Turbulent deposition of particulates and iodine in the drywell annular air gap are via different mechanisms to be discussed later. Natural deposition of iodine occurs on all surfaces with the rate controlled by natural convection as discussed for the PWR model. However, since the wall-bulk gas temperature difference that drives the natural convection is highly variable in a BWR, transient heat transfer analyses are made to estimate this temperature difference.

3.2.1 NATURAL DEPOSITION - EFFECT OF HEAT TRANSFER FROM BWR VESSEL WALLS

The mass transfer coefficient for I_2 removal (see Appendix J) is proportional to the temperature-difference,

$$T_{wall} - T_{bulk} = \Delta T_w$$

raised to the 1/4 or 1/3 power. For an order of magnitude range in ΔT_w, the mass transfer coefficient changes by only a factor of 2, a relatively insignificant change. However, during rapid cooling of the drywell (depressurization), ΔT_w can span more than an order of magnitude for short durations. During rapid heating, the condensing heat transfer coefficient is large ($h = 150$ Btu/hr ft^2 F) and a steady ΔT_w is rapidly reached. This is about 0.14 F in the drywell. In cooling, the heat transfer coefficient from the steel (approximately one inch thick) wall is low (2-5 Btu/hr ft F), and can lag behind the bulk gas temperature for some time. Neglecting any temperature gradient in the steel, for a sudden step change in bulk gas temperature, ΔT_s, the temperature-difference, ΔT_w, is given by

$$\Delta T_w = \Delta T_s \exp\left(-ht/\ell_\rho c_p\right) \qquad \text{(VII 3-20)}$$

where

h = heat transfer coefficient

t = time after ΔT_s

ℓ = wall thickness

ρ = wall mass density

C_p = wall heat capacity (per unit mass)

If the temperature change is gradual, i.e., linear with respect to time, the temperature-difference, ΔT_w, is now given by

$$\Delta T_w = (\beta\, \ell_\rho c_p/h)\left[\exp - (ht/\ell\rho c_p) - 1\right] \qquad \text{(VII 3-21)}$$

where β is the linear bulk-gas cooling rate, F/hr. Equations VII 3-20 and VII 3-21 are used to compute ΔT_w for various time intervals during cooling in the drywell and wetwell. Values of h depend on gas velocities in the above compartments as well as the drywell annular air gap.

Little information could be readily obtained to estimate ΔT_w's in the main reactor building. These would be highly dependent on positions in the building and the outside environment temperatures, as well as gas flow parameters from the reactor. To allow for some minimum natural deposition in the main building, $\Delta T_w = 0.1$ F was used. This would result in a natural deposition rate of $\lambda = 0.5\ hr^{-1}$ in the main reactor building for I_2. This λ is five times the gas displacement rate for the building under normal conditions (2,000 cfm through the Gas Treatment System).

3.2.2 POOL SCRUBBING

In a number of BWR accident sequences, gas flow occurs through the vent lines from the drywell to the wetwell water pool. The water pool occupies slightly over one-half the toroidal volume of the wetwell and is approximately 17-feet deep. Pool scrubbing is a major decontamination mechanism. Some data exists on pool scrubbing, but comprehensive experimental studies on pool scrubbing in a BWR wetwell pool that include investigations of all parameters (a wide range of particle sizes, steam quality, pool temperatures, flow rates, I_2 concentrations, downcomer L/D ratios, etc...) have not been reported. Applying such data, if available, would not have refined atmospheric source estimates greatly because the available data show that scrubbing is fairly effective on the fission products entering the pool. Also, trial calculations showed that often 30 percent or more of the available fission products in any sequence would escape the primary containment by other paths (such as through the drywell annular gap directly to the secondary containment system).

The best available data appear in a paper by Diffey, Rumary, et al. (Ref. 10), where I_2, methyl iodide, and .06 μ particles in a steam-air mixture were pool scrubbed. The typical decontamination factors were 100 for I_2, 2 for CH_3I, and 50-100 for the .06 μ particles with 90 percent steam-air mixtures (higher steam fractions give better decontamination). For CORRAL-BWR cases, the values used are 100 for both I_2 and particles, and 1.0 for CH_3I. A decontamination factor of 1.0 is also used for the noble gas fission products.

The frequent result of higher than 90 percent steam partially justifies the use of DF = 100 for particles. Even though the BWR accident particles are assumed to be 5-15 μ, or much more massive than those studied above, the scrubbing of particles is largely due to diffusiophoresis (condensing steam on the bubble wall carries particles), and therefore largely independent of particle size. However, larger particles would have more boundary layer penetration inertia in a rapidly circulating bubble and this should then further justify the choice of DF = 100 for particles, rather than the lower DF = 50.

3.2.3 STANDBY GAS TREATMENT SYSTEM - (SGTS)

The SGTS in a typical BWR is a set of two parallel filter trains upstream from three exhaust fans that releases filtered secondary containment building air at an elevated level via a stack. However, under accident conditions only one of the filter trains would normally be used; the other being held in reserve. The SGTS keeps the building at subatmospheric pressures to minimize ground level leaks.

Under normal conditions, the flow rate through the system is about 2,000 cfm but the exhaust fans are capable of 10,000 cfm. Sources in excess of this maximum would create positive building pressures and produce a ground level, unfiltered source. The filter trains, according to plant Technical Specifications, are routinely tested to insure the following removal efficiencies at all flow rates up to the 10,000 cfm maximum:

- 99% for particulates
- 99% for elemental iodine
- 99% for organic iodide

These specifications are derived essentially from in-place testing criteria published by the USAEC in Regulatory Guide 1.52. The criteria incorporate limits on bypass flow for the filter and adsorber sections. It is recognized that substantially better performance may be realized for the filter system during actual use. This is because the specifications implicitly anticipate some deterioration in system effectiveness between testing steps which may or may not occur. However, since filtered leakage will be a minor contributor to overall accident consequences for meltdown sequences in the BWR, the efficien-

cies given above were used in all CORRAL calculations. In addition, CORRAL is programmed to identify the filter and adsorber activity loadings to discover possible overheating conditions, at which time the filtration efficiencies would decrease significantly.

The overheating criteria for both the HEPA filters and for the charcoal beds were based upon typical thermal performance data obtained from Safety Analysis Reports and the design temperature limits for the components; 250 F at 2000 cfm for the HEPA filters and 640 F at 2000 cfm for the charcoal filters. The heating rate of the filters (Q_F) was assumed proportional to the temperature difference between the filter material and the flowing inlet air.

$$Q_F \alpha (T_{Filter} - T_{Air,\ inlet}) \qquad \text{(VII 3-22)}$$

For the maximum heating rate $T_{Filter} = T_{Design}$. The inlet air temperature, by definition, is

$$T_{Air,inlet} = \bar{T}_{Air} - \frac{\Delta T_{Air}}{2} . \qquad \text{(VII 3-23)}$$

The change in air temperature is given by a heat balance,

$$\Delta T_{Air} = \frac{Q_F}{\rho w C_p} \qquad \text{(VII 3-24)}$$

where

ρ = air density
w = air flow rate
C_p = air specific heat

Reference thermal performance data can be used to obtain an average air temperature from,

$$Q_F \alpha \left(T_{Filter} - \bar{T}_{Air}\right) . \qquad \text{(VII 3-25)}$$

Using Equations (VII 3-22) through (VII 3-25) and the reference data given in Table VII 3-4, the maximum heat loads for the HEPA and charcoal filters were obtained for an air flow rate of 2000 cfm. The results are also given in Table VII 3-4.

In CORRAL calculations the fraction of the core fission product inventory which is captured by the filter components (all particulate species on the HEPA filter and elemental and organic iodine on the charcoal filter) is continuously recorded. Data from inventory computations of fission product decay energy emission rates are used to convert the fractions to heat loads. If the calculated heat loads equal or exceed the design limits the filters are assumed to fail. At this point, the activity which has been sorbed by either filter type is assumed to remain fixed, but the filtering efficiency for any further activity which passes through the system is set equal to zero. This procedure is based on the conclusion that the filter media will experience a physical degradation due to the elevated temperature rather than chemical combustion. For HEPA's the degradation consists of deteriation of fiber binder materials and sealer materials such that structural damage to the filter media and bypass flow can occur. For the charcoal beds it is assumed that the water dousing system operates, so that combustion is prevented, but the waterlogged beds will develop channels resulting in bypass flow. The use of zero filter efficiencies under these conditions is probably overly pessimistic but conditions are too uncertain to estimate another value with reasonable confidence.

3.2.4 NATURAL DEPOSITION IN THE DRYWELL ANNULAR AIRSPACE

The drywell shell is surrounded by a two-inch air gap between the steel shell and the concrete shield containing the shell. Under normal leakage, isolation loss leakage, or under certain primary containment failure conditions, gas flow from the primary containment is assumed to pass through the space and exit at the operating floor of the reactor building. Therefore, any fission product transport and deposition which occurs in the region of secondary containment below the operating floor are approximated in CORRAL by behavior in this annular air space. For cases in which leakage occurs directly from the drywell shell, the wetwell torus, or the connecting vent pipes this provides an accurate description of the flow path to the operating floor level. For cases in which primary containment leakage occurs in one of the many subcompartments in the lower region of the secondary containment building, the model constitutes a simplified approximation of the geometry and flow paths between the various leakage locations and the operating floor level. However, the method

described below for calculating fission product transport and deposition in the annular region, is expected to produce overestimates rather than underestimates of fission product concentrations reaching the refueling building under this alternate leakage path condition. This is because the combination of longer residence time with deposition in the lower regions of secondary containment would usually be more effective than the decontamination factors predicted for the annulus. Only under high flow conditions should decontamination in the annulus predict concentrations lower than might be obtained for the other leak path.

The annular region cannot be modeled like the well-mixed compartments with deposition on the walls and/or floor. It is better described as plug flow along a cylindrical annulus with mass transfer to the walls. A simple first order differential equation defines a mass transfer coefficient, k, that can be estimated from known correlations for I_2 transfer. For particles, k can be estimated from particle deposition data from moving gas streams with more difficulty and uncertainty. The differential equation for transfer to the walls of an annular slit is:

$$\frac{dC}{(C-C_w)} = -\left(\frac{2k}{U\Delta r}\right)dx, \qquad \text{(VII 3-26)}$$

where

C = the concentration of the transferring substance

C_w = wall concentration

U = plug average annual velocity

Δr = annulus width

x = axial distance

k = mass transfer coefficient.

If $C_w = 0$, Equation (VII 3-26) integrates for $0 \leq x \leq \ell$ to

$$\frac{C}{C(x=0)} = \exp\left[-\left(\frac{2\,k}{\underline{U}\Delta r}\right)\ell\right], \qquad \text{(VII 3-27)}$$

assuming an average axial velocity, $\underline{U}$,

$$\underline{U} = \frac{Q}{A_{av}}$$

where

$A_{av} = \Delta r \int_0^{\ell} \pi\, r\, dx/\ell$, average annulus cross section, and

Q = volumetric flow rate

For the annular gap described earlier for a typical BWR, Equation (VII 3-27) becomes

$$\frac{C}{C(x=0)} = \exp(-1200\ k/\underline{U}) \qquad \text{(VII 3-28)}$$

The assumption that $C_w = 0$ for both particulates and I_2 is reasonable for most conditions in the BWR accident cases. Molecular I_2 has been experimentally verified to have a high affinity for steel and paint surfaces (Ref. 4,11). Normally the overall mass transfer coefficient for I_2 would be

$$k^{-1} = k_w^{-1} + K_g^{-1} \qquad \text{(VII 3-29)}$$

where k_g is the boundary layer coefficient and k_w is a first order rate constant for the surface reaction (Ref. 4). The value of k_w is difficult to predict for the annulus since it is a function of temperature, surface composition, surface roughness, I_2 concentration, and vapor pressure. Thus, for the drywell annulus the surface was assumed to be a "perfect sink" for I_2 with no desorption occurring.

The gas phase mass transfer coefficients for I_2 are estimated using the following analogies from heat transfer correlations (Ref. 5). For developed turbulent flow ($Re \leq 20{,}000$),

$$Sh = \frac{k\ 4Rh}{D_{I_2}} = 0.026\ Re^{0.8}\ Sc^{1/3}, \qquad \text{(VII 3-30)}$$

and for laminar isothermal flow ($Re < 2{,}100$),

$$Sh = 1.86\ (Re \cdot Sc \cdot 4Rh/\ell)^{1/3}. \qquad \text{(VII 3-31)}$$

where

Re = Reynolds number = $\frac{\rho \underline{U}(4Rh)}{\mu}$

Rh = Hydraulic radius

$$= \frac{\text{flow cross sectional area}}{\text{wetted parameter}}$$

$$= \Delta r/2 \text{ for the annulus.}$$

The transition region, 2100<Re<20,000, is not well understood and Equation (VII 3-30) could overestimate the mass transfer coefficient by a factor of 3-5 at Re = 2100. This error is offset by the non-smooth nature of the annular gap, which could also cause an underestimation of k for high Reynolds numbers. For BWR cases encountered, the Reynolds number ranges from the laminar region to about 30,000. The maximum DF's occur at Re = 0 and Re = 2101. A cutoff of DF = 100 maximum for I_2 is assumed in CORRAL-BWR calculations for the annular gap. This is done because of the possibility of desorption or saturation of the annular surface.

The behavior of particulates is more difficult to predict because deposition velocities from moving gas streams are a function of particle size as well as gas velocity. Sehmel (Ref. 12) has recently published experimental data that allow an estimation of particle deposition in the annular gap. The deposition velocity (or mass transfer coefficient) is highly affected by gravity. Most of Sehmel's data are for deposition on floors and ceilings, and the deposition in the drywell is on an essentially vertical wall. Wall deposition velocities are closest to floor deposition velocities, but are slightly lower for inertial particles (usually $\geq$ 0.1 μ). For these inertial particles, Brownian diffusion is nil, so k = 0 has been assigned a DF = 1 for Re < 2100 for all particles. Only the largest of the 5-15-μ particles have a significant turbulent deposition velocity.

An empirical fit of Sehmel's data is possible for $k = k(\underline{U}, d_p)$, but he has only two $\underline{U}$ values for vertical wall deposition. For this reason only a first order approximation can be made for k. This also eliminates major overhaul of CORRAL's matrix computations to incorporate a new set of variables. The ratio $k/\underline{U} = 1/300$ = constant for all k and $\underline{U}$ for a particle size midway between 10-15μ. Table VII 3-5 shows the wide range of particle DF's versus Reynolds number.

To be conservative, an upper limit of DF = 100 seems more reasonable to assign to d_p = 15 μ (for $k/\underline{U} = 1/300$, DF = 27). With this upper limit, the following empirical equation fits the particle range:

$$DF = 1.0 + 0.1 \left[\frac{d_p - 5}{5} \right]^{9.95} \qquad \text{(VII 3-32)}$$

for $10 < d_p < 15$ μ particles and DF = 1.0 for $d_p < 10$ μ. Integrating Equation VII 3-32 over the aging process of the particles as they settle out in 4 hours (see paragraph 3.1.2.2), produces DF (avg) - 10.0. Since the age of airborne particles undergoing natural deposition is important longer than the 4 hour time period (approximately two of these periods), the average DF = 5.5. This value was used in CORRAL-BWR calculations for all particles passing through the annular gap for $Re \geq 2100$. It is a conservative number because approximately 90 percent of the mass of particles released is >10 μ in the CSE data and also in the CORRAL calculations. The mass average particle is 13.5 μ which has a DF = 21. Thus picking DF = 5.5 over-estimates early atmospheric sources and under-estimates additional sources on a long time basis. Certainly on a mass average basis, DF = 5.5 is conservative.

3.2.5 THE COMPUTER CODE CORRAL

The multicompartment containment model was programmed with Fortran V for use on a Univac 1108. The program incorporates the models for fission product removal discussed in the previous section. Figure VII 3-4 shows the basic flow chart for CORRAL. A summary of each of the five flow chart sections follows.

a. Input Parameters

1. Constants

(a) Core fractions for gap, melt, steam explosion and vaporization releases.

(b) Numbers of compartments.

(c) Volumes, wall areas, floor areas, heights of each compartment.

(d) Spray parameters (flow rates, drop sizes, fall heights, equilibrium conditions for I_2 removal, I_2 distribution coefficients).

(e) Times of all events.

(f) Compartment filter decontamination rates.

(g) Fractions of compartments released during a puff release.

2. Variables (with time)

(a) Pressure, temperature, and water vapor content of each compartment. Temperature difference between bulk gas and walls.

(b) Flow rates between compartments.

(c) Decontamination factors between compartments.

(d) Particle sizes.

(e) Leak rates to atmosphere and leak DF's (decontamination factors).

b. Initial Conditions

1. All concentrations set equal to zero at t = 0 except gas release concentrations in first compartment.

2. Spray set to operate in main compartment (PWR).

3. All amounts released and DRF's (dose reduction factors) set equal to zero. A zero DRF means that nothing has been released.

c. Computation of Properties and Removal Rates

1. Pressure, temperature, and water vapor content and T(bulk)-T(wall) by parabolic interpolation.

2. Intercompartmental flow rates and decontamination factors and leak rates and respective DF's by parabolic interpolation.

3. Particle sizes by linear interpolation.

4. Gas phase viscosities and I_2 diffusivities and Schmidt numbers.

5. Mass transfer Grashof numbers and corresponding deposition rates.

6. Particles settling velocities and their natural deposition.

7. Spray lambdas for particle.

8. Terminal spray velocities, gas phase mass transfer coefficient, liquid phase mass transfer coefficient, and spray lambdas.

9. I_2 equilibrium equivalent lambdas (if needed).

10. Overall lambdas.

d. Solution of Differential Equations

The solution of the differential equations is discussed in the previous section. To properly age the continuous releases, it was necessary to divide these releases into discrete impulses releases. The melt release was divided into ten equally spaced and sized releases, each independent age wise from the other nine. The vaporization release (released at an exponentially decaying rate) was divided into 20 impulse releases, each successive release at an exponentially lower value than the first. The sum of the first ten releases equals 1/2 the total release, and the remaining ten equals the remaining 1/2. The duration of the period of the first ten is one half life. The duration of the second ten should be three half lives for a reasonable approximation of an exponential decay.

Thus the total number of differential equations solved (one each for particulates, organic iodides and I_2) for any time step is (N=number of compartments)

GAP RELEASE	3N equations
EXPLOSION RELEASE	3N
MELT RELEASE	30N
VAPORIZATION RELEASE	$\frac{60N}{96N}$ equations

The accuracy of the output depends on the rate of change of the rate coefficients, so short time steps would be desirable immediately after each discrete release (aging is rapid at first, especially if sprays are on). Long time steps are sufficient for old releases.

e. Output Variables

1. Airborne contained fractions relased at time, t.
   (a) For each release: I_2, organic iodides, particulates.
   (b) For each compartment for each release: I_2, organic iodides, particulates, at time, t.
2. Escaped fractions released (for each release: I_2, organic iodides, particulates, at time, t).
3. Escape fractions of the core for any desired isotope.
4. Dose reduction factor for each release (I_2 and particulates) at time, t.
5. Overall dose reduction factor (I_2 and particulates) at time, t.
6. Total fraction of core iodine escaped and core particulates escaped up to time, t.

3.3 ESTIMATION OF METHYL IODIDE FRACTION USED IN PWR AND BWR ANALYSES WITH THE CORRAL CODE

Considerable experimental evidence exists that some relatively small portion of the fission product iodine which is released from the reactor fuel will appear in the containment volume as organic iodide compounds. The dominant compound, methyl iodide, because of its chemical properties would tend to remain in the gas phase rather than deposit on surfaces, dissolve in water, or react with spray solutions. Trapping on charcoal filters is also less effective for organic iodides than for inorganic iodine species. Therefore, estimates of the amount of this difficult-to-remove form that could be produced in an accident are necessary. This task is hampered by uncertainties in the mechanism of formation and limited data, but conversion values have been obtained based on the information that is currently available. The approach used and the resulting values for each water reactor type are described in the two following subsections.

3.3.1 METHYL IODIDE FRACTION FOR PWR ANALYSES

The fraction of iodine airborne as methyl iodide following postulated accident cases has been estimated from the information summarized by Postma and Zavadoski (Ref. 13). The total percentage formation was obtained by adding that formed by radiolysis to that formed by nonradiolytic mechanisms.

For nonradiolytic formation, the least squares fit of experimental measurements indicates conversion of 0.056 percent of iodine. Upper and lower limits indicated by the measurements are 1 percent and 0.004 percent, respectively. These values were summarized as

Nonradiolytic Percent

$$\text{Conversion} = 0.1\% \quad {}^{+0.9\%}_{-0.1\%}$$

Radiolytic formation process lead to combination of elemental iodine and trace level organic materials in the gas phase. On the basis of available experimental data, the maximum percentage conversion for a DBA case is 2.1 percent. The minimum formation due to radiolysis is near zero. Therefore, for no removal, we estimate

Radiolytic Conversion For No Removal Case = $1.1\% \pm 1\%$.

The no-removal case can never be realized because natural processes will deplete an appreciable fraction of the airborne iodine, making it unavailable for radiolysis. For natural removal, the percentage conversion was reduced by a factor of 2. The result may be summarized as follows:

Radiolytic Conversion For Natural Removal Case = $0.6\% \pm 0.5\%$.

Sprays will remove iodine rapidly from the gas phase, further reducing the potential for organic iodide formation. The effect of spray removal was handled by reducing the conversion by an additional factor of 2. The result is summarized as follows:

Radiolytic Conversion For Spray Removal Case = $0.3\% \pm 0.2\%$.

Total formation of organic iodides will be the sum of that for radiolysis and that formed by nonradiolytic mechanisms. For the natural transport case the result is

Total Conversion For Natural Removal

$$\text{Case} = 0.7\% \quad {}^{+1.4\%}_{-0.6\%}$$

and for the spray case,

Total Conversion For Spray Removal

Case = $0.4\%^{+1.1\%}_{-0.3\%}$

It should be noted that this approach defines an instantaneous methyl iodide fraction existing near the beginning of the accident sequence when most of the core iodine has been released. A more sophisticated approach would account for nonradiolytic formation as above, but would account for gas phase radiolysis through use of a G value for formation. A continued formation of organic iodides, based on the instantaneous airborne iodine concentration, G value for formation, and radiation dose would be used in place of the fractional conversions listed for the two conditions. However, this was considered an unnecessary complication because overall accident consequences are only partly dependent on iodine releases to the environment.

3.3.2 METHYL IODIDE FRACTION FOR BWR ANALYSES

It appears there is not enough evidence that methyl iodide formation in a BWR should be significantly different than in a PWR. Although radiolytic formation rates are higher in a BWR due to higher dose, radiolytic destruction is higher too. The net rate is perhaps much the same in both reactor types. Natural deposition lambdas are nearly identical. The driving force for natural convection is the bulk gas - wall temperature difference (ΔT). For the condensing atmosphere of the accidental sequences

$$\Delta T\ (PWR) \triangleq 10\ \Delta T\ (BWR)$$

$$\lambda(BWR) = \lambda\left(\frac{\Delta T(BWR)}{\Delta T(PWR)}\right)^{1/3}\left(\frac{A(BWR)/V(BWR)}{A(PWR)/V(PWR)}\right)$$

If we compare the drywell A/V with the PWR, then $\{A(BWR)/V(BWR)\}/\{A(PWR)/V(PWR)\} \triangleq 10^{1/3}$, therefore

$$\lambda(BWR) \triangleq \lambda(PWR)\ .$$

Since the natural transport case is the only condition requiring consideration in BWR analyses, a total conversion value for organic iodides of

$$0.7\%^{+1.1\%}_{-0.6\%}$$

will be used.

3.3.3 FISSION PRODUCT DECONTAMINATION DURING LEAKAGES TO THE ATMOSPHERE

Several different types of leakage from reactor containment to the atmosphere can occur during accident sequences for either reactor system. These can be classified as follows: (1) low (design) leakage from one or a collection of small undefined paths, (2) isolation loss leakage from a single and relatively large open path, and (3) massive leakage (a puff) from a failed containment vessel. In PWR systems the key structure with respect to atmospheric leakage is the steel-lined concrete containment vessel, while in BWR systems the important structure is the concrete and metal panel reactor building, also known as the secondary containment. During leakage from these structures it is possible that some of the fission product vapors and aerosols, which are carried by the bulk gas flow, would deposit on surfaces along the leak passage. Leakage through a network of rough-walled cracks would favor deposition while little deposition should occur during flow through an orifice.

In analyses performed throughout this study no credit has been taken for fission product deposition along the leak path when the leak path leads directly to the atmosphere. For large leaks (classes (2) and (3) above) this approach is probably close to actual experience. However, it is also considered an acceptable, although conservative, approximation for small leaks because; (1) the generally undefined nature of small leak distributions inhibits the ability to predict accurate decontamination factors, and (2) the accident sequences which are analyzed include containment failure at some point in the accident scenario and fission-product leakages beyond these points overwhelm the earlier low leakage values. In calculations the assumption of no decontamination is represented by using DF = 1.

There is one containment leakage situation where the release of activity to the atmosphere is modified by using a DF value greater than one. This case occurs only in PWR analyses where melt-through of the concrete base mat is followed by a puff release of the contained gas until the internal pressure equalizes with the external pressure.[1] Any gases and airborne fission products

---

[1] Since the bottom steel containment liner is embedded and anchored in concrete all around the reactor cavity area, no significant gaseous release from the base of containment is expected until the mat is actually penetrated by the melt.

escaping in this manner would have to pass through many feet of ground material in order to reach the atmosphere. The base of large PWR containments typically extend 40 to 60 feet below grade and part of this height is usually saturated with subsurface groundwater. The ground material may be low or high permeability soils, but next to the containment wall (perhaps within a coffer dam) the material is likely to consist of layers of gravel, sand, and/or porous concrete backfill.

This combination of external media should act as an effective filter for water soluble and particulate contaminants in the permeating gas stream. Work reported in Appendix K indicates many minutes or hours will be required for active gas to penetrate to the ground surface; that is, containment pressure relief by a single huge puff is not expected. In the water saturated zone of this natural filter bed soluble vapor species such as elemental iodine should be absorbed. Even though partial channeling may occur along fissures caused by the pressure gradients, the interfaces between the several layers of different materials should act as crack arrestors to produce meandering transport paths. Aerosol particles should be efficiently removed during passage through the dry upper layers of the backfill material. Work on the effectiveness of sand filters for removing aerosols from air streams (Ref. 14,15) indicate that efficiencies in the range of 99 percent to 99.99 percent are typical for one to three foot deep beds depending upon gas flow velocity, particle size, and degree of bed packing. Equivalent or better efficiencies should be expected for the situation of interest here because dry bed depths of 10 to 20 feet are anticipated.

Based on the above rationale it was concluded that fission product escape to the atmosphere via pressure relief from the base of the containment would be characterized by a large DF value for most species. Preliminary calculations were performed which indicated that any DF greater than 1000 would produce at most a ten percent decrease in the total atmospheric source term for accident sequences involving containment meltthrough; that is for DF$\geq$1000 the leakage prior to meltthrough accounts for nearly all of the atmospheric release. Therefore, a conservative value of 1000 was used in all such calculations. This DF applies only to elemental iodine and the particulate fission products. A DF = 1 was always used for the fission product noble gases and the organic iodide fraction. It is also emphasized that this procedure is followed only in PWR accident sequence analyses. In BWR accident sequences containment failure by some other process always precedes the meltthrough pathway.

3.3.4 POTENTIAL GROUNDWATER CONTAMINATION IN A MELTDOWN ACCIDENT[1]

Most of the reactor meltdown accident sequences are considered to ultimately result in melthrough of the bottom of the containment structure. This event will bring the molten mass into contact with the natural soil system at estimated depths of 50 to 100 feet. Radioactive contamination of the local groundwater can occur by several processes during this event. In meltthrough accidents where sprays have operated, some portion of the spray liquid may be released to the soil-water system. In accidents where sprays have not operated, airborne activity in the containment may be carried into the groundwater during containment building depressurization. Finally, groundwater leaching of the core mass itself can provide a delayed but long-term contamination source. The radionuclides introduced by any of these processes can be transported along the groundwater route to locations of potential interaction with human usage. It is of interest to the present study to obtain an estimate of the magnitude of this potential contamination pathway.

3.3.4.1 Problem Definition.

The analysis assumes a 3200 MW(th) reactor, after operating for 550 days at full power, experiences an accident event which results in core meltdown followed by meltthrough of the concrete floor of the containment structure as described in Appendix I. It has been estimated that containment meltthrough would occur about one day after the accident-initiating event (Ref. 36). Therefore, contamination of groundwater is unlikely before this time. Two basic modes were defined for analysis; one to examine the implications of early radioactivity release and the other to examine the effect of delayed leaching of radioactivity from the solidified core mass.

---

[1]The discussion presented here is based on the analyses performed by A. E. Reisenaur and R. C. Routson of Battelle's Pacific Northwest Laboratories.

In the first mode, it is assumed that containment meltthrough at one day is followed by rapid depressurization, and the airborne radioactivity in containment is delivered to the underlying soil-water system. This condition is indicative of a meltthrough accident in which containment sprays have not operated. Since detailed accident sequence calculations were performed in the Reactor Safety Study for this type of accident, core activity release fraction data are available. The release fractions range from a fraction of a percent of the core inventory for the less volatile species up to several percent of the core inventory for the more volatile species. Exact values used will be defined later in this section. The above contamination source term for the groundwater system is probably excessive for those accident sequences in which contaminated spray solution might leak into the soil because an equivalent radioactivity release would require leakage of several thousand gallons of solution past the molten core material. It is more likely the solution would vaporize back into the containment atmosphere. Accordingly, the depressurization release should be considered a worst case assumption. The analysis further assumes the airborne activity which is so released dissolves rapidly and completely in the receiving groundwater. This is probably highly conservative because much of the radioactivity will be in the form of oxide aerosol particles which should experience a relatively slow dissolution rate. In addition, the particulate source may have to penetrate a "dried-out" soil zone around the molten mass in order to reach the groundwater system. These two effects should delay the appearance of contamination in the groundwater and lead to lower peak concentrations than will be obtained under the present groundrules.

The second mode considers the effect of long-term leaching of fission products from the core-soil mass after it has cooled and solidified in the ground underneath the containment floor. It is expected that, during penetration into the ground, the size of the melt will increase as soil material is melted. Additional oxide and silicate phases will probably form which should mix with or partially dissolve in the core material. Fission products would be expected to distribute among the several molten phases under the influence of convective transport and chemical reaction driving forces. During this time the molten material should be surrounded by a relatively dry soil zone so that direct contact with groundwater would be unlikely. Eventually the melt penetration would stop because of decreasing decay-heat generation and the diluting effect of the molten soil constituents. Then the melt should gradually cool forming a solidified glass-like mass (Ref. 16). It is expected the mass would fracture during the cooling process and subsequent return of groundwater to the surface could begin leaching out fission products. The dimensions of the core-soil mass and the time delay for leaching to begin are difficult to predict accurately. Bounding heat-transfer calculations have indicated melt sizes may increase to maximum radii of 30 to 50 feet in 1 or 2 years in dry soils (Ref. 18). The presence of groundwater would tend to lower the numbers but results of the overall analysis here are not highly sensitive to exact dimensions. Elementary heat balance calculations also indicate that at about 1 year the heat removal capacity of the anticipated water flow (without boiling) would balance the decay-heat generation rate of the mass. The above results provide some guidance for selecting source dimensions and the starting time for leaching.

In both modes the source is modeled as a cylinder 70 feet in diameter and extending over the assumed 60 feet depth of the groundwater system. Radioactivity released from this boundary enters the groundwater where it is transported by the groundwater flow to a nearby outlet water body such as a river, lake, or bay. Therefore the rate of appearance of radionuclides at the outlet will depend on: (1) the release rate, (2) the groundwater flow velocity, and (3) the distribution coefficients for sorption of the dissolved radionuclides on the soil material of the groundwater system. In other words the soil-water system acts as a large chromatographic column to selectively separate and delay the discharge of the individual radionuclides in aqueous solution.

3.3.4.2 The Hydraulic and Ion Transport Models.

The hydraulics model for the two modes defined above was formulated as follows. An analytic solution to a point source and point sink in a uniform flow field was expanded to include a fully penetrating cylindrical source of finite radius. A diagram of the flow system used is given in Fig. VIII 3-5. The data chosen for the slope of the groundwater system, distance to the outlet water body, and soil type were selected from examining several eastern United

States power reactor site reports and generally represent conditions which would cause the most rapid dispersion of the radionuclides. Table VII 3-6 shows the input values used in the hydraulics model calculations. The normal groundwater flow was assumed to be perpendicular to the outlet water body.

In performing calculations with the model, the presence of the cylindrical source was assumed to disturb the uniform flow system out to twice the source radius. Therefore, the cross section of the contaminated flow system was 140-feet wide by 60-feet deep. The volumetric rate of fluid flow in this rectangular channel was 11,200 ft^3/day, and the linear flow velocity was 7 feet/day. Accordingly, the travel time for water from the source to the outlet water body was 215 days or 0.59 year.

The radionuclide transport calculations were made using a model based on the theoretical cell concept in which equilibration between the liquid and solid phases is achieved before the fluid is convected into the next cell (Ref. 17). The equilibrium stage approach has traditionally been considered satisfactory for groundwater systems because of the speed of the chemical reactions in relation to the fluid flow rate.

Sorption coefficients (Kd) for each isotope of concern were determined in the following fashion

a. Kd's for Sr and Cs in a typical[1] groundwater system were determined from direct data.

b. The Kd's for all other components in the given solution were calculated by assuming that the ratio of Kd_x to Kd_{Cs} or Kd_{Sr} reported in other references is constant.

Using the best available data, a conservative distribution coefficient (Kd) was chosen for each specie of concern. These coefficients with appropriate references are listed in Table VII 3-7.

3.3.4.3 Results of the Depressurization Release Problem.

The radionuclides chosen for calculation in this mode were selected on the basis of their half-life, distribution coefficient, and inventory. The fraction of the reactor core inventory of each radioactive species released to the groundwater system was based on calculated depressurization release fractions for a core meltthrough accident. The values used are given in Table VII 3-8. In executing these calculations, the mixed cell transport model utilized 100 column segments, and the individual radionuclide inventories (corresponding to the release fractions in Table VII 3-8) were "injected" to the groundwater flow channel over a two segment interval. This translates to an injection period of about 4.3 days which may or may not correspond to actual periods. However, final results are not too sensitive to this factor, particularly for species which experience adsorption and delay during transport to the outlet water body.

Resulting activity release rates of selected radionuclides contained in the groundwater released to the water body have been plotted and the curves are shown in Fig. VII 3-6. The semi-log plots show the release rates in curies/day as a function of time. Note the analysis predicts breakthrough of the non-sorbed Ru-106 at about 0.35 year with the release rate peaking at 0.59 year (215 days). The indicated axial dispersion is an artifact of the mixed cell model and may overestimate actual conditions. However, less dispersion would lead to higher peak release rates because the activity balance of the radionuclide must be maintained. In contrast to the non-sorbed ruthenium-106, the sorbed ruthenium-106 ions break through only after about 7 years and the ions leached from the soil have a much lower and broader elution curve. Technicium 99, with a low distribution coefficient (Kd = 0.1) breaks through in significant concentrations in about 0.7 years and peaks before one year. Strontium-90 which has an intermediate distribution coefficient (Kd = 2) arrives in significant quantities in 3 to 4 years and peaks at about 6 years. The Antimony-125 and the Cesium-137 with their higher Kd values lag behind the other nuclides arriving approximately 22 and 30 years after release and reaching their peak concentrations at 35 and 51 years, respectively.

The other radionuclides investigated were significantly delayed allowing radioactive decay to reduce them to innocuous levels at the time of arrival in the water body. In order to place these results in perspective with respect to radiological impact, the peak effluent

---

[1] Groundwater having 28 ppt total salinity and having a composition of 0.38 M Na^+, 0.008 M K^+, 0.008 M Ca^{++} and 0.04 M Mg^+.

concentrations discharged from the groundwater system for each of the radionuclides calculated may be compared to the maximum permissible concentrations specified in 10CFR20 (Ref. 30) for waters discharged to uncontrolled areas. This comparison along with other information is given in Table VII 3-9. It may be noted that three of the radionuclide effluent concentrations (Ru-106, Sr-90, and Cs-137) are predicted to be much higher than their respective MPC values. However, it must be emphasized that these are likely to be overestimates and they do not include the effects of several processes which would act to limit human exposure to this contamination source. These processes will be discussed following presentation of the results for the glass leaching release mode.

3.3.4.4 Results of the Glass Leaching Release Problem.

In accordance with estimates given earlier, the inventory of radionuclides in the core mass one year after the initial event was used to specify the leaching source strength. The significant species and their inventories were determined from the fuel irradiation history and consideration of prior fission product releases from the molten core. All isotopes of the noble gases, halegens, alkali metals, and tellurium group elements were assumed absent from the core-soil mass.[1] From the remaining refractory elements the following key species were selected; Tc-99, Sr-90, Ce-141, Zr-95, Eu-155, Pm-147, Eu-153, Sm-151, U-235, U-238, Pu-241, Pu-239, Pu-240, and Pu-242. The relationship used to predict the rate of leaching for all components can be expressed as

$$y = -5.222 + 0.334x$$

y = $\log_{10}$ (fraction leached from time ϕ to time T)

x = $\log_{10}$ (elapsed time from time ϕ to time T)

Time is in hours, ϕ is fixed at 1 year and T is variable.

The relationship was derived from data presented by Saidl and other (Ref. 31,32,33). The melt was conservatively assumed to be basalt glass since it is probably much more soluble than any other glass, and the characteristic components were Sr and Cs which are the most leachable of the components of interest.

The elution curves obtained for several of the more important nuclides are presented in Fig. VII 3-7. All the curves characteristically rise to a peak and then slowly decay. The peak efflux rates and concentrations of the radionuclides for this case are generally a factor of 100 to 1000 lower than for the corresponding nuclides in the depressurization release case. However, the elution continues for extended periods of time. Each of these features is a direct result of the very slow leaching process. In Table VII 3-10, the peak effluent concentrations discharged from the groundwater system for each of the radionuclides calculated are compared to the maximum permissible concentrations specified in 10CFR20 (Ref. 30) for waters discharged to uncontrolled areas. It is apparent that except for Sr-90 all the predicted peak effluent concentrations are well below the MPC limits.

3.3.4.5 Exposure Reduction Processes and Contamination Control Measures.

It should be emphasized that the hydraulic model parameters, the radionuclide distribution coefficients, and the radionuclide leaching rate used in these analyses were selected to produce overestimates for the rate of appearance of the radionuclide sources at the outlet water body. For example, the soil permeability coefficient is indicative of well-sorted sands with gravel and of fissured limestone formations (Ref. 34), the distribution coefficients are probably low by factors of 10 or 100 (Ref. 35), and the leaching expression assumes a relatively highly soluble glass containing fissures which increase the effective surface area by a factor of 100 or more (Ref. 32). In addition, calculations of human radiation dose from use of the receiving water body resource would have to include the dilution effect that would occur in the water body beyond the efflux point for the contaminated groundwater. Thus, the groundwater contamination problem at many reactor sites is expected to be less severe than indicated here.

Another important factor to consider in evaluating the above results is the significant times which are required for

---

[1] This assumption is consistent with the release fractions presented earlier in this report for the volatile fission products.

movement of radionuclides through a groundwater system. Several months and in many cases years should elapse before contamination would appear in water bodies used for the support of a significant population group. This delay would allow ample time for instituting monitoring operations and for setting up an effective warning network. More importantly, the time would most likely be used to execute procedures for controlling or even eliminating the spread of contamination beyond the reactor site. This would involve drilling wells for monitoring and pumping purposes to control the local groundwater flow gradient. The withdrawn water could be stored temporarily in surface tanks or in sealed holding ponds for subsequent treatment. After movement of the radionuclides is under control, it would seem feasible if it were to be considered necessary to form a vault-like barrier around the radioactive zone using a combination of excavation, drilling, and concrete injection operations.

Even without the above engineered mitigating actions, the basic conclusion of this analysis would not be changed. Specifically, the analysis has shown the hydrologic contamination problem occurs on a much longer time scale than does the atmospheric contamination problem for a core meltthrough accident. Therefore, warning actions alone should be sufficient to limit population radiation doses from the hydrologic source to low levels compared to the doses received as a result of the atmospheric source.

References

1. Reactor Physics Quarterly Report, April-June 1969, BNWL-1150, Battelle-Northwest, Richland, Wash., (B. H. Duane, p 2.5-2.7), (1969).

2. Knudsen, J. G., "Properties of Air-Steam Mixtures Containing Small Amounts of Iodine", BNWL-1326, Battelle-Northwest (1970).

3. Knudsen, J. G., and R. K. Hilliard, "Fission Product Transport by Natural Processes in Containment Vessels", BNWL-943, Battelle-Northwest, Richland, Washington (1969).

4. Hilliard, R. K. and L. F. Coleman, "Natural Transport Effects On Fission Product Behavior in the Containment Systems Experiment", BNWL-1457, Battelle-Northwest, Richland, Washington (1970).

5. Bird, R. B., Stewart, W. E., and E. N. Lightfoot, "Transport Phenomena", John Wiley and Sons, N. Y. (1960).

6. Postma, A. K. and W. F. Pasedag, "A Review of Mathematical Models for Predicting Spray Removal of Fission Products in Reactor Containment Vessels", BNWL-B-268, Battelle-Northwest, Richland, Washington (1973).

7. Postma, A. K. and R. K. Hilliard, "Absorption of Methyl Iodine by Sodium Thiosulfate Sprays", AND Trans. 12, p 898-899 (November, 1969).

8. Hilliard, R. K., Postma, A. K., et al., "Removal of Iodine and Particles by Sprays in the Containment System Experiment", Nuclear Technology, 10, p 499-519 (1971).

9. Postma, A. K., L. F. Coleman, and R. K. Hilliard, "Iodine Removal from Containment Atmospheres by Boric Acid Spray", Report No. BNP-100, Battelle-Northwest, Richland, Washington (197).

10. Diffey, H. R., Fumary, C. H., M. J. S. Smith and R. A. Stinchcombe (AERE, Harwell, England), "Iodine Cleanup in a Steam Suppression System," CONF-650407 (Vol. 2), Internation Symposium on Fission Product Release and Transport Under Accident Conditions, Oak Ridge, Tennessee, p 776-804 (April, 1965).

11. Rosenberg, H. S., Genco, J. M., and D. L. Morrison, "Fission-Product Deposition and Its Enhancement Under Reactor Accident Conditions: Deposition on Containment-System Surfaces", BMI-1865, Battelle-Columbus (May, 1969).

12. Sehmel, G. A.,"Particle Eddy Diffusivities and Deposiition Velocities For Isothermal Flow and Smooth Surfaces", Aerosol Science 4, p 125-139 (1973).

13. Postma, A. K., and R. W. Zavadoski, "Review of Organic Iodine Formation Under Accident Conditions in Water-Cooled Reactors", WASH-1233, (October, 1972).

14. Yoder, R. E., and Empson, "The Effectiveness of Land as a Filter Medium", Amer. Ind. Hyg. Assoc. J., 19, 107 (1958).

15. McFee, D. R., and Sedlet, J., "Plutonium-Uranium-Molybdenum Fume Characteristics and Land Filtration", J. Nucl. Energy, 22, 641 (1968).

16. Jansen, G. and D. D. Stepnewski, "Fast Reactor Fuel Interactions with Floor Material After a Hypothetical Core Meltdown,", Nucl Tech, 17, 85 (1973).

17. Routson, R. C. and R. J. Serne, "One-Dimensional Model of the Movement of Trace Radioactive Solute Through Soil Columns" The PERCOL Model", BNWL-1718 (1972).

18. Ergen, W. K., et al., "Emergency Core Cooling: Report of Advisory Task Force on Power Reactor Emergency Cooling (USAEC).

19. Schroeder, M. C., "Laboratory Studies of the Radioactive Contamination of Aquifers", AEC Document UCRL 13074 (1963).

20. Rhodes, D. W., "The Effect of pH on the Update of Radioactive Isotopes from Solution by a Soil", Soil Sci. Soc. Amer. Proc. 21:389-396 (1957).

21. Pillai, K. C. and T. R. Folson, "The Concentration of Lithium, Potassium, Rubidium and Cesium in some Western American Rivers", Geochim. and Cosmochim. Acta, 32:1229-1234 (1968).

22. Barrow, N. J., "Comparison of the Adsorption of Molybdate, Sulfate, and Phosphate by Soil", Soil Sci., 109:282-288 (1970).

23. Geering, H. R., E. E. Gary, L. H. P. Jones and W. H. Allaway, "Solubility and Redox Criteria for the Possible Forms of Selenium in Soil", Soil Sci. Soc. Amer. Proc., 32:35-40 (1968).

24. Pourboug, M., "Atlas of Electrochemical Equilibria in Aqueous Solution", Pergamon Press, New York (1966).

25. Touhill, C. J., B. W. Mercer and A. J. Schuckrow, "Treatment of Waste Solidification Condensates", AEC Document BNWL-723 (1968).

26. Raja, M. E. and K. L. Babcock, "On the Soil Chemistry of Radio-Iodine", Soil Sci., 91:1-5 (1961).

27. Price, K. R., Unpublished Data, Battelle-Northwest, Richland, Washington (1973).

28. Wildung, R. E., Unpublished Data, Battelle-Northwest, Richland, Washington (1973).

29. Routson, R. C., Unpublished Data, Battelle-Northwest, Richland, Washington (1973).

30. Code of Federal Regulations, Title 10, Part 20, "Standards for Protection Against Radiation". USAEC. Appendix B, Table II.

31. Ralkova, J. and J. Saidl, "Solidification of High Level Wastes: Part 3, Diffusion and Rates of Radionuclides Incorporated in Basalts", Kernergie, 10:161 (1967).

32. Mendell, J. E., "A Review of Leaching Test Methods and the Leachability of Various Solid Media Containing Radioactive Wastes", AEC Document BNWL-1765 (1973).

33. Saidl, J. and J. Ralkova, "Immobilization of Strontium and Cesium by Fixation of Radioactive Waste in Baslat", Collection, Czechoslov. Comun., 31, 871 (1966).

34. Fisher, H. L., "Prediction of the Dosage to Man From Fallout of Nuclear Devices - Transport of Nuclear Debris by Surface and Groundwater" UCRL-50163 Pt. 6 (January, 1972).

35. Higgins, G. H. "Evaluation of the Groundwater Contamination Hazard from Underground Nuclear Explosions", J. Geoph. Res, 64, 1509 (1959).

36. Carbiener, W. A., et al "Physical Processes in Reactor Meltdown Accidents", WASH-1400, Appendix VIII, October, 1975.

TABLE VII 3-1 FISSION PRODUCT REMOVAL RATE CONSTANTS CALCULATED FOR A LARGE PWR CONTAINMENT VESSEL

Spray System	Flow Rate gpm	Fraction Initial Release	λ, hr^{-1}
Molecular Iodine			
1 CSR, Boric Acid	3500	1.0 → .01	3.12
2 CSR[(a)], Boric Acid (pH = 5)	7000	1.0 → .01	6.24
Equilibrium Conditions: Boric Acid	--	$10^{-2} \rightarrow 1.8 \times 10^{-3}$	1.15
Equilibrium Conditions: Boric Acid	--	$1.8 \times 10^{-3} \rightarrow 3 \times 10^{-5}$	
Equilibrium Conditions: Boric Acid	--	$< 3 \times 10^{-5}$	0
1 CSR, NaOH (pH 9.5)	3500	1.0 → .01	67
2 CSR, NaOh	7000	1.0 → .01	134
Equilibrium Conditions: NaOH	--	Next 2 hrs	0
Equilibrium Conditions: NaOH	--	$10^{-2} \rightarrow 3 \times 10^{-5}$	0.223
Equilibrium Conditions: NaOH	--	$3.8 \times 10^{-4} \rightarrow 3 \times 10^{-5}$	0.0422
Equilibrium Conditions: NaOH	--	$< 3 \times 10^{-5}$	0
1 CSI[(a)], Boric Acid	3200	1.0 → 0.1	2.85
Boric Acid	--	<.01	Same as boric acid equilibrium
No spray (natural deposition)		1.0 → .01	1.38
No spray		<.01	0
Particulates			
1 CSR	3500	1.0 → .02	6.0
2 CSR	7000	1.0 → .02	12.0
2 CSR	7000	<.02	0.9
1 CSI	3200	1.0 → .02	12.6
1 CSI	3200	<.02	0.945
No spray (natural deposition)		1.0 → .02	0.13
No spray		<.02	0

(a) CSR = Recirculation spray. CSI = Injection spray.

TABLE VII 3-2 EQUILIBRIUM DATA FOR I_2 WITH BORIC ACID SPRAYS (Ref. 9)

Time, min	H	C_g/C_{go}
0	2676	.01
100	1.5×10^4	1.8×10^{-3}
500	4.0×10^4	6.75×10^{-4}
1000	7.0×10^4	3.86×10^{-4}
2000	1.5×10^5	1.8×10^{-4}
4000	5×10^5	5.4×10^{-5}
$\geq$7000	1×10^6	2.7×10^{-5}

TABLE VII 3-3 EQUILIBRIUM DATA FOR I_2 WITH CAUSTIC SPRAYS (Ref. 9)

Time, min	H	C_g/C_{go}
0-100	Constant H, λ=0	.01
100-1000	Variable H, λ=.095 hr^{-1}	.01
1000	7.0×10^4	3.86×10^{-4}
2000	1.5×10^5	1.8×10^{-4}
4000	5×10^5	5.4×10^{-5}
$\geq$7000	1×10^6	2.7×10^{-5}

TABLE VII 3-4 INPUT DATA AND RESULTS FOR FILTER OVERBEATING CRITERIA

Filter Type	Air Flow cfm	Filter Temperature F	Heat Load Watts
HEPA	2000	105	2.2×10^3
HEPA	2000	112	5.7×10^3
HEPA	2000	250(a)	5.4×10^4(a)
Charcoal	2000	110	1.3×10^3
Charcoal	2000	126	3.4×10^3
Charcoal	2000	640(a)	6.4×10^4(a)

(a) Design Limit

TABLE VII 3-5 DF vs PARTICLE SIZE AND REYNOLDS NUMBER IN DRYWELL ANNULAR GAP

d_p, μ	DF (Re $\leq$2100)	DF (Re = 2100)	DF (Re = 30,000)
5	1.0	1.0	1.0
10	1.0	1.1	1.1
15	1.0	4.4×10^5	2.2×10^4

TABLE VII 3-6 HYDRAULICS MODEL PARAMETERS

Length of Flow Field	1500 Feet
Slope of the Groundwater	1 Foot in 5000 Feet
Depth of the Groundwater System	60 Feet
Soil Permeability Coefficient	6666. Feet/Day
Radius of Source	35 Feet
Effective Porosity	0.19

TABLE VII 3-7 DISTRIBUTION COEFFICIENTS FOR VARIOUS RADIONUCLIDES IN GROUNDWATER

Radionuclide	Kd (ml/g)	Reference
I	0.1	25
Br	0.1	25
Cs	20	18
Rb	15	20
Te	20	23
Se	20	22
Sb	15	27
Ba	3	18,23
Sr	2	18
1/2 Ru	4	24
1/2 Ru	0	24
Mo	5	21
Pd	25	23
Rh	25	23
Tc	0.1	23,25
Y	200	19
Zr	200	19
Ce	50	28
Pr	60	28
Pm	60	28
Sm	60	28
Eu	60	28
U	100	26
Pu	200	19

TABLE VII 3-8 CORE INVENTORY DEPRESSURIZATION RELEASE FRACTIONS[(a)]

Group	Chemical Element	Release Fraction
1	I, Br	0.011
2	Cs, Rb	0.027
3	Te, Se, Sb	0.040
4	Ba, Sr	0.029
5	Ru, Mo, Pd, Rh, Tc	0.0028
6	Others	0.0005

(a) Obtained from CORRAL calculated output for PWR accident sequence ABε.

TABLE VII 3-9 COMPARISON OF CALCULATED GROUNDWATER EFFLUENT CONCENTRATIONS TO MPC LIMITS - DEPRESSURIZATION RELEASE CASE

Nuclide	Source Inventory, Curies	Time of Peak, years	Peak Effluent Concentration µCi/cc (a)	MPC µCi/cc
Ru-106 (b)	2.6×10^{4}	0.59	5.1×10^{-1}	1×10^{-5}
Tc-99	2.1×10^{0}	0.85	1.4×10^{-4}	2×10^{-4}
Ba-140	4.5×10^{6}	3.3	7.2×10^{-43}	2×10^{-5}
Sr-89	3.1×10^{6}	4.7	7.4×10^{-10}	3×10^{-6}
Sr-90	1.5×10^{5}	5.6	7.0×10^{-1}	3×10^{-7}
Ru-103	2.7×10^{5}	6.5	1.1×10^{-23}	8×10^{-5}
Ru-106	2.6×10^{4}	10	5.5×10^{-5}	1×10^{-5}
Te-129	4.2×10^{5}	11	2.9×10^{-71}	8×10^{-4}
Te-127m	5.1×10^{4}	24	1.9×10^{-36}	5×10^{-5}
Sb-125	1.1×10^{4}	35	6.6×10^{-7}	1×10^{-4}
Cs-134	4.5×10^{4}	43	2.0×10^{-9}	9×10^{-6}
Cs-135	3.7×10^{-1}	51	2.2×10^{-7}	1×10^{-4}
Cs-137	1.5×10^{5}	51	2.8×10^{-2}	2×10^{-5}

(a) Taken at 1500 ft from the point of release
(b) Non-sorbed fraction

TABLE VII 3-10 COMPARISON OF CALCULATED GROUNDWATER EFFLUENT CONCENTRATIONS TO MPC LIMITS - GLASS LEACHING RELEASE CASE

Nuclide	Source Inventory, Curies	Time of (a) Peak, years	Peak Effluent Concentration µCi/cc (c)	MPC µCi/cc
Tc-99	7.5×10^{2}	0.9	3.6×10^{-6}	2×10^{-4}
Sr-90	5.1×10^{6}	5.9	7.1×10^{-4}	3×10^{-7}
Ce-141	7.6×10^{4}	13	(b)	9×10^{-5}
Zr-95	3.2×10^{6}	27	(b)	6×10^{-5}
Eu-155	6.9×10^{4}	103	(b)	2×10^{-4}
Pm-147	1.4×10^{7}	115	(b)	2×10^{-4}
Eu-154	5.6×10^{4}	148	1.3×10^{-8}	2×10^{-5}
Sm-151	5.8×10^{3}	158	2.3×10^{-7}	4×10^{-4}
U-235	2.3×10^{0}	267	2.5×10^{-10}	3×10^{-5}
U-238	3.2×10^{1}	267	3.5×10^{-9}	4×10^{-5}
Pu-241	3.8×10^{6}	418	(b)	2×10^{-4}
Pu-239	1.2×10^{4}	535	8.0×10^{-7}	5×10^{-6}
Pu-240	1.2×10^{4}	535	8.0×10^{-7}	5×10^{-6}
Pu-242	3.9×10^{1}	535	2.6×10^{-9}	5×10^{-6}

(a) Time started from beginning of leaching or 1 year after the incident.
(b) Peak concentration less than 1×10^{-10} µCi/cc.
(c) Taken at 1500 ft from the point of release.

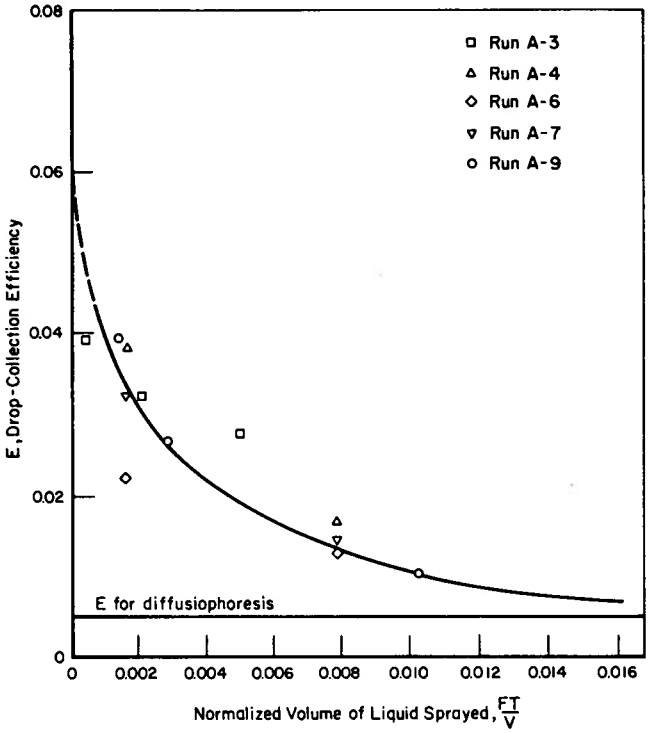

FIGURE VII 3-1 Drop-Collection Efficiency as a Function of Liquid Volume Sprayed

Points are plotted at mid-times of spray periods (fresh spray only)

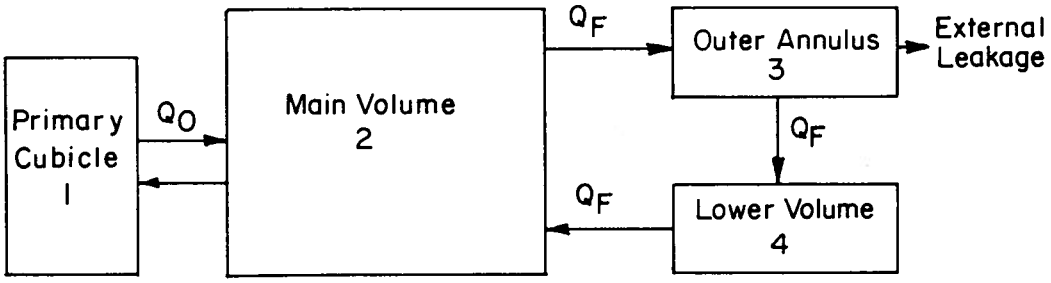

Compartment	Removal Processes	Fission Product Sources
1	Natural deposition	Gap and melt releases
2	Natural deposition	Steam explosion releases
	Spray absorption	
	Recirculation filters	
3	Natural deposition	
	Leakage	
4	Natural deposition	Vaporization release

FIGURE VII 3-2 Schematic of CORRAL-PWR

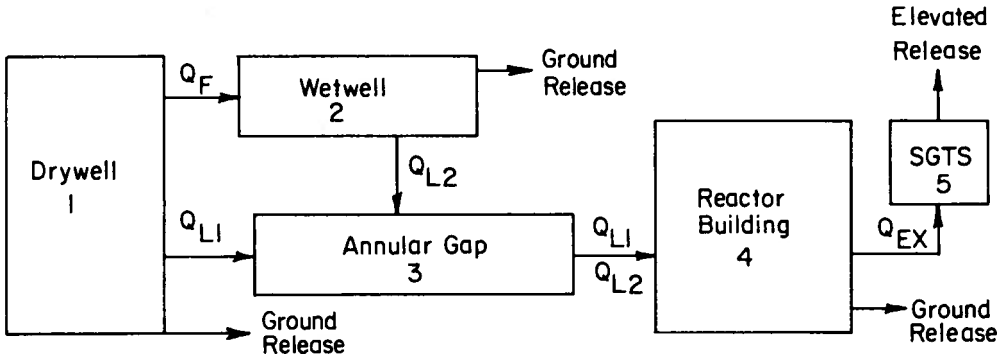

Compartment	Removal Processes	Fission Product Sources
1	Natural deposition External leakage	Gap, melt, steam explosion, and vaporization releases
2	Pool scrubbing Natural deposition External leakage	
3	Natural deposition	
4	Natural deposition External leakage	
5	Once-through filtration	

FIGURE VII 3-3 Schematic of CORRAL-BWR

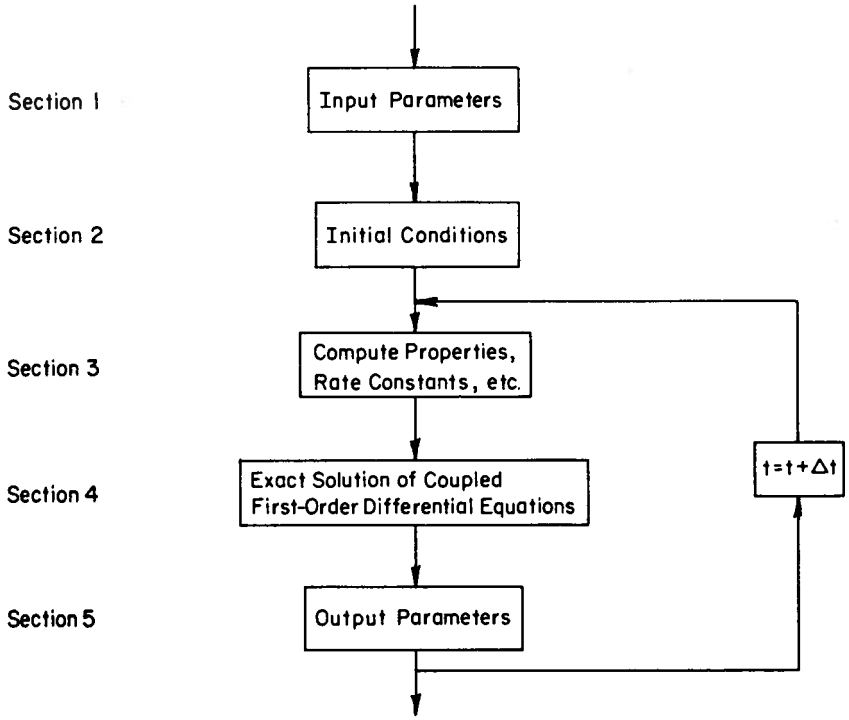

FIGURE VII 3-4 Computer Code CORRAL Flow Diagrams

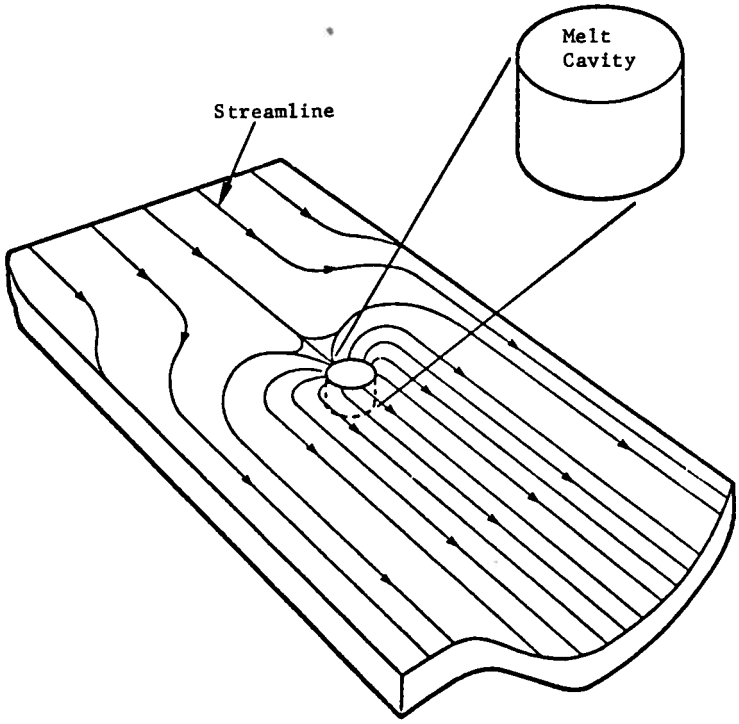

FIGURE VII 3-5 Idealized Flow System Used for Analysis

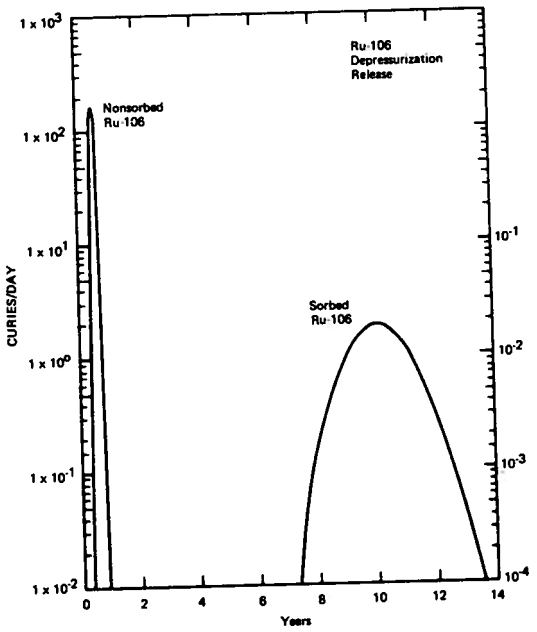

FIGURE VII 3-6 Radionuclide Elution Curves for Depressurization Release

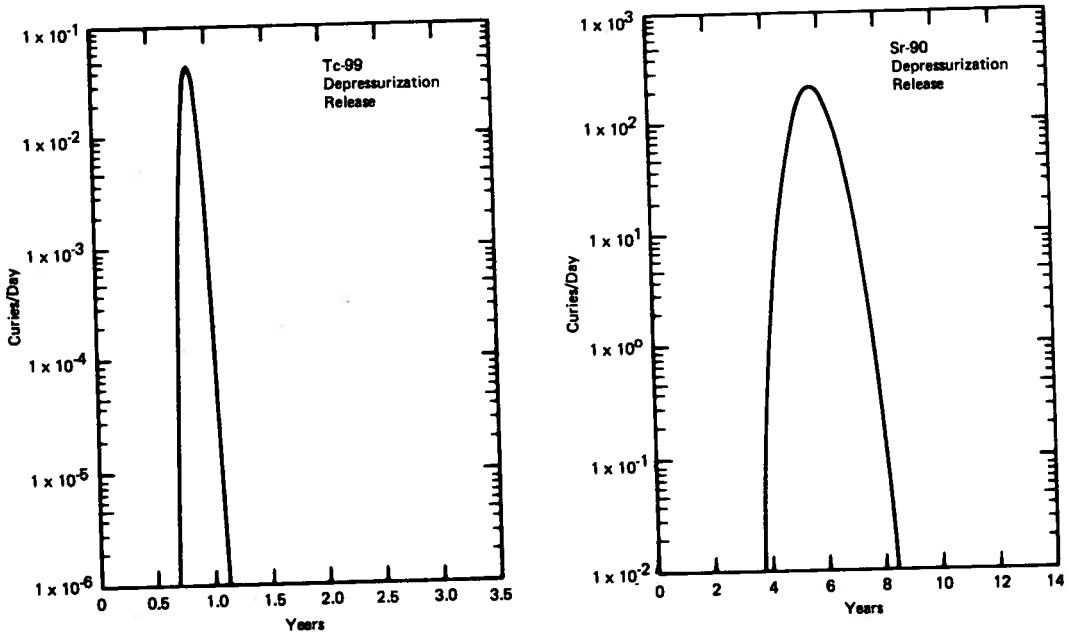

FIGURE VII 3-6 (Continued)

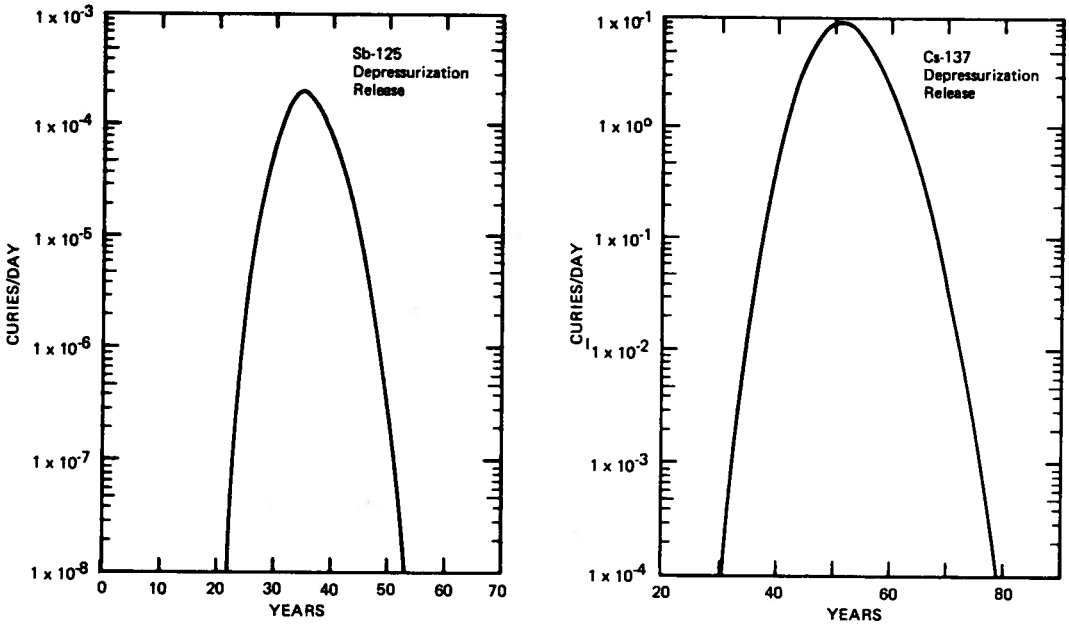

FIGURE VII 3-6 (Continued)

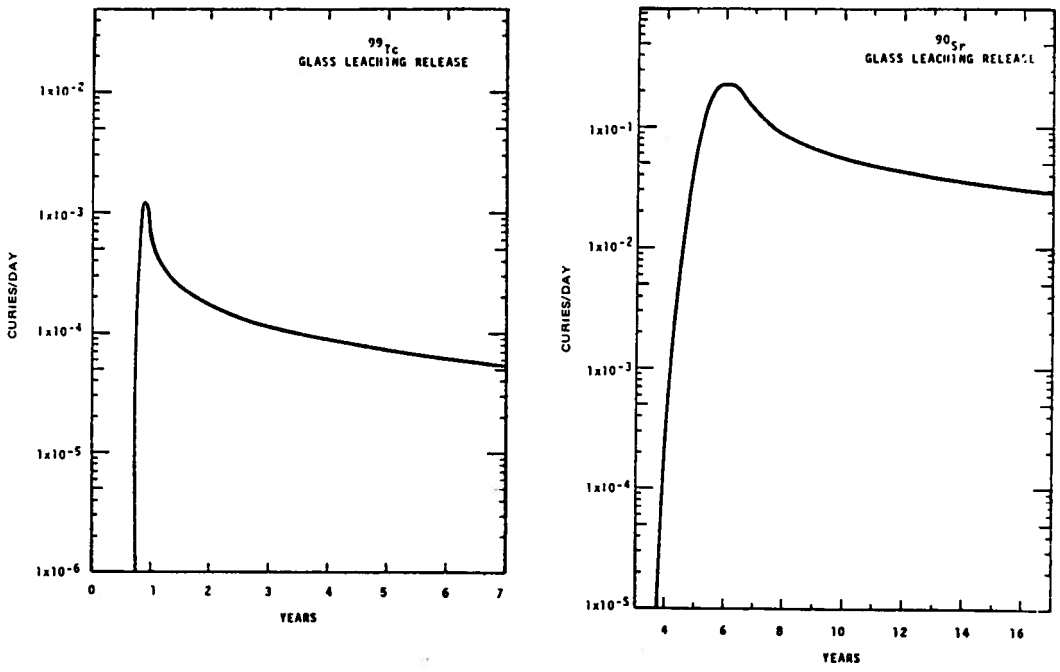

FIGURE VII 3-7 Radionuclide Elution Curves for Glass Leaching Release

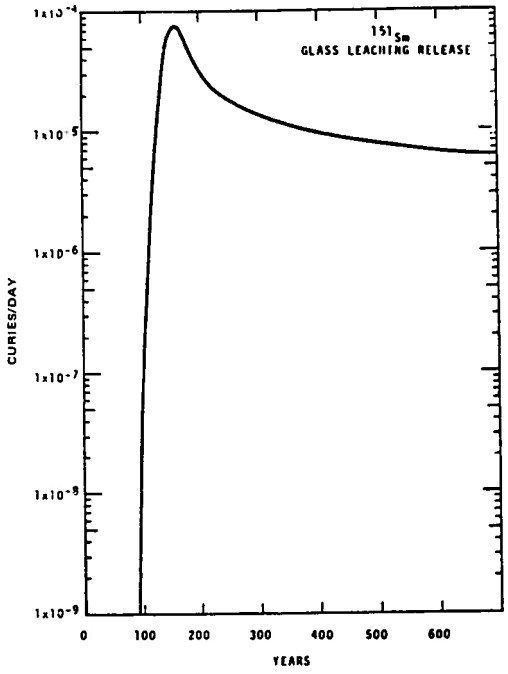

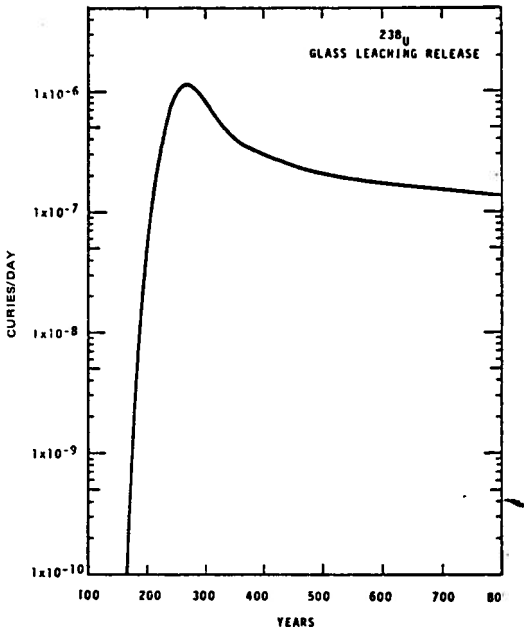

FIGURE VII 3-7 (Continued)

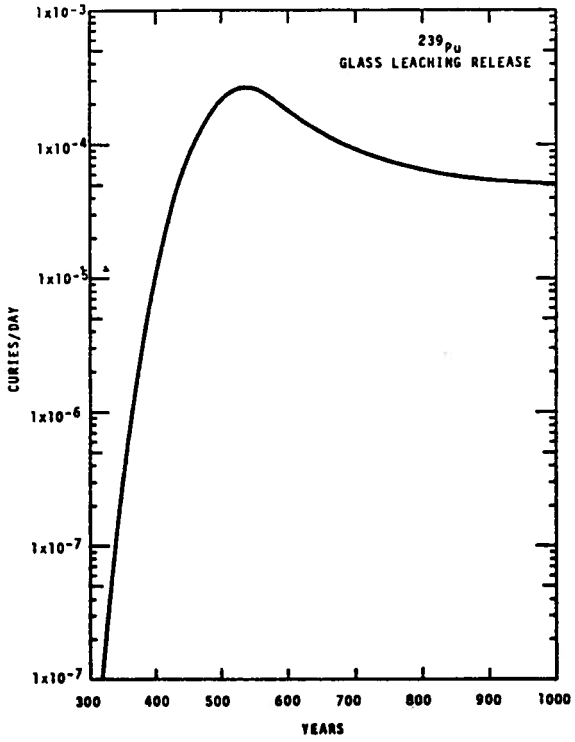

FIGURE VII 3-7 (Continued)

Appendix D

Survey of Experimental Work on Fission Product Release From Molten UO_2

by

R. L. Ritzman
Battelle, Columbus Laboratories

and

G. W. Parker
Oak Ridge National Laboratory

Experimental work on the release of a number of important fission products during melting of UO_2 samples has been performed at several laboratories. Numerous factors which can affect release magnitudes or rates have been examined to various degrees, but an extensive data base for use in predicting release during a reactor core meltdown does not exist. This is mainly because no moderate or large amounts of irradiated UO_2 have been melted, particularly in a reactor core configuration. The studies that have been done with small fuel samples do, however, provide useful insights to the general release behavior of the more important fission products. The purpose of this survey is to summarize the more pertinent findings of these studies without developing a comprehensive review of all the work that has been done. Emphasis will be placed on the general conclusions that can be drawn from the data as a whole regarding release magnitudes and significant interactions which should affect the magnitudes.

D1. OUT-OF-PILE MELTING STUDIES

Most of the experimental work of this type has been performed at Oak Ridge National Laboratory (ORNL), but some additional useful data have been obtained at the Contamination-Decontamination Experiment (CDE). Much of the ORNL work consisted of melting small samples of irradiated UO_2 using different furnace heating techniques. The work has been described in a report by Parker, et al. (Ref. 1). Limited investigation of parameters which can affect fission product release was made including burnup, sample size, time molten, atmosphere composition, melting method, and type of cladding. Most of the melting experiments were performed in helium because of reactivity of container or heater materials with oxygen, but a few experiments were performed with CO_2 and air.

D1.1 ARC-IMAGE FURNACE EXPERIMENTS

The first melting experiments were conducted with small (0.2 to 0.6 gram) trace-irradiated and unclad UO_2 specimens held in a BeO support tube. The entire assembly was melted (sometimes incompletely) in an arc-image furnace for periods of 1-1/2 to 3 minutes. Following melting the release of rare gases, iodine, tellurium, cesium, ruthenium, strontium, barium, and rare earth elements was measured by radiochemical analysis. Release was defined as the percentage of each specie that escaped the UO_2-BeO assembly. The helium cover gas used in the experiment contained small amounts of air as an impurity. Table VII D-1 lists the results of the fission product release measurements for these experiments. The rare gas release values should be considered indicative of the degree of melting that was achieved. In general, the data from these small specimens indicate two ranges of release values; one set of high releases which includes rare gases, iodine, tellurium, cesium, and ruthenium, and another set of low releases which include strontium, barium, and rare earths. It is possible that the air impurity in the helium cover gas influenced some of the release values. Strontium, the rare earth elements, and to some extent barium, are known to form quite stable oxides with volatilities significantly less than the respective metals (Ref. 2 and 3). Such reactions may have contributed to the low releases observed for these fission products. On the other hand, ruthenium can form volatile oxides (Ref. 2), and this may have caused the observed high release values. The releases of the remaining fission products would not be expected to be particularly sensitive to the presence of air impurities, since at UO_2 melting temperatures both the oxides, if formed, and the elements exhibit high volatility.

Limited additional experiments of this type were performed in air and carbon dioxide and impure helium atmospheres using UO_2 having burnup levels up to 11,000 Mwd/T. All fission product release data were very similar to the results described above; i.e., either high or low release for the identical sets of fission products. A weak positive correlation of release with burnup level was suggested, but the effect also correlates with differences in sample sizes. No appreciable effect of the different cover gases used on the extent of release was indicated. This was probably because each of the atmospheres created an essentially oxidizing environment. Generally, the data indicate that burnup level should be considered no more than a secondary factor and that air and CO_2 have about the same effect on fission product release from molten UO_2.

D1.2 TUNGSTEN CRUCIBLE MELTING EXPERIMENTS

The next series of experiments consisted of trace-irradiated UO_2 specimens that were melted by induction in tungsten crucibles. The results of these experiments are more useful for two reasons: (1) the larger samples, bout 29 grams, are comparable to actual reactor fuel pellet sizes, and (2) an essentially inert furnace atmosphere was maintained so that release data are indicative of non-oxidizing conditions. The data obtained from these experiments are given in Table VII D-2. Comparison with Table VII D-1 shows that, generally, the same release results were obtained by the two melting techniques except for the fission product ruthenium. As noted earlier, ruthenium is known to be quite oxygen sensitive and it is quite possible that its higher release on melting in the arc-image furnace can be attributed to traces of oxygen in the helium supply and the absence of the good oxygen getter (tungsten) that was available in the later experiments with larger samples. Note also in Table VII D-2 that the certain (rare earths) release values approximately correspond to the percent UO_2 that vaporized. This observation is consistent with the known refractory nature of the rare earth oxides. The time that the UO_2 remained molten in these experiments varied to some extent and a weak correlation may exist between release and time molten for the more volatile elements. Nevertheless, the data lead to the conclusion that the melting of bare UO_2 fuel pellets will cause rapid and high release of the more volatile fission products (rare gases, iodine, tellurium, and cesium). The release of ruthenium is very sensitive to the oxidizing nature of the system. Strontium and rare earth release rates should be low and comparable to UO_2 vaporization rates while barium release rates may be somewhat higher (probably due to the lesser stability or higher volatility of its oxide).

D1.3 TUNGSTEN RESISTOR MELTING EXPERIMENTS

The third and final type of laboratory scale out-of-pile melting experiment involved use of a tungsten rod resistor heating element which was passed through cored UO_2 pellets. Both clad and unclad elements were employed in these experiments, but they were limited to a helium atmosphere and complete melting of specimens could not be accomplished before the tungsten rods melted. Nevertheless, the results are quite useful because the high interior fuel temperature and cooler surface achieved with this heating method more nearly simulate nuclear heating than any other out-of-pile technique. The release data obtained from the melting of trace-irradiated UO_2 are given in Table VII D-3. The results from the unclad specimens, after adjusting for the fraction melted, are very similar to the results of the other melting methods with respect to rare gases, iodine, tellurium, cesium, and cerium (rare earths). The releases of strontium and barium are somewhat higher and the release of ruthenium is again low, which suggests that the oxygen activity in the system was even lower than in the tungsten crucible melting experiments. The release from the stainless-steel clad specimen was quite similar to that from unclad fuel.

However, it is evident that the zirconium clad specimens gave very different results for some fission products. The releases of strontium and barium were significantly higher while tellurium release experienced a sharp decrease. Post-melting examinations indicated that the molten zirconium had wet the UO_2 and spread over the surface. Since zirconium is known to have a high affinity for oxygen, this behavior probably caused the clad to serve as a very effective oxygen getter. This led to a very low oxygen activity in the system causing conversion of both strontium and barium to the more volatile metallic forms. The low tellurium release can apparently be explained on the basis of reaction with and retention by the molten zirconium. This conclusion is supported by independent results obtained by Genco, et al. (Ref. 4) which shows that tellurium vapor reacts extensively with zir-

conium metal at temperatures above about 400 C. Since tellurium belongs to the same periodic group as oxygen, it is not too surprising that stable zirconium tellurides could exist at high temperatures. The same considerations provide some insight regarding the lack of effect of stainless steel cladding on fission product releases. Iron, the major component of stainless steel, has a much lower affinity for oxygen (less negative free energy of formation) (Ref. 5) than does zirconium. Consequently, it should not have a strong effect on the oxygen activity in the system (which can influence strontium, barium, and perhaps ruthenium volatility), and by analogy should not tend to form thermally stable tellurides either.

D1.4 MELTING EXPERIMENTS AT THE NSPP

A different series of UO_2 melting experiments were performed at ORNL as part of the Nuclear Safety Pilot Plant (NSPP) program (Refs. 6-9). Samples of clad UO_2 were passed under a plasma torch in different atmospheres to generate an aerosol source for the study of containment behavior processes in an adjacent model containment vessel. The experiments were characterized by many differing conditions and material balances were poor in some instances but the results provide some useful general observations. The release data for these experiments are summarized in Table VII D-4. Two sets of release percentages for various fission products are listed; one for release from the immediate fuel region and another for release from the steel transfer line to the model containment vessel. Looking at the first five experiments (stainless-steel cladding) the data in general indicate high releases from molten fuel for iodine, tellurium, and cesium with much lower releases for the other species. Ruthenium behavior was erratic and probably indicative of the oxygen level in the furnace. None of the release results appear to depend on changes in furnace atmosphere except ruthenium. The latter two experiments with Zircaloy clad high burnup UO_2 are more difficult to interpret. The difference in degree of melting probably masks most atmosphere effects except for ruthenium. Consistent with other data the ruthenium release was relatively high in an air atmosphere. The low ruthenium release in steam could be attributed to a more reducing environment resulting from hydrogen produced by the zirconium-water reaction that would take place between cladding and steam. Also consistent with the out-of-pile melting work described earlier, iodine and cesium releases remain high and apparently independent of atmosphere. The barium release in Experiment 14 and strontium, barium, and cerium releases in Experiment 15 appear somewhat anomalous. The oxygen gettering ability of Zircaloy leading to volatilization of strontium and barium metal could possibly explain the high releases in Experiment 15, but cerium should not be strongly affected and the ruthenium release is not consistent with this hypothesis. The explanation is unknown and much more information about exact conditions in the furnace during melting would be needed in order to analyze the data further. The second set of release numbers in Table VII D-4 provides an indication of the effectiveness with which fission products released from the fuel region were transported to the MCV. Even though temperatures in the transfer line were low (probably several hundred degrees) the transit time was short. In general, plateout factors for all species during this transfer were about the same and ranged from factors of about 2 to factors of about 10. Thus, plateout in the transfer line did not cause a major change in the character of the fission product source that was transported to the model containment vessel.

D1.5 MELTING EXPERIMENTS AT THE CDE

Another short series of out-of-pile experiments in which fission product release from molten UO_2 was measured was conducted at the CDE by Freeby, et al. (Ref. 10). These consisted of five runs in which Zircaloy clad UO_2 pellets were melted by induction in steam atmospheres. The fuel weight ranged from 70 to 80 grams and molten times of about 30 minutes were achieved in each case. Fuel burnups among the five samples ranged from about 500 to 2000 Mwd/T. Some difficulties in achieving material balances were encountered, particularly for iodine and tellurium. However, these experiments are specifically relevant to the conditions that would exist during reactor core melting. The combined results of the five experiments are given in Table VII D-5 along with other pertinent data that investigators obtained from reports of related work. The CDE results generally agree with other out-of-pile release data in that high volatility is indicated for the noble gases, iodine, tellurium, and cesium, and relatively low volatility for strontium, barium, and ruthenium. However, contrary to the ORNL results, the release data do not indicate a dominant effect of the Zircaloy cladding on tellurium or strontium and barium release.

This may be due to the steam atmosphere in the CDE experiments which caused extensive oxidation of the Zircaloy cladding (possibly liberating some retained tellurium) and perhaps producing a high enough oxygen activity in the system to hold strontium and barium as their oxides. The data listed in the table under CMF were the result of a single melting experiment under a steam-air atmosphere in that facility at ORNL. The data continue to support the earlier observations at ORNL concerning the effect of zirconium cladding on tellurium and strontium release. Therefore, the release behavior of tellurium and strontium and barium during melting of Zircaloy clad UO_2 is somewhat uncertain. A comparison of the data obtained in the different experiments identified in Table VII D-5 shows a possible trend toward increase in iodine release with increasing fuel burnup. However, differences in specimen temperatures or melting periods probably influence the results such that the indicated burnup effect is quite indefinite.

In the CDE experiments efforts were made to record the plateout of released fission products that occurred within a short stainless steel transfer line to a containment vessel. The temperature of the line was maintained at about 800 F and transit times ranged from about one to two seconds. In general, it was found that less than 1/3 of the entering fission products deposited in the line except for cerium which was nearly all deposited. The results roughly agree with experience at the NSPP and indicate that longer residence times or higher surface areas would be needed to promote efficient plateout. Another significant observation was recorded during the CDE melting experiments. Even though the small fuel pins were kept molten for 30 minutes or so, most of the fission product release took place within a one- to two-minute period relatively early in the experiments. This rapid release coincided with melt-through of the Zircaloy cladding (pin lying on its side in UO_2 powder). Subsequently large quantities of particulates (cladding and fuel) were released creating a white smoke in the furnace. A continuous slow release of fission products occurred during the period the fuel was maintained in the molten state. Although unconfirmed, it seems probable that the early rapid release was due to escape of the highly volatile fission products while the slower continuous release was due to the low volatility species. The appearance of a dense aerosol in the furnace is indicative of the ease with which released vapors will condense and agglomerate to form a particulate source.

D2. IN-PILE MELTING STUDIES

In addition to the out-of-pile melting experiments, a series of in-pile fuel melting experiments were conducted at ORNL (Ref. 15). These experiments consisted of melting miniature stainless-steel-clad UO_2 fuel elements ($\sim$30 grams UO_2) in various atmospheres in the Oak Ridge Research Reactor and measuring the fission products released. Fission and gamma heat in the reactor raised the temperature of the miniature fuel elements sufficiently high to melt the UO_2 without the use of external heat. Data were obtained for fission product release from the fuel zone (fuel element and thoria holder) and from the high temperature zone (thoria and zirconia insulation) which had a minimum temperature of 1000 C. Although over twenty experiments were run most of the major results are contained in the summary of seven runs that are given in Table VII D-6. The first set of values (release from the fuel zone) show extensive release of iodine, tellurium, and cesium regardless of the type of atmosphere. The other fission products and the UO_2 fuel also experienced relatively large releases which were reduced somewhat in high steam concentration atmospheres. The second set of values in the table (release from the high temperature zone) are more useful to reactor accident analysis because they give a better indication of escape from a core region which is not entirely molten. These data are also more comparable with out-of-pile studies which often achieve incomplete melting and have steep thermal gradients in the sample region of the furnaces. The release data in Table VII D-6 can, in general, be divided into two groups, a group having high values and another group having low values. Iodine, tellurium, and cesium belong to the high group while ruthenium, strontium-barium, and zirconium - cerium belong to the low group. In Experiments 13 and 18 ruthenium release was exceptionally high which was probably due to the highly oxidizing nature of the atmosphere in the system. These observations are generally consistent with the results that have been obtained from the various out-of-pile melting studies. The in-pile experiments resulted in a number of other conclusions (Ref. 17) which are pertinent to reactor core meltdown analysis.

a. Stainless steel appears to retain ruthenium and, under oxidizing conditions, to lower the melting

point of the UO_2. However, retention of the ruthenium by oxidized stainless steel was not observed.

b. Fission product release showed only a weak, if any, correlation with a factor of 1,000 increase in fuel burnup.

c. Electron photomicrographs of particles collected on filters in the in-pile apparatus indicated the source consisted of sub-micron sized particles which were generally spherical in shape.

D3. SUMMARY AND CONCLUSIONS

The experimental work that has been done regarding fission product release from UO_2 during melting can be generally summarized as follows:

a. Nearly total release of the noble gases, iodine, cesium, tellurium should be expected within a few minutes from standard pellet-size masses of UO_2. The release of these species seems largely independent of whether oxidizing or reducing conditions exist during melting. Release of the four elements is unaffected by stainless steel cladding and only tellurium is influenced by Zircaloy cladding. Considerable retention of tellurium, probably through compound formation with zirconium, can occur but complete oxidation of the Zircaloy would be expected to liberate such reacted tellurium.

b. The release behavior of ruthenium can be quite complex because it forms volatile oxides. The degree of oxide formation appears quite sensitive to the oxygen activity in the system. The oxygen activity depends on both the gaseous atmosphere that exists and the other oxygen reactive materials that are present. Air, carbon dioxide, and also steam represent oxidizing atmospheres for ruthenium. However, zirconium (and Zircaloy) is a very effective oxygen getter. Consequently, the release of ruthenium from Zircaloy clad UO_2 in the above atmospheres should be expected to depend on the degree of cladding oxidation. If the cladding is completely oxidized, then excess air, CO_2, or steam would be available and fission product ruthenium should experience large release. If the Zircaloy is only partly oxidized, the oxygen activity would be low, ruthenium should remain in the metallic state and be expected to experience only small release. Since stainless steel is less reactive with oxygen, it should have less effect on oxygen activities than Zircaloy. However, evidence indicates that metallic ruthenium will partition into stainless steel from UO_2 and considerable oxidation of the stainless-steel may be necessary to cause release of the dissolved ruthenium.

c. The release behavior of strontium and barium should also depend on the oxygen activity in the system but not to the degree nor in the manner of ruthenium. Metallic strontium and barium are not very volatile and their oxides are even less volatile. Therefore, the higher releases of these fission products should occur under conditions of low oxygen activity, or, for clad UO_2, in situations where incomplete oxidation of the Zircaloy has left some free zirconium. The limited experimental data tend to confirm this behavior and indicate that even under very reducing conditions, the release of these elements will not reach high values. The data also show that stainless-steel has essentially no effect on strontium or barium release from UO_2. Thus, stainless steel is apparently not effective in reducing the oxygen activity far enough to cause conversion of the alkaline earth oxides to the respective metals. If these fission products exist as oxides then low release from molten UO_2 is to be expected.

d. The release of cerium (a rare earth) and fission product zirconium were found to be quite low in essentially all the melting experiments. These elements form very stable nonvolatile oxides and their release from UO_2 should be nearly insensitive to external atmosphere and chemical effects of cladding materials. The experimental results almost entirely support this conclusion.

References

1. Parker, G. W., et al., "Out-of-Pile Studies of Fission-Product Release from Overheated Reactor Fuels at ORNL, 1955-1965", ORNL-3981 (July, 1967), p. 92-102.

2. Bedford, R. G., and Jackson, D. D., "Volatilities of the Fission Product and Uranium Oxides", UCRL-12314 (January, 1965).

3. Gabelnick, S. D., and Chasanov, M. G., "A Calculational Approach to the Estimation of Fuel and Fission-Product Vapor Pressure and Oxidation States to 6000 K", ANL-7867 (October, 1972).

4. Genco, J. M., et al., "Fission-Product Deposition and Its Enhancement Under Reactor Accident Conditions: Deposition on Primary System Surfaces", BMI-1863 (March, 1969) p. 38-42.

5. Coughlin, J. P., "Contributions to the Data on Theoretical Metallurgy. XII Heats and Free Energies of Formation of Inorganic Oxides", U.S. Bureau of Mines Bulletin 542 (1954).

6. Parsly, L. F. and Row, T. H., "Study of Fission Products Released from Trace-Irradiated UO_2 into Steam-Air Atmospheres (Nuclear Safety Pilot Plant Runs 8 and 9)", ORNL-TM-1588 (May, 1966).

7. Parsly, L. F. and Row, T. H., "Behavior of Fission Products Released From Synthetic High Burnup UO_2 in Steam Atmospheres (Nuclear Safety Pilot Plant Runs 10-12)", ORNL-TM-1698 (February, 1967).

8. Parsly, L. F. and Row, T. H., "Behavior of Fission Products Released into a Steam-Air Atmosphere From Overheated UO_2 Previously Irradiated to 20,000 Mwd/T (Nuclear Safety Pilot Plant Run No. 14, Part I), ORNL-TM-1908 (September, 1967).

9. Parsly, L. F., et al., "Release and Transport of Fission Products Released From Fuel Pins Irradiated to 20,000 Mwd/T: Summary Report of NSPP Run 15", ORNL-TM-3533 (February, 1972).

10. Freeby, W. A., Lakey, L. T., and Black, D. E., "Fission Product Behavior Under Simulated Loss-of-Coolant Conditions in the Contamination-Decontamination Experiment", IN-1172 (January, 1969).

11. Collins, R. D., and Hillary, J. J., "Some Experiments Related to the Behavior or Gas-Borne Iodine", TRG-933 (W) (1967), p. 5.

12. Collins, R. D., Hillary, J. J., and Taylor, J. C., "Air Cleaning for Reactors With Vented Containment", TRG-1318 (W) (August, 1966), p. 18.

13. Cottrell, WM., B (prog. dir.), "Nuclear Safety Program Annual Progress Report for Period Ending December 31, 1966", ORNL-4071 (March, 1967), p. 76.

14. Browning, W. E., Jr., et al, "Release of Fission Products During In-Pile Melting of UO_2", Nucl. Sci. and Eng., 18, 151-162 (1964).

15. Cottrell, Wm. B. (prog. dir.), "Nuclear Safety Program Semiannual Progress Report for Period Ending June 30, 1964", ORNL-3691 (November, 1964), p. 32.

16. Cottrell, Wm. B. (prog. dir.), "Nuclear Safety Program Semiannual Progress Report for Period Ending December 31, 1964", ORNL-3776 (March, 1965) p. 113.

17. Cottrell, Wm. B. (prog. dir.) "Nuclear Safety Program Semiannual Progress Report for Period Ending June 30, 1965", ORNL-3843 (September, 1965), p. 37.

18. Fischer, J., Schilb, J. D., and Chasanov, M.G., Investigation of the Distribution of Fission Products Among Molten Fuel and Reactor Phases. (Part I - The Distribution of Fission Products Between Molten Iron and Molten Uranium Dioxide)", ANL-7864 (October, 1971).

TABLE VII D-I FISSION PRODUCT RELEASE FROM UO_2[(a)] MELTED IN IMPURE HELIUM[(b)]

Run No.	Sample Weight (g)	Time at Temp. (sec)	Percentage of Individual Fission Product Released							
			Rare Gases	I	Te	Cs	Ru	Sr	Ba	TRE[(c)]
1	0.57	120	64	71	60	59	28	0.18		
2	0.34	120	91	70	72	25	60	0.07	0.8	0.2
3	0.56	120	93	84	86	34	32	0.16	0.9	1.1
4	0.56	180	56	67	63	24	75	0.11	1.3	0.7
5	0.58	180	63	46	54	12	36	0.11	2.6	0.5
6	0.37	120	69	51	43	7.1	20	0.26	0.5	0.3
7	0.18	120	99.4	84	86	90	72	0.20	2.0	0.7
8	0.25	90	99.6	95	96	93	76	3.9	7.3	3.8

(a) Trace-irradiated pellet melted simultaneously with BeO support tube in arc-image furnace.

(b) Helium flow rate, 100 cc/min.

(c) Total rare earths.

TABLE VII D-2 FISSION PRODUCT RELEASE FROM UO_2[(a)] MELTED IN PURE HELIUM[(b)] BY THE TUNGSTEN-CRUCIBLE METHOD

Molten Time (min.)	Percent UO_2 Vaporized	Percentage of Individual Fission Product Released							
		Xe-Kr	I	Te	Cs	Ru	Sr	Ba	Ce
1.0	0.10	93	77	90	63	0.45	0.33	4.8	0.05
1.5	0.16	98	98	98	66	0.05	0.47	2.6	0.07
2.0	0.16	99	99	99	60	0.32	0.41	3.0	0.17
2.5	0.25	99	95	99	72	0.33	0.53	2.4	0.13
1.5[(c)]	-	99	88	92	80	0.20	0.26	2.6	0.40
2.5[(c)]	-	99	93	96	89	0.70	0.50	3.6	0.10

(a) Sample: 29g PWR UO_2 irradiated at tracer level and preheated in helium for 4.5 to 5.0 min.
(b) Atmosphere: purified helium flowing at a rate of 700 cc/min.
(c) UO_2 sample had a slightly higher density than the first four samples.

TABLE VII D-3 FISSION PRODUCT RELEASE[a] FROM TRACE-IRRADIATED PWR-TYPE UO_2 MELTED IN A SINGLE ELEMENT TUNGSTEN-RESISTOR FURNACE FILLED WITH HELIUM[b]

Element	Heat Duration (min.)	UO_2 Vaporized (%)	Percentage of Individual Fission Product Released							
			Xe-Kr	I	Te	Cs	Ru	Sr	Ba	Ce/RE
UO_2	5.0	0.8	63	47	56	44	1.6	1.6	5.3	0.6
UO_2	4.0	0.2	50	30	42	41	0.4	0.8	2.9	0.5
UO_2	4.4	0.3	34	25	33	40	0.05	1.2	4.3	0.5
UO_2 (SS clad)	4.7	0.2	56	52	31	46	0.5	1.0	4.2	0.3
UO_2 (Zr clad)	7.0	0.1	52	24	1.1	28	0.1	10.1	10.6	0.5
UO_2 (Zr clad)	6.7	0.04	41	50	0.6	32	0.2	10.0	7.5	0.5

(a) Results are not corrected for the fraction of the sample melted which is approximately equal to the percent rare gas release. Release is from fuel and cladding.

(b) Helium flow rate, 400 cc/min.

TABLE VII D-4 SUMMARY OF FISSION PRODUCT RELEASES OBSERVED IN NSPP UO_2 MELTING EXPERIMENTS

Expt. No.	Furnace Atmos.	Clad Mater.	Degree Melted	Percent Release From Fuel Mass								
				I	Te	Cs	Sr	Ba	Ru	Ce	Zr	U
8[a]	He-steam	SS	5%	9	2	6	0.1	1.0	0.3	0.1	0.01	0.1
9[a]	He-steam	SS	80%	61	30	29	0.1	0.3	16.0	0.7	0.1	1.0
10[b]	A-H_2	SS	70-80%	26	--	20	0.07	--	2.0	0.2	--	0.3
11[b]	Air	SS	70-80%	96	--	44	0.05	--	27.0	0.2	--	1.0
12[b]	A-H_2	SS	50%	74	32	85	--	2.0	0.9	0.5	--	2.0
14[c]	Steam	Zry-2	limited	10	--	6	0.9	64.0	0.4	0.3	--	--
15[c]	He-air	Zry-2	high	70	--	56	41.0	32.0	29.0	10.0	--	--
				Percent Transferred to MCV								
8	He-steam	SS	5%	2	0.3	0.1	0.02	0.2	0.02	0.02	--	0.01
9	He-steam	SS	80%	35	8.0	10.0	0.08	0.06	2.0	0.2	0.03	0.3
10	A-H_2	SS	70-80%	24	--	19.0	0.03	--	1.0	0.2	--	0.2
11	Air	SS	70-80%	84	--	26.0	0.02	--	12.0	0.008	--	0.6
12	A-H_2	SS	50%	9	3.0	4.0	--	0.02	0.09	0.05	--	0.02
14	Steam	Zry-2	limited	2	--	0.7	0.2	2.0	0.1	0.2	--	--
15	He-Air	Zry-2	high	27	--	42.0	14.0	12.0	0.4	1.0	--	--

(a) Clad UO_2 trace irradiated.
(b) Simulated high burnup UO_2-premixed.
(c) Irradiated to 20,000 Mwd/T.

TABLE VII D-5 FISSION PRODUCT RELEASE FROM HEATED ZIRCALOY-CLAD UO_2

Experiment	CDE	CMF[b]
Fuel Burnup (Mwd/T)	460-2000	7000
Fission Product Releases - Percent of Fuel Inventory		
Xe, Kr	86-90	
I[a]	15-44	91.0
Te	7-22	2.0
Cs	3-21	30.0
Sr	0.01-0.05	0.2
Ba	0.04-0.20	-
Mo	2-8	-
Ru	0.003-0.7	0.2
Zr-Nb	0.0001-0.1	

(a) Some British work at low burnup has been performed:

Reference	Burnup	Iodine Release,%
11	1-2	14-15
12	100	8-35

(b) See Reference 13.

TABLE VII D-6 RESULTS OF ORNL EXPERIMENTS ON FISSION-PRODUCT RELEASE DURING IN-PILE MELTING OF STAINLESS-STEEL CLAD UO_2

Expt. No.	Sweep Gas	UO_2 Melted, %	I	Te	Cs	Ru	Sr-Ba	Zr-Ce	UO_2
				Material Released from the Fuel Zone[b] - %					
4,5,9	Dry He	100	99+	99	99	78	77	65	48
13,18	Moist air[a]	100	98	97	95	38	33	28	27
16	87% steam 13% air	100	90	96	96	13	16	9	7
17	87% steam 12% He 1% H_2	100	95	90	89	21	19	5	3
				Material Released from the High Temperature Zone[c] - %					
4,5,9	Dry He	100	86	86	71	4	1.4	0.4	0.09
13,18	Moist air[a]	100	95	89	83	16	1.4	0.6	0.90
16	87% steam 13% air	100	67	92	42	0.8	0.8	0.1	0.2
17	86% steam 12% He 1% H_2	100	73	87	30	1.2	3.6	0.5	1.3

(a) The steam concentration in this atmosphere was low, corresponding to air saturated with water vapor at 23 C.

(b) Molten times lasted about 5 minutes.

(c) Minimum temperature, 1000 C.

Appendix E

An Evaluation of Fission Product and Fuel Constituent Release From Reactor Fuels Based on a Thermodynamic Analysis of the Compound Species Present in the Fuel

by

M. Pobereskin, C. Alexander and R. Ritzman
Battelle's Columbus Laboratories

E1. INTRODUCTION

Considerable research has been performed aimed at establishing the nature and amount of fission products released from the core of a light water nuclear reactor in event of a loss-of-coolant. Experimental and analytical approaches have both been attempted (Ref. 1). Generally speaking, the experiments have been on a laboratory scale, and require extensive interpretation to reflect real life conditions. Similarly, the analytical approaches have been predicted on existence of chemical species presumed from general knowledge of the chemistry of the element.

In this study, the evaluation of fission product behavior is based upon a thermodynamic analysis of the fission product and fuel species present in the fuel under pertinent conditions. This is made possible through the application of the EQUICA computer program to the analysis of the nature, amount, and state of the species at thermodynamic equilibrium.

EQUICA rapidly computes the composition of a given set of reaction species. It is especially versatile in its ability to accept input data which can incorporate thermal and entropy effects other than those of the tabulated values given in handbooks and the JANAF Tables.

EQUICA consists of a basis which may contain 20 species in which all elements present in the computation are present in either elemental or some combined form. An additional 40 species may be included in the computation. There are no other stipulations applied to the basis other than it can contain no more than 20 different elements. As a matter of fact, the program has provision for shifting the basis so that the species richest in a certain element would form the basis for that element in all species in which it appeared, and all equilibrium constants would be based on its equilibrium value in that particular composition. For instance, in a computation at very high temperature gaseous carbon may form the basis for carbon, under pyrolysis conditions elemental carbon may form the basis, and under combustion conditions carbon in carbon dioxide may form the basis for carbon. This ability to shift basis greatly improves the convergence for complex systems when the final composition differs markedly from the initial estimate. Unlike most thermochemical programs there is no limit on the number of solids in either the basis or nonbasis sets, and one can have the same chemical substance present as both a gas or vapor and a condensed phase or as a component in a solution. Under these conditions EQUICA will correctly determine the saturation vapor pressure of the vapor species. EQUICA will also allow for the vanishing of a condensed phase if it is established thermodynamically that the phase should not exist. This is in keeping with the phase rule and ensures that the proper degrees of freedom are maintained.

The program utilizes a composition matrix made up of N molecular species comprised of S chemical elements. A composition matrix relates the species to the elements. If one considers then that the composition N_i of the I^{th} species be changed by $\Delta\xi$, then to preserve stoichiometry the following changes in the composition of the basis are needed:

$$N_i^1 = N_i + \Delta\xi.$$

It is possible that for some minor species N_i^1 could go negative, and since N_i enters the program for the form of ($\ln N_i$), then this relation becomes undefined as $N_i \to 0$. For this reason a subroutine FUDGE has been written and

incorporated to determine if the current $\Delta\xi$ produces non-positive N_i values. If it is found that negative compositions exist then the subroutine computes a new $\Delta\xi$ value which allows all N_i's to remain constant. The input data include initial estimates of composition and Gibbs free energies of all species at the desired temperature and pressure. The output consists of the following:

a. The equilibrium compositions of all species.

b. The equilibrium constants of all species. (Although equilibrium constants for the basis species are not defined, the program sets their value to one. Thus a one in the equilibrium constant column indicates that this species currently is a basis species.)

c. A defined by $A = \frac{P}{\sum_{i}^{n} \gamma_i N_i}$

This A value is then related to the volume the gaseous products would occupy at pressure P and temperature T.

d. The convergence vector, C, which defines the extent of convergence of all major and minor species.

e. Partial pressure for each species.

f. Total pressure (sum of partial pressures).

E2. ANALYSIS FOR TEMPERATURES BELOW FUEL MELTING

In the present analysis, it was necessary, of course, to include uranium, oxygen, zirconium, hydrogen, and helium among the element inputs to the program. This left room in the program for fifteen elements to be selected from the major fission products. It was found that selecting these elements was not as limiting as was the condition that only 60 compound species could be considered. In addition to the elements listed above, Cs, Ba, La, Sm, Mo, Ru, Te, I, Br, and Sr were included in the analysis. This choice of elements was based not only on abundance in fission yield and representation of the major chemical groups, but also on uniqueness of thermochemical properties. For example, the lanthanum oxide would satisfactorily represent the sesquioxides except that elemental samarium was considered to be sufficiently volatile that in the first analysis samarium needed to be considered apart from the other rare earths.

Two computer runs were made based on approximate preaccident and postaccident conditions. The initial run was designed to provide some prediction of the chemical species that could exist in fuel rods just before the accident, and to indicate fission product volatility as a function of temperature for periods after this. The effect of several parameters was examined.

a. Fuel burnup - 1 and 4 percent were used to produce variations in fission product concentration.

b. Temperature - equilibrium calculations were made for 800, 1300, 1900, and 2500K, corresponding roughly to temperature regions in operating fuel rods and to accident temperatures for an overheating reactor core.

c. Pressure - 1000 and 2000 psia were used to simulate internal rod pressures.

d. Steam concentration - 30 ppm water in the fuel and unlimited steam supply were used to simulate normal conditions and more oxidizing conditions for the fuel-fission product-cladding system.

Elemental compositions were predicted on a nominal fuel rod containing 10 pounds of UO_2 and 2 pounds of zirconium. Solution effects of oxides in the parent fuel were not included because, for the most part, the oxides have very limited solid solubility in UO_2.

The results of the parametric analysis to 2500K are summarized in Tables VII E-1 through VII E-4, which for each temperature give the predicted dominant condensed phase and vapor phase forms and the approximate mole ratio of material in the vapor phase to material in the condensed phase. This ratio indicates the volatility of the fission product species. Several conclusions were drawn from the data.

a. The degree of burnup and the total pressure had negligible effects on the results.

b. The volatility of some species (generally Ba, La, Sm, Zr, and Sr) is depressed by excess steam (more oxidizing conditions) with the effect more evident at lower temperatures.

c. The volatility of some species is enhanced by excess steam - Ru and U at higher temperatures and Te, I, Br, and Cs at lower temperatures.

d. The most volatile fission product species are Cs, Te, and CsI. At higher temperatures, particularly under more reducing conditions, Ba and Sr begin to approach the above three in volatility.

Generally speaking, the results confirmed what one might have predicted from a general knowledge of the chemistry of the involved elements. An exception was the indication that iodine and bromine react with the excess cesium in the fuel. In the subsequent runs, with HI as a species in the matrix, the CsI was still the indicated major iodine carrying species, even at temperatures to 3100K. Furthermore, CsI will not oxidize in air to Cs_2O and I_2 nor in water vapor to $Cs_2O + 2HI$. Therefore, based on these calculations it appears that CsI may be present in the released fission product vapors. It should be noted though that no experimental confirmation of this prediction is available, and other reactions that cesium might undergo could alter the conclusion.

E3. ANALYSIS FOR MOLTEN FUEL

In this computer run, several new species were introduced; e.g., stainless steel constituents Fe, Cr, Ni (and their oxides), and Zr(g), Mo(g), Ru(g), and HI(g). To make room for these species a number of the nonreactive species from the first run were dropped from the matrix. Conditions were fixed at 3100K, 1000 psia, 1 percent burnup, and unlimited water. For this run the free energies were adjusted and the oxides were considered to form an ideal solution.

The results of the run showed that the Fe, Cr, Ni compound species did not affect the reaction patterns established in the systems at temperatures to 2500K. The overall situation with excess water present was quite oxidizing in that the partial pressure of UO_3 was more than two orders of magnitude greater than UO_2 in all cases.

The data were used to calculate volatilization rates utilizing the Knudsen-Mayer equation:

$$Z = 44\ P\sqrt{M/T} \qquad \text{(VII E-1)}$$

where Z is the volatilization rate in grams per second per square centimeter, P is the vapor pressure in atmospheres, M the molecular weight, and T is the temperature in degrees Kelvin. Although this relationship holds for molecular flow in vacuum, Fonda (Ref. 2) has indicated that in the presence of an inert cover gas, the same relationship applies but the rate is effectively reduced by a factor of 1/80 to 1/100. For practical purposes, at temperatures near 3000K, one may utilize the relation:

$$Z \sim 0.01\ P\sqrt{M}\ \text{g/sec/cm}^2 \qquad \text{(VII E-2)}$$

as long as the rate-controlling step of diffusion through a boundary layer film Equation (VII E-2) is expected to be applicable. Under conditions tending to be more static, the evolution rate would be even lower. Thus Equation (VII E-2) may be considered as an upper limit for vaporization loss. Equation (VII E-2) appears to be only a slowly changing function of pressure at atmospheric pressure or greater. Thus at pressures as high as 50 psia Equation (VII E-2) should closely approximate actual release conditions.

The vapor species expected to be released and the maximum-volatilization rates obtained for the molten fuel case are given in Table VII E-5.

It is assumed that convective forces are operative in the gas phase which will lift the volatiles along with the gaseous currents and these species will be entrained in the gas at least until the species are contacted by a surface where they may condense. They could be carried as aerosol particles however.

These results indicate that uranium is about as volatile as anything else and its volatilization should assist the loss of volatile fission products from the receding surface. Care must be used in attempting to extrapolate the volatilization rates to any real core meltdown situation. The values given in Table VII E-5 should be considered only indicative of the relative volatility of the different species under the precise conditions selected for the calculation; i.e., excess water and 3100K. In this context the data show the potential volatile nature of species in molten UO_2--even some species which are normally considered refractory.

E4. CONCLUSIONS

In order to provide a basis for evaluating the dynamics of release, an analysis

was made of the degree of volatilization of the fission product species as a function of temperature. These data are summarized in Tables VII E-1 to VII E-4. Assuming cladding rupture at 800 K, three major phases in the release process are recognized. These are identified below and estimates of release magnitudes are provided.

a. Release at Time of Rupture

Cs - Several percent of inventory

Te - Less than 1 percent of inventory

I_2 - Less than 1 percent of inventory

b. Release During Heat-up to Melting

Cs - remainder, mostly as Cs vapor (early in period)

Te - remainder as Te vapor (early in period)

I - remainder, as CsI vapor (later in period)

Ba - a large percent as Ba or BaO vapor

Sr - a few percent as Sr vapor

c. Release from Molten Fuel

Ru - potential for rapid release as RuO_3

Sr - potential for rapid release as Sr

Mo - potential for rapid release as MoO_3

La - potential for slow release as LaO

Zr - potential for very slow release as ZrO_2

U - potential for rapid vaporization as UO_3

Certainly, the release characteristics of the fission products indicated above are restricted to the thermodynamic systems, components, and conditions that were analyzed. Kinetic limitations and an exhaustive treatment of all potential compound species could not be included. Nevertheless the predictions in many cases tend to agree with other methods used to estimate fission product releases. Exceptions appear to be tellurium and iodine release during fuel heatup to melting, but here possible tellurium reaction with the cladding was not included and cesium iodide stability was considered only with respect to formation of cesium oxide or formation of hydrogen iodide. The results indicated for molten fuel are based on a rather extreme condition; i.e., pure molten fuel in equilibrium with excess water. In fact fuel will probably be diluted with lower melting oxides of structural materials, the mass is likely to be non-isothermal, and the availability of water should be limited. Consequently, the releases from molten fuel have only a potential for occurring and acutally represent upper limit predictions at this time. Considerable experimental work is needed in the area of core meltdown and materials interactions before much improved projections of fission product escape can be made. Thermodynamic analyses such as these are very useful in revealing the important problems which require investigation.

References

1. Morrison, D. L., et al., "An Evaluation of the Applicability of Existing Data to the Analytical Description of a Nuclear Reactor Accident", BMI-1779 (August, 1966).

2. Fonda, G. R., "Evaporation of Tungsten Under Various Pressures of Argon", Phys. Rev., 31, 260 (1928).

TABLE VII E-1 RESULTS OF THERMODYNAMIC ANALYSIS AT T = 800 K

Fission Product	Dominant Condensed Form	Dominant Vapor Form	Approximate Composition Ratio Vapor/Condensed
	Limited Steam		
Cs	Cs	Cs	2×10^{-2}
Ba	Ba	Ba	2×10^{-9}
La	La_2O_3	LaO	1×10^{-25}
Sm	Sm_2O_3	Sm	1×10^{-14}
Zr	Zr	N.C.	-
Mo	MoO_2	N.C.	-
Ru	Ru	N.C.	-
Te	Te	Te	7×10^{-4}
I	CsI	I_2	1×10^{-3}
Br	CsBr	Br_2	1×10^{-3}
Sr	SrO	Sr	4×10^{-8}
U	UO_2	N.C.	-
	Unlimited Steam		
Cs	Cs	Cs	5×10^{-1}
Ba	BaO	BaO	1×10^{-20}
La	La_2O_3	N.C.	-
Sm	Sm_2O_3	N.C.	-
Zr	ZrO_2	N.C.	-
Mo	N.C.	N.C.	-
Ru	Ru	N.C.	-
Te	Te	Te	1×10^{-2}
I	CsI	CsI	1×10^{-3}
Br	CsBr	CsBr	5×10^{-3}
Sr	SrO	Sr	3×10^{-23}
U	UO_2	N.C.	-

N.C. = Not certain because convergence not achieved in the iteration limit.

TABLE VII E-2 RESULTS OF THERMODYNAMIC ANALYSIS AT T = 1300 K

Fission Product	Dominant Condensed Form	Dominant Vapor Form	Approximate Composition Ratio Vapor/Condensed
	Limited Steam		
Cs	Cs_2O	Cs	1×10^{5}
Ba	Ba	Ba	2×10^{-5}
La	La_2O_3	LaO	2×10^{-13}
Sm	Sm_2O_3	Sm	2×10^{-7}
Zr	Zr	ZrO	1×10^{-18}
Mo	MoO_2	N.C.	-
Ru	Ru	N.C.	-
Te	Te	Te	4×10^{0}
I	CsI	CsI	3×10^{-2}
Br	CsBr	CsBr	2×10^{-1}
Sr	SrO	Sr	5×10^{-5}
U	UO_2	UO	5×10^{-17}
	Unlimited Steam		
Cs	CS_2O	Cs	1×10^{5}
Ba	BaO	BaO	1×10^{-9}
La	La_2O_3	LaO	1×10^{-16}
Sm	Sm_2O_3	Sm	2×10^{-19}
Zr	ZrO_2	ZrO_2	1×10^{-23}
Mo	N.C.	N.C.	-
Ru	Ru	RuO_3	1×10^{-27}
Te	TeO_2	Te	3×10^{4}
I	CsI	CsI	7×10^{-1}
Br	CsBr	CsBr	4×10^{3}
Sr	SrO	Sr	1×10^{-11}
U	UO_2	UO_2	1×10^{-17}

N.C. = Not certain because convergence not achieved in the iteration limit.

TABLE VII E-3 RESULTS OF THERMODYNAMIC ANALYSIS AT T = 1900 K

Fission Product	Dominant Condensed Form	Dominant Vapor Form	Approximate Composition Ratio Vapor/Condensed
	Limited Steam		
Cs	None	Cs	$>1 \times 10^{8}$
Ba	Ba	Ba	2×10^{-3}
La	La_2O_3	LaO	2×10^{-7}
Sm	Sm_2O_3	Sm	7×10^{-4}
Zr	Zr	ZrO	4×10^{-11}
Mo	N.C.	N.C.	-
Ru	Ru	RuO_3	2×10^{-33}
Te	TeO_2	Te	3×10^{4}
I	CsI	CsI	$>8 \times 10^{3}$
Br	CsBr	CsBr	$>4 \times 10^{3}$
Sr	SrO	Sr	7×10^{-2}
U	UO_2	UO	1×10^{-10}
	Unlimited Steam		
Cs	None	Cs	$>1 \times 10^{8}$
Ba	BaO	BaO	2×10^{-4}
La	La_2O_3	LaO	7×10^{-9}
Sm	Sm_2O_3	Sm	2×10^{-9}
Zr	ZrO_2	ZrO_2	1×10^{-13}
Mo	N.C.	N.C.	-
Ru	Ru	RuO_3	1×10^{-16}
Te	None	Te	$>2 \times 10^{7}$
I	CsI	CsI	$>8 \times 10^{3}$
Br	CsBr	CsBr	$>4 \times 10^{3}$
Sr	SrO	Sr	5×10^{-6}
U	UO_2	UO_3	2×10^{-9}

N.C. = Not certain because convergence not achieved in the iteration limit.

TABLE VII E-4 RESULTS OF THERMODYNAMIC ANALYSIS AT T = 2500 K

Fission Product	Dominant Condensed Form	Dominant Vapor Form	Approximate Composition Ratio Vapor/Condensed
	Limited Steam		
Cs	None	Cs	$>1 \times 10^{8}$
Ba	Ba	Ba	3×10^{-2}
La	La_2O_3	LaO	3×10^{-4}
Sm	Sm_2O_3	Sm	3×10^{-3}
Zr	Zr	ZrO	3×10^{-7}
Mo	N.C.	N.C.	-
Ru	Ru	RuO_3	2×10^{-23}
Te	None	Te	$>2 \times 10^{7}$
I	CsI	CsI	$>8 \times 10^{3}$
Br	CsBr	CsBr	$>4 \times 10^{3}$
Sr	SrO	Sr	3×10^{4}
U	UO_2	UO	2×10^{-7}
	Unlimited Steam		
Cs	None	Cs	$>1 \times 10^{8}$
Ba	BaO	BaO	8×10^{-2}
La	La_2O_3	LaO	1×10^{-4}
Sm	Sm_2O_3	Sm	7×10^{-7}
Zr	ZrO_2	ZrO_2	1×10^{-8}
Mo	N.C.	N.C.	-
Ru	Ru	RuO_3	6×10^{-13}
Te	None	Te	$>2 \times 10^{7}$
I	CsI	CsI	7×10^{3}
Br	CsBr	CsBr	3×10^{3}
Sr	SrO	Sr	1×10^{-2}
U	UO_2	UO_2	1×10^{-6}

N.C. = Not certain because convergence not achieved in the iteration limit.

TABLE VII E-5 VAPOR SPECIES AND MAXIMUM VOLATILIZATION RATE ESTIMATES, T = 3100K

Species	Equilibrium Vapor Fraction	Equilibrium Partial Pressure, atm	Limiting Volatilization Rate, $g/cm^2/sec$
Cs	1.0	-	(a)
BaO	1.0	-	(a)
Te, TeO	1.0	-	(a)
CsI	1.0	-	(a)
RuO_3	0.47	1×10^{-2}	1×10^{-3}
Sr	0.034	8×10^{-4}	8×10^{-5}
MoO_3	0.024	1×10^{-3}	1×10^{-4}
LaO	0.017	8×10^{-5}	1×10^{-5}
ZrO_2	0.009	2×10^{-6}	2×10^{-7}
UO_3	0.51	7	~1

(a) These are too highly volatile to estimate rates. No condensed phase exists at 3100 K.

Appendix F

Summary of Data on Fission Product Release From UO_2 During Oxidation in Air

by

R. L. Ritzman

Battelle's Columbus Laboratories

and

G. W. Parker

Oak Ridge National Laboratory

When uranium dioxide is heated in air at temperatures below about 1550 C, the UO_2 is oxidized to U_3O_8 with an accompanying expansion of the solid lattice (Ref. 1). The U_3O_8 surface layer cracks upon accumulation of sufficient stress and exposes the underlying UO_2 to continued oxidation (Ref. 2). The oxidation reaction is exothermic and ignition or burning of UO_2 has been observed (Ref. 3). These conditions--increased surface area, phase change with lattice expansion, and elevated temperatures--are conductive to fission product release during the oxidation process. Parker et al.(Ref. 2) first studied release from trace-irradiated PWR-type UO_2 pellets of 94 percent theoretical density and later (Ref. 4) from the same type of fuel irradiated to different levels of burnup to a maximum of 7000 Mwd/T. Approximately one-gram samples were heated for different periods in air flowing at 100 cc/minute at temperatures ranging from 500 C to 1400 C.

The pertinent fission product release data that were obtained in these series of experiments at ORNL are summarized in Fig. VII F-1 and in Tables VII F-1, VII F-2, and VII F-3. Release values determined with specimens irradiated at trace level ($\sim$1 Mwd/T) are plotted in Fig. VII F-1. Results show that release is not a simple function of temperature, but above 900 C releases tend to increase with temperature.

The effect of varying the heating time at different temperatures is shown in Tables VII F-2 and VII F-3. Specimens employed to obtain these data were PWR-type material with a density of 93 to 94 percent of theoretical, irradiated to a burnup of 1000 Mwd/T and 4000 Mwd/T, respectively. Increasing exposure time in air in the range investigated seemed to have no significant effct on fission-product release below 800 C, but at this temperature and above, increasing release of some isotopes with increasing exposure was observed.

The effect of burnup on oxidation release of the more volatile fission products is shown graphically in Fig. VII F-2 for two temperatures. The largest effect in the case of iodine and ruthenium came in the first 1000 Mwd/T of burnup and this was also true of the rare gases at 1200 C. The release of tellurium appeared to increase more or less regularly with increasing burnup in the range tested. The release of cesium, even at 1200 C, was too low to establish an unequivocal correlation but the results obtained indicate a slight increase in release with increasing burnup.

The outstanding feature of these results, particularly at the higher temperatures, is the high release of rare gases, iodine, ruthenium, and tellurium. Tellurium release is not quite as large as the other three but still much greater than cesium, strontium, or barium. Ruthenium release is probably largely due to formation of a volatile oxide. Tellurium oxide is also reasonably volatile at the higher temperatures. The very low releases of cesium, strontium, and barium are indicative of the lower volatility of their oxides. In general, the results also indicate that only a few minutes exposure to air at temperatures of 1200 C or above would be necessary to cause large releases of rare gas, iodine, ruthenium, and tellurium fission products.

References

1. Belle, J., Editor, Uranium Dioxide: Properties and Nuclear Applications, USAEC, 1961, Chapter 8.

2. Parker, G. W., G. E. Creek, and W. J. Martin in "Chemistry Division Annual Progress Report for Period Ending June 30, 1961", ORNL-3176 (Sept 1961), p 68.

3. Leitnaker, J. M., M. L. Smith, and C. M. Fitzpatrick, "Conversion of Uranium Nitrate to Ceramic Grade Oxide for the Light Water Breeder Reactor: Process Development", ORNL-4755 (April 1972).

4. Parker, G. W., et al., in "Nuclear Safety Program Semiannual Progress Report for Period Ending June 30, 1962", ORNL-3319 (Aug 1962), p 11.

TABLE VII F-1 FISSION PRODUCT RELEASE FROM UO_2 OXIDIZED IN AIR
Sample: Intermediate density PWR UO_2 (93-94%)
Irradiation: 1000 Mwd/ton
Air flow: 100 cc/min

Temp (C)	Time at Temperature (min)		Percentage of Individual Fission Products Released							
	He	Air	Rare Gases	I	Te	Cs	Ru	Sr	Ba	U
500		9	4.4	4.6	<0.014	0.02	0.013	<0.001	<0.0009	
	15.0	13	4.0	2.5	<0.003	<0.0008	<0.014	<0.004	<0.001	
	15.0	90	4.0	4.7	0.008	<0.002	0.36	<0.004	<0.0008	
600		11	6.6	3.4	0.003	0.004	0.33	0.003		
	15.0	13	6.0	5.6	<0.003	<0.0007	<0.23	<0.001	0.0009	
	12.0	90	5.5	6.0	0.005	0.003	0.9	<0.0009	<0.0009	
700		12	8.5	9.4	0.01	0.001	0.63	0.001		
	15.0	12	7.2	10.1	<0.003	<0.003	1.25	<0.0009	<0.001	
	13.0	90	8.3	10.0	<0.003	0.02	3.8	<0.0008	<0.0007	
800		15	10.5	9.1	0.05	0.016	5.2	0.0006		
	13.0	14	8.56	11.2	0.033	0.038	6.6	0.008	0.0006	
	13.5	90	15.1	14.1	0.08	<0.007	35.3	<0.001	0.002	
900		15	11.2	15.2	<0.4	0.005	18.9	<0.001		
	10.0	14	11.9	14.4	<0.85	0.03	11.5	<0.002	<0.01	
	12.5	90	13.7	26.9	0.41	<0.002	30.3	<0.001	<0.0015	
1000		26	30.3	55.2	<7.7	0.07	81.5	<0.001	<0.007	
	10.0	18	22.2	42.2	<0.6	~0.03	69.8	<0.001	0.002	0.007
	12.0	90	30.5	73.3	31.3	0.02	97.9	0.002	0.005	<0.0012
1100	8.0	10	60.0	70.4	75.3	2.8	85.7	<0.001	<0.002	0.002
	12.5	11	49.9	64.1	28.0	<0.01	95.5	0.001	<0.016	
	12.5	90	52.7	71.2	58.0	<0.4	99.9	<0.2	<0.2	0.19
1200	17.0	15	79.6	86.6	59.4	<0.1	97.8	<0.03	0.1	
	14.5	90	77.0	83.4	75.9	4.5	99.7	0.14	0.14	0.142

TABLE VII F-2 FISSION-PRODUCT RELEASE FROM PWR-TYPE UO_2 [(a)] Irradiated to 4000 Mwd/T and Heated in Air [(b)]

Temp (c)	Time at Temperature (min.) He	Air	Percentage of Individual Fission Products Released: Rare Gases	I	Te	Cs	Ru	Sr	Ba	U
500	16.0	23.0	1.5	3.6	<0.007	<0.0004	<0.005	<0.0004		
	18.0	90.0	2.9	3.2	<0.01	<0.0007	<0.01	<0.0004	<0.0008	
600	14.0	18.0	4.4	10.0	<0.006	0.002	0.08	<0.001		
	15.0	90.0	4.5	8.0	8.4	<0.001	1.8	<0.001	<0.004	
700	14.0	12.0	9.3	9.6	0.01	0.001	1.7	<0.0002	<0.0004	
	13.5	15.0	7.0	10.0	0.004	<0.001	0.4	<0.0003	<0.0006	
	14.0	90.0	6.8	6.5	<0.05	<0.0005	2.3	<0.0004	<0.002	
800	13.0	15.0	14.0	7.1	0.007	0.015	1.0	<0.0004	<0.0007	
	14.0	90.0	14.0	16.0	<0.06	<0.01	12.0	<0.0004	<0.001	
900	14.0	19.0	21.0	49.0	0.4	0.001	17.0	<0.001	0.01	
	15.0	90.0	22.0	47.0	6.0	0.015	53.0	<0.0008	<0.004	
1000	16.0	15.0	40.0	84.0	12.0	0.09	72.0	<0.003	<0.02	
	13.5	90.0	44.0	75.0	32.0	0.37	92.0	0.1	0.08	0.06
1100	14.0	14.0	66.0	79.0	16.0	<0.02	91.0	<0.05	<0.003	
	14.0	90.0	73.0	84.0	39.0	0.2	99.0	0.006	0.01	<0.003
1200	14.0	16.5	71.0	82.0	37.0	0.8	99.0	<0.01	<0.001	
	13.0	90.0	80.0	95.0	66.0	6.4	99.6	0.007	0.7	<0.003

(a) Sample approximately 1g of intermediate density (93 to 94 percent) material in porous alundum cups.

(b) Air flow, 100 cc/min.

TABLE VII F-3 FISSION-PRODUCT RELEASE FROM PWR-TYPE UO_2 [(a)] Irradiated to 7000 Mwd/T and Heated in Air [(b)] for 90 Minutes

Temp (C)	Percent of Individual Fission Products Released: Rare Gases	I	Te	Cs	Ru	Sr	Ba
500	3.1	4.1	<0.5	0.0006	0.1	<0.0007	<0.0004
600	4.2	3.1	<0.1	<0.002	0.7	<0.0004	<0.009
700	6.1	15.0	<0.08	<0.005	0.1	<0.0005	<0.007
800	9.4	9.0	<0.3	0.002	9.8	<0.0005	0.03
850	15.0	34.0	1.4	0.02	35.0	<0.005	<0.08
900	34.0	29.0	80.0	<0.01	78.0	<0.03	<0.08
1000	86.0	78.0	37.0	<0.03	93.0	<0.04	<0.3

(a) Samples 0.5 to 0.9 g of 96 percent density material in porous alundum cups, preheated for 13 to 16 minutes in helium.

(b) Air flow, 100 cc/min.

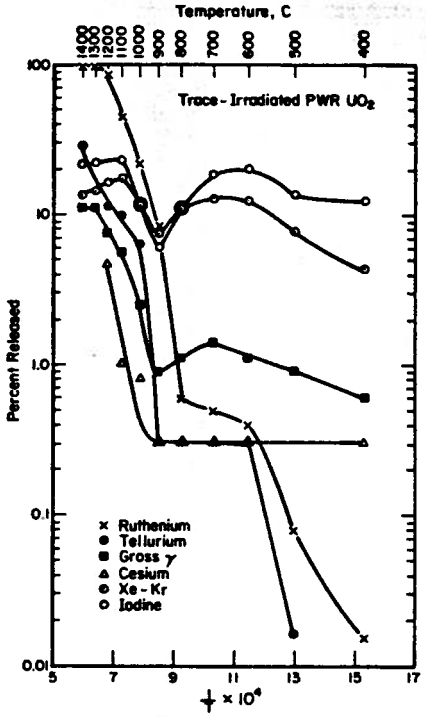

FIGURE VII F-1 Fission Product Release by the Oxidation of UO_2 to U_3O_8 in Air, Showing Discontinuity between 600 and 900 C

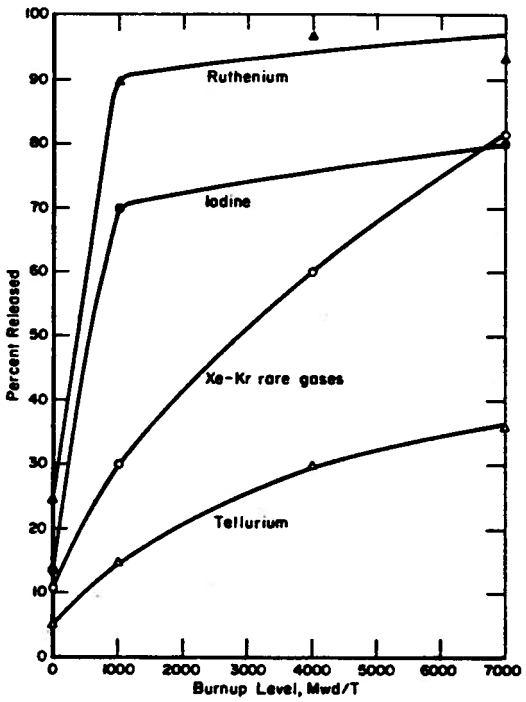

FIGURE VII F-2 Effect of Burnup on Fission-Product Release by Oxidation at 100 and 1200 C

Appendix G

Estimations of Fission Product Release From Melt During Concrete Penetration

by

L. F. Parsly, Jr., and M. H. Fontana
Oak Ridge National Laboratory

Conditions are created which could promote fission product release from the molten core material during its penetration of the containment concrete base. Carbon dioxide generated from decomposition of limestone aggregate, and steam liberated from solid hydrates or included water, may pass through the melt producing a gas sparging effect. Analyses performed in the core meltdown task indicate that high-gas generation rates would occur during the first half-hour after the molten core contacts the concrete base. Subsequently, the gas generation rates should decrease as concrete penetration slows, but the cumulative gas generation during this period would exceed that of the early period. In order to obtain an estimate of the effectiveness of this process in promoting fission product release, simple volatilization calculations were performed.

RELEASE DURING GAS SPARGING

The assumption was made that concrete would be decomposed and that a significant decomposition product would be CO_2. The CO_2 at 3000 K and 1 atm pressure was assumed to bubble through the molten core, and it was assumed that equilibrium distribution of fission products between the melt and the gas bubbles would be established. Distribution coefficients for the fission products between the melt and the CO_2 were calculated from the data given in Gabelnick and Chassnov (Ref. 1) for 3000 K, 5 percent burnup and 5 g/cc smear density. These were assumed to be independent of concentration. Based on the assumed equilibrium, a differential material balance can be written. From this we find that:

$$C = C_o \exp\left(-\frac{H V_G}{V_L}\right), \qquad \text{(VII G-1)}$$

where

C = final concentration

C_o = initial concentration

H = distribution coefficient = concentration in gas/concentration in liquid

V_G = volume of gas which has bubbled through the melt

V_L = volume of melt.

Thus, the fraction retained is

$$\frac{C}{C_o} = \exp\left(-\frac{H V_G}{V_L}\right) \qquad \text{(VII G-2)}$$

and the fraction removed is

$$\frac{C_o - C}{C_o} = 1 - \exp\left(-\frac{H V_G}{V_L}\right) \qquad \text{(VII G-3)}$$

The calculated distribution coefficients and the fraction removed values obtained from Equation (VII G-3) are given in Table VII G-1. The results are based on a melt volume (V_L) of 932 ft^3 and a total CO_2 volume (V_G) of 1.25×10^6 ft^3. This volume of CO_2 corresponds to decomposition of approximately 5.8×10^4 lb of concrete (Ref. 2). Complete decomposition of this mass may not occur and/or the generated CO_2 may partially bypass the melt. Thus, two columns of fraction removed values are given in Table VII G-1; one assuming only 20 percent of the total CO_2 volume sparges the melt and another which assumes 100 percent. The V_G/V_L values in Equation (VII G-3) applying to these two conditions are respectively 268 and 1340.

The results of these calculations indicate that the fission products can be grouped into four classes as follows:

a. Highly volatile - essentially completely removed by even limited sparging. These include Ag, Cd, Cs, In, I, Rb, Sb, Se, Sn, and Te.

b. Refractory - almost completely retained after sparging. These include Ce, Nb, Rh, and Zr.

c. Moderately volatile - extent of removal depends on amount of sparging. These include Eu, La, Mo, Nd, and Pd.

d. Uncertain - has one volatile and one non-volatile form. These include Ba, Gd, Pm, Pr, Ru, Sm, Sr, Tc, and Y. However, as noted in the table, the volatile form of each of these fission products is the minor species in the thermodynamic system analyzed. The sparging process would create highly oxidizing conditions. On this basis, Ba, Gd, Pm, Pr, Sm, Sr, and Y should exist as oxides and can legitimately be considered refractory. Under the same conditions Ru and Tc should form the volatile oxides but the presence of metallic iron in the real melt system would interfere. Therefore, only the volatility classification for these two fission products remains questionable.

It must be cautioned that the volatilization fractions listed in Table VII G-1 were obtained using a simple rate expression based on convenient assumptions regarding chemical and physical equilibrium. While very useful in developing the qualitative conclusions just presented, the data should not be considered a quantitative prediction of actual releases in a containment melt-through situation.

References

1. Gabelnick, S. D. and Chasanov, M. G., "A Calculational Approach to the Estimation of Fuel and Fission Product Vapor Pressures and Oxidation States to 6000 K", ANL-7867 (October, 1972).

2. Reimers, R. A., and Seidenfeld, A., "Investigation of the Consequences of a Nuclear Reactor Core Melt-through Accident, ORNL-MIT-62 (October, 1968).

TABLE VII G-1 REMOVAL OF FISSION PRODUCTS FROM MELT BY SPARGING WITH CO_2 FROM CONCRETE DECOMPOSITION

Fission Product	Distribution Coefficient[b]	Percent Sparge Gas Volume	
		20	100
		Fraction Removed from Melt	
Ag	3.26×10^{-2}	>0.999	>0.999
Ag_2O	1.62×10^{-1}	>0.999	>0.999
Ba[a]	9.35×10^{-2}	>0.999	>0.999
BaO	4.09×10^{-5}	0.01	0.045
Cd	4.93	>0.999	>0.999
CdO	3.45×10^{-2}	>0.999	>0.999
Ce	4.14×10^{-5}	0.01	0.045
Ce_2O_3	1.25×10^{-5}	<0.01	0.017
Cs	6.51×10^{-1}	>0.999	>0.999
Cs_2O	1.53	>0.999	>0.999
Eu	2.73×10^{-1}	>0.999	>0.999
Eu_2O_3	2.43×10^{-3}	0.48	0.96
Gd[a]	3.33×10^{-3}	0.59	>0.999
Gd_2O_3	5.68×10^{-6}	<0.01	<0.01
I		>0.999	>0.999
In	4.78×10^{-2}	>0.999	>0.999
In_2O_3	406.0	>0.999	>0.999
La[a]	2.00×10^{-4}	0.05	0.23
La_2O_3	3.67×10^{-5}	0.01	0.051
Mo	3.35×10^{-7}	<0.001	<0.001
MoO_2	1.21×10^{-4}	0.03	0.15
Nb	2.47×10^{-8}	<0.001	<0.001
NbO_2	2.92×10^{-6}	<0.001	<0.001
Nd[a]	9.65×10^{-4}	0.23	0.73
Nd_2O_3	1.27×10^{-4}	0.03	0.16
Pd	6.12×10^{-4}	0.15	0.56
PdO	3.80×10^{-4}	0.10	0.40
Pm[a]	8.84×10^{-3}	0.91	>0.999
Pm_2O_3	3.25×10^{-6}	<0.001	0.001
Pr[a]	1.03×10^{-3}	0.24	0.75
Pr_2O_3	1.38×10^{-5}	<0.01	0.02
Rb	7.53×10^{-1}	>0.999	>0.999
Rb_2O	4.08×10^{-1}	>0.999	>0.999
Rh	2.06×10^{-5}	<0.01	0.03
Rh_2O	7.93×10^{-6}	<0.01	0.01
Ru	1.11×10^{-5}	<0.01	0.02
RuO_2[a]	6.12×10^{-1}	>0.999	>0.999
Sb	4.40×10^{-2}	>0.999	>0.999
Sb_2O_3	8.80	>0.999	>0.999

TABLE VII G-1 (Continued)

Fission Product	Distribution Coefficient[b]	Percent Sparge Gas Volume	
		20	100
		Fraction Removed from Melt	
Se	4.49×10^{-1}	>0.999	>0.999
SeO_2	4.10	>0.999	>0.999
Sm[a]	3.24×10^{-1}	>0.999	>0.999
Sm_2O_3	5.45×10^{-5}	0.01	0.07
Sn	4.02×10^{-3}	0.66	0.995
SnO	3.62×10^{-2}	>0.999	>0.999
Sr[a]	2.45×10^{-1}	>0.999	>0.999
SrO	8.18×10^{-7}	<0.001	0.001
Tc	3.69×10^{-7}	<0.001	<0.001
TcO_2[a]	1.57×10^{-3}	0.34	0.88
Te	0.62×10^{-1}	>0.999	>0.999
TeO_2	3.40×10^{-1}	>0.999	>0.999
Y[a]	3.45×10^{-4}	0.056	0.384
Y_2O_3	1.77×10^{-5}	0.01	0.02
Zr	5.2×10^{-7}	<0.001	<0.001
ZrO_2	1.59×10^{-8}	<0.001	<0.001
UO_2	4.71×10^{-6}	0.001	0.006
PuO_2	2.64×10^{-7}	<0.001	<0.001

(a) Minor species

(b) Distribution coefficient = $\frac{\text{Concentration in gas}}{\text{Concentration in liquid}}$

Appendix I

Iodine Deposition in PWR and BWR Reactor Vessels and Associated Equipment

H. S. Rosenberg and D. K. Landstrom
Battelle's Columbus Laboratories

A model to predict the deposition of fission-product iodine on the internals and associated equipment of PWR and BWR reactors was developed and calculations were made as a function of temperature, concentration, gas flow rate, gas composition, and puff versus constant release rate. It can be shown that the amount of iodine deposited is independent of the release model and depends only on the steam boil-off rate (Q), the surface area available for deposition (A), and the overall deposition coefficient, (K_t). Further, it can be shown that the deposition of iodine is controlled by the wall deposition velocity (K_w), and for all cases of interest $K_t \doteq K_w$.

I1. CONSTANT RELEASE VERSUS PUFF RELEASE[1]

I1.1 CONSTANT RELEASE RATE

For a constant release over a time period, the concentration of iodine is given by the following equation:

$$C_g = \frac{W}{Q}\left[1 - e^{-(Q/V)t}\right] \qquad \text{(VII I-1)}$$

where, C_g = concentration of I_2 in gas, W = mass release rate of I_2, Q = volumetric flow rate, V = volume of chamber, and t = time period.

The amount of iodine deposited is given by:

$$M_d = \int_o^t C_g K_t A dt \qquad \text{(VII I-2)}$$

where, K_t = overall deposition coefficient, A = deposition area and C_g is as defined in Equation (VII I-1).

Inserting and integrating gives:

$$M_d = \frac{WK_tA}{Q}\left[t + \frac{V}{Q}\left(e^{-(Q/V)t} - 1\right)\right]. \qquad \text{(VII I-3)}$$

Now, by definition

$$W = M_o/t \qquad \text{(VII I-4)}$$

where M_o = the total mass of I_2, and since the product of Q and t is large compared to V, Equation (VII I-3) reduces to

$$M_d = M_o K_t A/Q \qquad \text{(VII I-5)}$$

I1.2 PUFF RELEASE

For the case of a puff release of a mass (M_o) of iodine into a chamber of volume V, the concentration is given by:

$$C_o = M_o/V \qquad \text{(VII I-6)}$$

Steam being produced at a rate (Q) removes iodine at a rate $C_g'Q$.

Therefore:

$$V\frac{dC_g'}{dt} = -C_g'Q \qquad \text{(VII I-7)}$$

and

$$\frac{dC_g'}{dt} = -QC_g'/V\ . \qquad \text{(VII I-8)}$$

Therefore:

$$C_g' = C_o e^{-Qt/V} \qquad \text{(VII I-9)}$$

where t is the deposition time.

The amount of iodine deposited is therefore:

---

[1] See Table VII I-5 for units and definitions of terms.

$$M_d = \int_o^t C'_g K_t A dt \qquad \text{(VII I-10)}$$

$$M_d = K_t A C_o \int_o^t e^{-Qt/V} dt \qquad \text{(VII I-11)}$$

$$M_d = \frac{-K_t A C_o V}{Q}\left[e^{-Qt/V} - 1\right] \qquad \text{(VII I-12)}$$

Since the product of Q and t is large with respect to V, this equation will reduce to:

$$M_d = K_t A C_o V/Q. \qquad \text{(VII I-13)}$$

Since from Equation (VII I-6) $C_o = M_o/V$, Equation (VII I-13) further reduces to

$$M_d = M_o K_t A/Q. \qquad \text{(VII I-14)}$$

Equation (VII I-14) is the same as Equation (VII I-5) for the constant release case so that M_d is independent of the release model and depends only on the steam boil-off rate (Q), the surface area available for deposition (A), and the overall deposition coefficient, K_t.

I2. DETERMINATION OF THE OVERALL DEPOSITION COEFFICIENT, K_t, AND CALCULATION OF DEPOSITION FRACTIONS

As will be described later, it was determined for both the PWR and BWR reactors that the deposition of iodine is essentially controlled by the wall deposition velocity, K_w, since the calculated value of the mass-transport coefficient, K_g is large with respect to K_w. The following relationship exists between the coefficients:

$$\frac{1}{K_t} = \frac{1}{K_g} + \frac{1}{K_w}. \qquad \text{(VII I-15)}$$

If K_g is large with respect to K_w, Equation (VII I-13) will reduce to a simple equivalent between K_t and K_w, i.e.:

$$K_t = K_w \qquad \text{(VII I-16)}$$

If the above is true then Equations (VII I-3) and (VII I-12) can be written as follows:

$$M_d = M_o K_w A/Q. \qquad \text{(VII I-17)}$$

I2.1 PWR REACTOR, UPPER INTERNALS

In order to prove the validity of using Equation (VII I-16) it was necessary to calculate values of K_g and compare them to previously determined values of K_w (Ref. 1). For the PWR reactor upper internals this was done by using the Chilton-Colburn analogy between heat and mass transfer to determine K_g, since an empirical equation is available to calculate the heat transfer coefficient, h_m, for fluid flowing normal to banks of staggered tubes. The heat transfer coefficient equation is (Ref. 2)

$$\frac{h_m D_o}{k_f} = 0.33 \left[\frac{C_p \mu}{k_f}\right]^{1/3} \left[\frac{D_o G_{max}}{\mu}\right]^{0.6}. \qquad \text{(VII I-18)}$$

where D_o = outside diameter of tubes, C_p = fluid heat capacity, μ = viscosity of fluid, k_f = thermal conductivity of fluid, G_{max} = mass velocity of fluid through minimum cross section.

Using the definitions of Chilton and Colburn (Ref. 3) for j_H and J_D:

$$j_H = \frac{h_m}{C_p \rho U_{ave}}\left[\frac{C_p \mu}{k_f}\right]^{2/3} \qquad \text{(VII I-19)}$$

$$j_D = \frac{K'_g P_{Bm}}{G_{max}}\left[\frac{\mu}{\rho D_v}\right]^{2/3} \qquad \text{(VII I-20)}$$

where h_m, C_p, μ, k_f, G_{max} are previously defined, K'_g = gas film coefficient P_{Bm} = logarithmic mean of the partial pressure, ρ = density, D_v = diffusivity of iodine in fluid, U_{ave} = mean fluid velocity.

Assuming $j_H = j_D$, adjusting the units of K'_g such that

$$Kg = \frac{K'_g U_{ave} P_{Bm}}{G_{max}},$$

defining

$$\frac{C_p \mu}{k_f} = \text{Prandtl Number} = N_{pr} \text{ and } \frac{\mu}{\rho D_v}$$

$$= \text{Schmidt Number} = N_{sc}, \text{ then}$$

$$\frac{h_m}{C_p \rho}\left[N_{pr}\right]^{2/3} = K_g \left[N_{sc}\right]^{2/3} \qquad \text{(VII I-21)}$$

Thus

$$K_g = \frac{h_m}{C_p \rho}\left[N_{pr}\right]^{2/3}\left[N_{sc}\right]^{-2/3} \qquad \text{(VII I-22)}$$

h_m is obtained from Equation (VII I-16) and the diffusivity term, D_v, in the Schmidt number is evaluated using the following equation (Ref. 4)

$$D_{12} = \frac{1.858 \times 10^{-3}\, T^{3/2}\left[\frac{m_1 + m_2}{m_1 m_2}\right]^{1/2}}{P\, G_{12}^{\,2}\, \Omega_D} \qquad \text{(VII I-23)}$$

where T = temperature (K), m_1 and m_2 are the molecular weights of the two components, G_{12} = Lennard-Jones force constant, and Ω_D = Collision integral for diffusion.

Values of G_{12} and Ω_D can be obtained from tables listed in Reference 4. Solving Equation (VII I-22) for K_g at various conditions produce the values listed in Table VII I-1, which also shows the values of K_w taken from Reference 1. Table VII 1-1 also shows the amount of iodine deposited (M_d) from Equation (VII I-17) and the fraction deposited $f_d = M_d/M_o$ for various conditions. All calculations assume an iodine mass release of 22 lbs (10kg), deposition surfaces of pre-filmed 304 stainless steel, the atmosphere in the pressure vessel is well-mixed, and steam boil-off rates of 12 lbs/sec (3×10^6 cc/sec) and 1.2 lbs/sec (3×10^5 cc/sec). The area available for deposition was estimated from scale drawings and is approximately 3000 sq ft. for PWR upper internals (see Table VII I-6). Calculations were performed for temperatures of 250 F, 500 F, 1000 F, and 2000 F. At the two higher temperatures, two iodine species, elemental iodine and hydrogen iodide, were considered along with different fluid compositions because iodine could conceivably react with hydrogen in the core region to form HI.

I2.2 PWR REACTOR, STEAM GENERATOR

For the deposition of iodine in the steam generator, Gilliland's Equation (VII I-7) which represents mass transfer inside wetted-wall columns was used to obtain j_D as follows:

$$j_D = 0.023\ (Re)^{-0.17}\ (N_{sc})^{0.11}, \qquad \text{(VII I-24)}$$

where

$$Re = \text{Reynolds Number} = \frac{4 R_H G_{max}}{\mu},$$

where

R_H = hydraulic radius

and N_{sc} is the Schmidt number as previously defined. Therefore combining Equations (VII I-20) and (VII I-21)

$$K'_g = \frac{0.023\ G_{max}}{P_{Bm}}(Re)^{-0.17}(N_{sc})^{-0.56}. \qquad \text{(VII I-25)}$$

By adjusting units to obtain K_g in ft/hr. we have:

$$K_g = \frac{0.023\ G_{max}}{\rho}(Re)^{-0.17}(N_{sc})^{-0.56}. \qquad \text{(VII I-26)}$$

Solving Equation (VII I-26) for K_g at various conditions produces the values listed in Table I-2. K_w is taken from Reference 1 and M_d was calculated using Equation (VII I-17). All calculations assume the same conditions used for the upper internal calculations except that the deposition area is approximately 51,500 sq. ft. Table VII I-2 also lists the M_d (total) and f_d (total) by summing the deposition from the reactor upper internals and the steam generators.

I2.3 BWR REACTOR, STEAM SEPARATORS

A procedure identical to that used to calculate deposition in a PWR steam generator was used to calculate the iodine deposition in the steam separators of a BWR. Gilliland's Equation (Ref. 5) was used with a suitable

modification of the Reynolds Number to the steam separator geometry. The same steam generation conditions as noted previously were used with a deposition area of approximately 9,850 sq. ft. Since the results were expected to be similar to the previous cases only the depositions at 500 and 1000 F were calculated. Table VII I-3 lists the values of K_g, K_w, K_t, M_d, and f_d for these conditions.

I2.4 BWR REACTOR STEAM DRYERS

A procedure similar to that used to calculate deposition in the BWR steam separators was used to calculate the iodine deposition in the steam dryers of a BWR. Gilliland's Equation (Ref. 5) was again used with a modification of the Reynolds Number to the steam dryer geometry. The same steam generating conditions as noted previously were used with a deposition area of 32,400 sq. ft. Again, deposition was calculated only at 500 and 1000 F. Table VII I-4 lists the values of K_g, K_w, K_t, M_d, F_d (total), and f_d (total) for these conditions.

I3. SUMMARY OF RESULTS

In all the cases examined for both the PWR and BWR primary systems, comparison of K_g and K_w values show that iodine deposition would be surface rate controlled even at relatively low bulk gas flows. The results in Table VII I-2 also show that minimal deposition of elemental iodine should be expected in the PWR primary system under LOCA conditions; that is, at temperatures above 500 F and at bulk steam generation rates in the range of 5 to 10 lb per second. In addition, considerably less than half the HI (if it should form) would be expected to deposit under these conditions either.

Deposition predictions for iodine in the upper regions of a BWR vessel (Tables VII I-3 and VII I-4) show results that are very similar to those obtained for the PWR cases. Therefore, primary system deposition should not cause significant retention of iodine during its transport to the containment region in either reactor system.

References

1. Genco, J. M., W. E. Berry, H. S. Rosenberg, D. L. Morrison, "Fission-Product Deposition and its Enhancement under Reactor Accident Conditions: Deposition on Primary-System Surfaces", BMI Report No. 1863 (March, 1969).

2. McAdams, W. H., Heat Transmission, McGraw Hill Book Co., pg. 272 (1954).

3. Sherwood, T. K., R. L. Pigford, "Absorption and Extraction", McGraw-Hill Book Co., Inc., pg. 61 (1952).

4. Reid, R. C., T. K. Sherwood, "The Properties of Gases and Liquids", McGraw Hill Book Co., Incl, pg 523 (1966).

5. Sherwood and Pigford, op. cit., p 78.

TABLE VII I-1 VALUES OF K_g, K_w, K_t, M_d AND f_d FOR VARIOUS CONDITIONS OF IODINE DEPOSITION

PWR UPPER INTERNALS[a]

Temperature F	Iodine Species	Fluid Composition	Steam Boil-off Rate lbs/sec	K_g ft/hr	K_w[b] ft/hr	K_t ft/hr	M_d lbs.	f_d
250	I_2	100% H_2O	12.0	339.0	0.354	0.354	6.13×10^{-2}	2.79×10^{-3}
250	I_2	100% H_2O	1.2	85.2	0.354	0.352	6.10×10^{-1}	2.77×10^{-2}
500	I_2	100% H_2O	12.0	233.7	0.0236	0.0236	4.09×10^{-3}	1.86×10^{-4}
500	I_2	100% H_2O	1.2	58.7	0.0236	0.0236	4.09×10^{-2}	1.86×10^{-3}
1000	I_2	100% H_2O	12.0	421.8	1.53×10^{-3}	1.53×10^{-3}	2.65×10^{-4}	1.20×10^{-5}
1000	I_2	100% H_2O	1.2	106.0	1.53×10^{-3}	1.53×10^{-3}	2.65×10^{-3}	1.20×10^{-4}
1000	HI	50% H_2O 50% H_2	12.0	906.7	0.590	0.590	0.102	4.64×10^{-3}
1000	HI	50% H_2	1.2	227.7	0.590	0.588	1.02	0.0463
2000	I_2	100% H_2O	12.0	844.8	2.01×10^{-4}	2.01×10^{-4}	3.48×10^{-5}	1.58×10^{-6}
2000	I_2	100% H_2O	1.2	212.1	2.01×10^{-4}	2.01×10^{-4}	3.48×10^{-4}	1.58×10^{-5}
2000	HI	50% H_2O 50% H_2	12.0	1807.7	0.354	0.354	6.13×10^{-2}	2.79×10^{-3}
2000	HI	50% H_2O 50% H_2	1.2	454.1	0.354	0.354	6.13×10^{-1}	2.79×10^{-2}

(a) Based on Deposition area of approximately 3000 sq. ft. - See Table VII I-6.
(b) Values obtained from Reference 1.

TABLE VII I-2 VALUES OF K_g, K_w, K_t, M_d, f_d, M_d (TOTAL) AND f_d FOR VARIOUS CONDITIONS OF IODINE DEPOSITION

PWR STEAM GENERATORS[a]

Temperature F	Iodine Species	Steam Boil-off Rate lbs/sec	K_g ft/hr	K_w[d] ft/hr	K_t ft/hr	M_d lbs	f_d	M_d Total lbs	f_d Total
250[b]	I_2	12.0	520.0	0.354	0.354	1.05	4.78×10^{-2}	1.11	0.051
250[b]	I_2	1.2	76.9	0.354	0.354	10.52	4.78×10^{-1}	1.09	0.51
500[b]	I_2	12.0	327.0	0.0236	0.0236	7.02×10^{-2}	3.19×10^{-3}	7.28×10^{-3}	3.38×10^{-3}
500[b]	I_2	1.2	48.4	0.0236	0.0236	7.02×10^{-1}	3.19×10^{-2}	0.0729	0.0338
1000[b]	I_2	12.0	545.0	1.53×10^{-3}	1.53×10^{-3}	4.55×10^{-3}	2.07×10^{-3}	4.82×10^{-3}	2.08×10^{-3}
1000[b]	I_2	1.2	80.6	1.53×10^{-3}	1.53×10^{-3}	4.55×10^{-2}	2.07×0.0^{-2}	0.023	0.021
1000[c]	HI	12.0	1142.0	0.590	0.590	1.754	7.97×10^{-2}	1.855	0.0843
1000[c]	HI	1.2	169.0	0.590	0.590	17.54	7.97×10^{-1}	18.55	0.844
2000[b]	I_2	12.0	972.0	2.01×10^{-4}	2.01×10^{-4}	5.98×10^{-4}	2.72×10^{-5}	6.33×10^{-4}	2.88×10^{-5}
2000[b]	I_2	1.2	143.0	2.01×10^{-4}	2.01×10^{-4}	5.98×10^{-3}	2.72×10^{-4}	6.33×10^{-3}	2.88×10^{-4}
2000[c]	HI	12.0	2057.0	0.354	0.354	1.05	4.77×10^{-2}	1.11	0.051
2000[c]	HI	1.2	304.0	0.354	0.354	10.52	4.77×10^{-1}	11.1	0.506

(a) Based on deposition area of approximately 51,500 sq. ft. - See Table VII I-6.
(b) Fluid composition, 100% H_2O.
(c) Fluid composition, 50% H_2O - 50% H_2.
(d) Values obtained from Reference 1.

TABLE VII I-3 VALUES OF K_g, K_w, K_t, M_d AND f_d FOR VARIOUS CONDITIONS OF IODINE DEPOSITION

BWR, STEAM SEPARATORS[a]

Temperature F	Iodine Species	Fluid Composition	Steam Boil-off Rate lbs/sec	K_g ft/hr	K_w[b] ft/hr	K_t ft/hr	M_d lbs.	f_d
500	I_2	100% H_2O	12.0	8.98	0.0236	0.0235	0.0134	6.90×10^{-4}
500	I_2	100% H_2O	1.2	1.33	0.0236	0.0232	0.133	6.02×10^{-3}
1000	I_2	100% H_2O	12.0	14.34	1.53×10^{-3}	1.53×10^{-3}	8.7×10^{-4}	3.96×10^{-5}
1000	I_2	100% H_2O	1.2	2.12	1.53×10^{-3}	1.53×10^{-3}	8.7×10^{-3}	3.96×10^{-4}

(a) Based on deposition area of approximately 9,850 sq. ft. - See Table VII I-7.
(b) Values obtained from Reference 1.

TABLE VII I-4 VALUES OF K_g, K_w, K_t, M_d, f_d, M_d (TOTAL) AND f_d TOTAL FOR VARIOUS CONDITIONS OF IODINE DEPOSITION

BWR, STEAM DRYERS[a]

Temperature F	Iodine Species	Steam Boil-off Rate lbs/sec	K_g ft/hr	K_w[c] ft/hr	K_t ft/hr	M_d lbs	f_d	M_d Total lbs	f_d Total
500[b]	I_2	12.0	2.131	0.0236	0.0233	0.043	1.95×0.0^{-3}	0.0564	2.56×10^{-3}
500[b]	I_2	1.2	0.3156	0.0236	0.0220	0.412	0.019	0.545	0.025
1000[b]	I_2	12.0	4.088	1.53×10^{-3}	1.53×10^{-3}	2.86×10^{-3}	1.3×10^{-4}	3.73×10^{-3}	1.69×10^{-4}
1000[b]	I_2	1.2	0.504	1.53×10^{-3}	1.52×10^{-3}	0.0286	1.3×10^{-3}	0.0373	1.69×10^{-3}

(a) Based on deposition area of approximately 32,400 sq. ft. - See Table VII I-7.
(b) Fluid Composition, 100% H_2O.
(c) Values obtained from Reference 1.

TABLE VII I-5 DEFINITION OF TERMS AND UNITS USED TO CALCULATE IODINE DEPOSITION

A	=	Deposition Area, ft^2
C_g	=	Concentration of iodine in gas (constant release), lbs/ft^3
C'_g	=	Iodine concentration (puff release), lbs/ft^3
C_o	=	Initial concentration of iodine in gas (puff release), lbs/ft^3
C_P	=	Fluid heat capacity, Btu/(lb) (°F)
D_o	=	Outside diameter of tubes, ft.
D_{12}	=	Diffusion coefficient (diffusivity of species 1 through a mixture of 1 and 2) cm^2/sec.
D_v	=	Molecular diffusivity of iodine in fluid, ft^2/hr
f_d	=	Fraction of iodine deposited, dimensionless
G_{max}	=	Mass velocity of fluid through minimum cross section, lbs/(hr) (ft^2)
G_{12}	=	Lennard-Jones force constant
h_m	=	heat transfer coefficient, Btu/(hr) (ft^2) (F)
k_f	=	thermal conductivity of fluid, Btu/(hr) (ft) (F)
k_g	=	mass transport coefficient, ft/hr
K'_g	=	Individual or gas-film coefficient, lb-moles/(hr) (ft^2) (atm)
K_t	=	Overall deposition coefficient, ft/hr
K_w	=	Wall deposition velocity, ft/hr
M_d	=	Amount of iodine deposited, lbs
M_o	=	Initial mass of iodine, lbs
m_1	=	Molecular weight of species 1
m_2	=	Molecular weight of species 2
N_{pr}	=	Prandtl Number, dimensionless
N_{sc}	=	Schmidt Number, dimensionless
P	=	Pressure, atm
P_{Bm}	=	Logarithmic means of the partial pressure, atm.
Q	=	Volumetric flow rate (steam boil off rate) ft^3/hr
Re	=	Reynolds Number, dimensionless
R_H	=	Hydraulic radius, ft
T	=	Temperature, (°K)
t	=	time period, hr.
U_{ave}	=	Mean fluid velocity (volumetric flow rate, Q divided by cross section), ft/hr
V	=	Volume, ft^3
Ω_D	=	Collision integral for diffusion
ρ	=	fluid density, lbs/ft^3
μ	=	fluid viscosity, lbs/(ft) (hr)

TABLE VII I-6 SUMMARY OF TYPICAL PWR SURFACE AREAS

Thermal Shield

Surface Area (Inside) = 7.75×10^4 in^2 = 538.2 ft^2

Surface Area (Outside) = 8.0×10^4 in^2 = 555.8 ft^2

Core Barrel (Lower)

Surface Area (Inside) = 6.99×10^4 in^2 = 485.5 ft^2

Surface Area (Outside) = 7.20×10^4 in^2 = 500.0 ft^2

Core Barrel (Upper)

Surface Area (Inside) = 4.1×10^4 in^2 = 284.8 ft^2

Surface Area (Outside) = 4.2×10^4 in^2 = 294.1 ft^2

Coolant opening area (3764 in^2 = 26 ft^2) subtracted from above.

Top Support Plate

Under Surface Area = 17,066 in^2 = 118.5 ft^2 (hole area subtracted)

Volume (minus holes) = 54,612 in^3 = 31.6 ft^3

Mass = 15,834 lbs (for 304 SS)

Upper Structural Support Columns

External Surface area (per column) = 15 ft^2

For 14 Support Columns = 210 ft^2

For 25 Support Columns = 375 ft^2

Volume of each Support Column = 4951 in^3 = 2.87 ft^3

For 14 Columns = 40.1 ft^3

For 25 Columns = 71.6 ft^3

Mass of each Support Column = 1438 lbs

For 14 Columns = 20,130 lbs

For 25 Columns = 35,950 lbs

Control Rod Guide Tubes

Surface Area (per tube) = 37.3 ft^2

53 Control rods = 1,976 ft^2

Mass (per tube) = 283 lbs

53 Tubes = 15,000 lbs (total)

Pressure Vessel

Inside Surface Area (Upper Core Plate to Upper Support plate) = 364 ft^2

Areas of water inlets and outlets subtracted

Bottom Support Casting

Assuming approximately 50% open area

Volume = 43 ft^3

Mass = 21,650 lbs

Instrument Guide Tubes

Information not available to estimate total number of tubes.

Estimated weight for each tube = 144.7 lbs.

TABLE VII I-6 (Continued)

Steam Generator (Heat Exchanger U tubes) Single Unit

Internal Surface Area	=	51,500 ft^2 (3338 U tubes)
I.D. of tubes	=	0.775 in
Length of single tube	=	914 in = 76 feet
Surface Area/tube	=	2222 in^2 = 15.4 ft^2/tube

Reactor Coolant Pumps

Internal Surface Area (approx.) = 61.5 ft^2 per pump (3 total)

Piping (Single Loop)

Approx. total length of piping	=	81 ft
Approx. total Internal Surface Area	=	600 ft^2
Approx. length Reactor to Steam Generator	=	25 ft (29" I.D.)
Approx. length Steam Generator to Pump	=	22 ft (31" I.D.)
Approx. length Pump to Reactor	=	34 ft (27.5" I.D.)

TABLE VII I-7 SUMMARY OF TYPICAL BWR SURFACE AREAS

Steam Dome		
Volume	=	1,560 ft^3
Surface Area	=	515 ft^2
Core		
Empty Volume (without bypass)	=	2,420 ft^3
Bypass Volume	=	267 ft^3
Fuel Rod Volume	=	221 ft^3
Fuel Assembly Volume	=	99.1 ft^3
Net Core Volume	=	2,100 ft^3
Cladding Surface Area	=	59,100 ft^2
Channel Surface Area	=	29,800 ft^2
Core Shroud		
Inside and Outside Surface Area	=	2,160 ft^2
Mass	=	84,122 lb
Lower Plenum and Control Rod Drives		
Empty Volume	=	2,910 ft^3
Control Rod Guide Tube Displaced Volume	=	426 ft^3
Net Volume	=	2,482 ft^3
Guide Tube Outside Surface Area	=	3,410 ft^2
Total Surface Area	=	4,439 ft^2
Downcomer and Jet Pumps		
Empty Volume	=	1,510 ft^3
Jet Pump Volume	=	182 ft^3
Net Volume	=	1,328 ft^3
Jet Pump Outside Surface Area	=	874 ft^2
Total Surface Area	=	3,244 ft^2
Jet Pumps Total Mass (20 Pumps)	=	20,000 lb
Steam Separators		
Empty Volume	=	4,300 ft^3
Separator Displaced Volume	=	2,500 ft^3
Separator Volume	=	224 ft^3
Net Volume	=	1,800 ft^3
Separator Outside Surface Area	=	8,900 ft^2
Total Surface Area	=	9,850 ft^2

TABLE VII I-7 (Continued)

Steam Driers		
Empty Volume	=	2,970 ft^3
Drier Volume	=	132 ft^3
Net Volume	=	2,838 ft^3
Drier Surface Area	=	31,700 ft^2
Total Surface Area (approx.)	=	32,400 ft^2
Recirculation Piping		
Length (approx.)	=	80 ft
Inside Volume	=	64 ft^3
Inside Surface Area	=	254 ft^2
Inlets (approx. length)	=	15 ft
Inlets (volume)	=	75 ft^3
Inlets (inside surface area)	=	375 ft^2
Suction Lines and Pumps Approx. Length	=	100 ft each (2 total)
Suction Lines and Pumps Inside Volume	=	340 ft^3
Suction Lines and Pumps Inside Surface Area	=	920 ft^2

Section 2

Releases from Containment

2.1 GENERAL REMARKS

A large portion of the work of the Reactor Safety Study was expended in determining the probability and magnitude of various radioactive releases. This work is described in detail in the preceding appendices as well as Appendices VII, and VIII. In order to define the various releases that might occur, a series of release categories were identified for the postulated types of containment failure in both BWRs and PWRs. The probability of each release category and the associated magnitude of radioactive releases (as fractions of the initial core radioactivity that might leak from the containment structure) are used as input data to the consequence model.

In addition to probability and release magnitude, the parameters that characterize the various hypothetical accident sequences are time of release, duration of release, warning time for evacuation, height of release, and energy content of the released plume.

The time of release refers to the time interval between the start of the hypothetical accident and the release of radioactive material from the containment building to the atmosphere; it is used to calculate the initial decay of radioactivity. The duration of release is the total time during which radioactive material is emitted into the atmosphere; it is used to account for continuous releases by adjusting for horizontal dispersion due to wind meander. These parameters, time and duration of release, represent the temporal behavior of the release in the dispersion model. They are used to model a "puff" release from the calculations of release versus time presented in Appendix V.

The warning time for evacuation (see section 11.1.1) is the interval between awareness of impending core melt and the release of radioactive material from the containment building. Finally, the height of release and the energy content of the released plume gas affect the manner in which the plume would be dispersed in the atmosphere.

Table VI 2-1 lists the leakage parameters that characterize the PWR and BWR release categories. It should be understood that these categories are composites of numerous event tree sequences with similar characteristics, as discussed in Appendix V.

2.2 ACCIDENT DESCRIPTIONS

To help the reader understand the postulated containment releases, this section presents brief descriptions of the various physical processes that define each release category. For more detailed information on the release categories and the techniques employed to compute the radioactive releases to the atmosphere, the reader is referred to Appendices V, VII, and VIII. The dominant event tree sequences in each release category are discussed in detail in section 4.6 of Appendix V.

PWR 1

This release category can be characterized by a core meltdown followed by a steam explosion on contact of molten fuel with the residual water in the reactor vessel. The containment spray and heat removal systems are also assumed to have failed and, therefore, the containment could be at a pressure above ambient at the time of the steam explosion. It is assumed that the steam explosion would rupture the upper portion of the reactor vessel and breach the containment barrier, with the result that a substantial amount of radioactivity might be released from the containment in a puff over a period of about 10 minutes. Due to the sweeping action of gases generated during containment-vessel meltthrough, the release of radioactive materials would continue at a relatively low rate thereafter. The total release would contain

approximately 70% of the iodines and 40% of the alkali metals present in the core at the time of release.[1] Because the containment would contain hot pressurized gases at the time of failure, a relatively high release rate of sensible energy from the containment could be associated with this category. This category also includes certain potential accident sequences that would involve the occurrence of core melting and a steam explosion after containment rupture due to overpressure. In these sequences, the rate of energy release would be lower, although still relatively high.

PWR 2

This category is associated with the failure of core-cooling systems and core melting concurrent with the failure of containment spray and heat-removal systems. Failure of the containment barrier would occur through overpressure, causing a substantial fraction of the containment atmosphere to be released in a puff over a period of about 30 minutes. Due to the sweeping action of gases generated during containment vessel meltthrough, the release of radioactive material would continue at a relatively low rate thereafter. The total release would contain approximately 70% of the iodines and 50% of the alkali metals present in the core at the time of release. As in PWR release category 1, the high temperature and pressure within containment at the time of containment failure would result in a relatively high release rate of sensible energy from the containment.

PWR 3

This category involves an overpressure failure of the containment due to failure of containment heat removal. Containment failure would occur prior to the commencement of core melting. Core melting then would cause radioactive materials to be released through a ruptured containment barrier. Approximately 20% of the iodines and 20% of the alkali metals present in the core at the time of release would be released to the atmosphere. Most of the release would occur over a period of about 1.5 hours. The release of radioactive material from containment would be caused by the sweeping action of gases generated by the reaction of the molten fuel with concrete. Since these gases would be initially heated by contact with the melt, the rate of sensible energy release to the atmosphere would be moderately high.

PWR 4

This category involves failure of the core-cooling system and the containment spray injection system after a loss-of-coolant accident, together with a concurrent failure of the containment system to properly isolate. This would result in the release of 9% of the iodines and 4% of the alkali metals present in the core at the time of release. Most of the release would occur continuously over a period of 2 to 3 hours. Because the containment recirculation spray and heat-removal systems would operate to remove heat from the containment atmosphere during core melting, a relatively low rate of release of sensible energy would be associated with this category.

PWR 5

This category involves failure of the core cooling systems and is similar to PWR release category 4, except that the containment spray injection system would operate to further reduce the quantity of airborne radioactive material and to initially suppress containment temperature and pressure. The containment barrier would have a large leakage rate due to a concurrent failure of the containment system to properly isolate, and most of the radioactive material would be released continuously over a period of several hours. Approximately 3% of the iodines and 0.9% of the alkali metals present in the core would be released. Because of the operation of the containment heat-removal systems, the energy release rate would be low.

[1]The release fractions of all the chemical species are listed in Table VI 2-1. The release fractions of iodine and alkali metals are indicated here to illustrate the variations in release with release category.

PWR 6

This category involves a core meltdown due to failure in the core cooling systems. The containment sprays would not operate, but the containment barrier would retain its integrity until the molten core proceeded to melt through the concrete containment base mat. The radioactive materials would be released into the ground, with some leakage to the atmosphere occurring upward through the ground. Direct leakage to the atmosphere would also occur at a low rate prior to containment-vessel meltthrough. Most of the release would occur continuously over a period of about 10 hours. The release would include approximately 0.08% of the iodines and alkali metals present in the core at the time of release. Because leakage from containment to the atmosphere would be low and gases escaping through the ground would be cooled by contact with the soil, the energy release rate would be very low.

PWR 7

This category is similar to PWR release category 6, except that containment sprays would operate to reduce the containment temperature and pressure as well as the amount of airborne radioactivity. The release would involve 0.002% of the iodines and 0.001% of the alkali metals present in the core at the time of release. Most of the release would occur over a period of 10 hours. As in PWR release category 6, the energy release rate would be very low.

PWR 8

This category approximates a PWR design basis accident (large pipe break), except that the containment would fail to isolate properly on demand. The other engineered safeguards are assumed to function properly. The core would not melt. The release would involve approximately 0.01% of the iodines and 0.05% of the alkali metals. Most of the release would occur in the 0.5-hour period during which containment pressure would be above ambient. Because containment sprays would operate and core melting would not occur, the energy release rate would also be low.

PWR 9

This category approximates a PWR design basis accident (large pipe break), in which only the activity initially contained within the gap between the fuel pellet and cladding would be released into the containment. The core would not melt. It is assumed that the minimum required engineered safeguards would function satisfactorily to remove heat from the core and containment. The release would occur over the 0.5-hour period during which the containment pressure would be above ambient. Approximately 0.00001% of the iodines and 0.00006% of the alkali metals would be released. As in PWR release category 8, the energy release rate would be very low.

BWR 1

This release category is representative of a core meltdown followed by a steam explosion in the reactor vessel. The latter would cause the release of a substantial quantity of radioactive material to the atmosphere. The total release would contain approximately 40% of the iodines and alkali metals present in the core at the time of containment failure. Most of the release would occur over a 1/2 hour period. Because of the energy generated in the steam explosion, this category would be characterized by a relatively high rate of energy release to the atmosphere. This category also includes certain sequences that involve overpressure failure of the containment prior to the occurrence of core melting and a steam explosion. In these sequences, the rate of energy release would be somewhat smaller than for those discussed above, although it would still be relatively high.

BWR 2

This release category is representative of a core meltdown resulting from a transient event in which decay-heat-removal systems are assumed to fail. Containment overpressure failure would result, and core melting would follow. Most of the release would occur over a period of about 3 hours. The containment failure would be such that radioactivity would be released directly to the atmosphere without significant retention of fission products. This category involves a relatively high rate of energy release due to the sweeping action of the gases generated by the molten mass. Approximately 90% of the iodines and 50% of the alkali metals present in the core would be released to the atmosphere.

BWR 3

This release category represents a core meltdown caused by a transient event accompanied by a failure to scram or failure to remove decay heat. Containment failure would occur either before core melt or as a result of gases generated during the interaction of the molten fuel with concrete after reactor-vessel meltthrough. Some fission-product retention would occur either in the suppression pool or the reactor building prior to release to the atmosphere. Most of the release would occur over a period of about 3 hours and would involve 10% of the iodines and 10% of the alkali metals. For those sequences in which the containment would fail due to overpressure after core melt, the rate of energy release to the atmosphere would be relatively high. For those sequences in which overpressure failure would occur before core melt, the energy release rate would be somewhat smaller, although still moderately high.

BWR 4

This release category is representative of a core meltdown with enough containment leakage to the reactor building to prevent containment failure by overpressure. The quantity of radioactivity released to the atmosphere would be significantly reduced by normal ventilation paths in the reactor building and potential mitigation by the secondary containment filter systems. Condensation in the containment and the action of the standby gas treatment system on the releases would also lead to a low rate of energy release. The radioactive material would be released from the reactor building or the stack at an elevated level. Most of the release would occur over a 2-hour period and would involve approximately 0.08% of the iodines and 0.5% of the alkali metals.

BWR 5

This category approximates a BWR design basis accident (large pipe break) in which only the activity initially contained within the gap between the fuel pellet and cladding would be released into containment. The core would not melt, and containment leakage would be small. It is assumed that the minimum required engineered safeguards would function satisfactorily. The release would be filtered and pass through the elevated stack. It would occur over a period of about 5 hours while the containment is pressurized above ambient and would involve approximately 6×10^{-9} % of the iodines and 4×10^{-7} % of the alkali metals. Since core melt would not occur and containment heat-removal systems would operate, the release to the atmosphere would involve a negligibly small amount of thermal energy.

TABLE 8 BWR ACCIDENT SUMMARY

Sequence		Core Melting			Reactor Vessel Meltthrough (c)		Containment Overpressure	Containment Meltthrough		
		Start, min	End, (a) min	Pressure, psia	Time, min	Pressure, psia	Failure, min	Start, (b) min	Pressure, psia	End, min
1.	A	—	—	—	—	—	—	—	—	—
2.	AJ	1520	1640	15	1730	15	1500	1750	15	5000
3.	AI	1520	1640	15	1730	15	1500	1750	15	5000
4.	AH	—	—	—	—	—	—	—	—	—
5.	AHJ	1520	1640	15	1730	15	1500	1750	15	5000
6.	AHI	20	80	52	140	128	220	160	165	2000
7.	AG	—	—	—	—	—	—	—	—	—
8.	AGJ	270	330	15	390	15	—	410	15	2500
9.	AGI	270	330	15	390	15	—	410	15	2500
10.	AGH	—	—	—	—	—	—	—	—	—
11.	AHGJ	270	30	15	390	15	—	410	15	2500
12.	AGHI	20	80	24	140	19	—	160	34	2000
13.	AF	5	150	58	210	58	290	230	165	2000
14.	AFG	5	150	18	210	16	—	230	34	2000
15a.	AE	20	150	17	210	82	640	230	107	2000
15b.	AE	20	150	17	180	17	640	200	107	2000
16a.	AEG	20	150	15	210	47	—	230	66	2000
16b.	AEG	20	150	15	180	15	—	200	66	2000
17.	AD	—	—	—	—	—	—	—	—	—
18.	ADJ	420	510	15	600	15	0.5	620	15	3000
19.	ADI	420	510	15	600	15	0.5	620	15	3000
20.	ADH	—	—	—	—	—	—	—	—	—
21.	ADHJ	420	510	15	600	15	0.5	620	15	3000
22.	ADHI	20	80	15	140	15	0.5	160	15	2000
23.	ADF	5	150	15	210	15	0.5	230	15	2000
24a.	ADE	20	150	15	210	15	0.5	230	15	2000
24b.	ADE	20	150	15	180	15	0.5	200	15	2000
25.	AC	5	150	58	210	58	290	230	165	2000
26.	ACG	5	150	18	210	16	—	230	34	2000
27.	ACD	5	150	15	210	15	0.5	230	15	2000
28.	AB	20	150	17	180	17	640	200	107	2000
29.	ABG	20	150	15	180	15	—	200	66	2000
30.	ABD	20	150	15	180	15	0.5	200	15	2000
31.	TC	30	180	93	180	93	190	200	15	2000
32.	TW	1740	1860	15	1950	15	1540	1970	15	5000
33.	TQUV	115	180	56	210	57	300	230	162	2000

(a) End of core melting is taken as ~80 percent molten.

(b) After the initial rapid interaction between the molten core and concrete.

(c) For accident sequences in which the primary system is at higher pressure during core melting the reactor vessel fails by a combination of melting and pressure stress.

TABLE 10. (CONTINUED)

Subsequence	Puff Release Time, min.	Puff Release Fraction, v/o[a]	Time Interval, min.	Leakage Leak Rate, v/o/hr[a]	Leakage Pressure, psia	Leakage Temperature, F Drywell	Leakage Temperature, F Wetwell	Flow to Suppression Pool, v/o/hr[a,b]	Remarks
ADEγ (dry)	0.5	91	0-20	0.25	15	212	126	—	Core heating
			-150	0.25	15	212	126	--	Core melting
			-180	0.25	15	212	126	—	Reactor vessel melting
			-200	1030	15	212	126	—	Boiloff and concrete decomposition
			-460	420	15	212	126	--	Boiloff and concrete decomposition
			-520	48	15	212	126	—	Concrete decomposition
			520-	41	15	212	126	—	Concrete decomposition
TC-α			0-30	0.021	48	250	250	—	Primary system at 1100-1250 psia, boiloff through relief and safety valves, core cooled
			30-50	0.021	71	250	250	3650[c,e]	Primary system at 1100 psia, core heatup and initial melt, fission products released to suppression pool
	50	99/79[d]	50	--	15	212	212	--	Steam Explosion, Reactor Vessel, and Containment Failure
			50-180	585	15	212	212	—	Completion of Core melt
			180-240	190	15	212	212	--	Reactor Vessel Melt
			240-260	300	15	212	212	--	Initial Concrete Attack
			260-320	22	15	212	212	—	Concrete Decomposition
			320-380	17	15	212	212	--	Concrete Decomposition
TC-γ			0-30	0.021	48	250	250	--	Primary system at 1100-1250 psia, boiloff through relif and safety valves, core cooled
			30-50	0.021	71	250	250	3650[c,e]	Primary system at 1100 psia, core heatup and initial melt, fission products released to suppression pool
			50-180	0.021	93	250	250	3650[c,e]	Primary system at 1100 psia, completion of core melt, reactor vessel failure
			180-190	0.021	175	337	250	390	Initial Concrete Attack
	190	92	190	--	15	212	212	--	Containmnet Failure
			190-200	600	15	212	212	—	Concrete Decomposition
			200-260	43	15	212	212	—	Concrete Decomposition
			260-320	34	15	212	212	--	Concrete Decomposition
TW-α			0-1540	0.021	175	360	360	—	Heating of suppression pool water, core cooled
			1540		15	212	212	—	Containment Failure, core cooled
			1540-1740	570[e]	15	212	212		Boiloff through relief valvas, core cooled
			1740-1860	660[e]	15	212	212		Boiloff and core melt
	1860	80	1860	--	15	212	212	--	Steam explosion, primary system failure
			1860-1980	115	15	212	212	--	Reactor Vessel melt
			1980-2000	300	15	212	212	--	Initial Concrete Attack
			2000-2060	14	15	212	212	--	Concrete decomposition
			2060-2120	12	15	212	212	--	Concrete decomposition
TWγ or TWγ'			0-1540	0.021	175	360	360	--	Heating of suppression pool water, core cooled
			1540		15	212	212	--	Containment Failure, core cooled
			1540-1740	570[e]	15	212	212		Boiloff through relief valves, core cooled
			1740-1860	660[e]	15	212	212		Boiloff and core melt
			1860-1950	660[e]	15	212	212		Reactor Vessel Melt
			1950-1970	600	15	212	212	--	Initial Concrets Attack
			1970-2030	28	15	212	212	--	Concrete Decomposition
			2030-2090	24	15	212	212	--	Concrete Decomposition

(a) Normalized to a containment free volume of 278,000 ft^3.
(b) Flow of gas and vapor, excluding that during primary system blowdown.
(c) Normalized to a primary system free volume of 28,835 ft^3.
(d) Fractions of primary cooling system/primary containment volume.
(e) Flow from primary coolant system directly to suppression pool.

TABLE 11 (CONTINUED)

Sequence	Release Component[a]	Time of Release, minutes	Fraction of Core Inventory Released to Containment[b]						
			Xe	I	Cs	Te	Sr	Ru	La
AGJδθ	Gap	1	.030	.0017	.005	10^{-5}	10^{-7}	0	0
	Melt	270-330	.870	.883	.760	.150	.100	.030	.003
	Vaporiz.	370-490	.100	.100	.190	.850	.010	.050	.010
AEGδ (dry)	Gap	1	.030	.017	.050	10^{-4}	10^{-6}	0	0
	Melt	85-150	.580	.590	.507	.100	.067	.020	.002
	Vaporiz.	180-300	.390	.393	.443	.900	.043	.060	.011
AEGδη (dry)	Gap	1	.030	.017	.050	10^{-4}	10^{-6}	0	0
	Melt	85-150	.580	.590	.507	.100	.067	.020	.002
	Vaporiz.	180-300	.390	.393	.443	.900	.043	.060	.011
AGJε, εη, and εζ	Gap	1	.030	.0017	.0050	10^{-5}	10^{-7}	0	0
	Melt	270-330	.870	.883	.760	.150	.100	.030	.003
	Vaporiz.	370-490	.100	.100	.190	.850	.010	.050	.010
AFGε, εη, and εζ	Gap	10	.465	.047	.048	.0076	.005	.0015	.00015
	Melt	20-150	.435	.043	.035	.0075	.005	.0015	.00015
	Vaporiz.	210-330	.100	.100	.170	.850	.010	.050	.010
TCγ	Gap	-	-	-	-	-	-	-	-
	Melt	180	.900	-	-	-	-	-	-
	Vaporiz.	180-300	.100	.100	.190	.850	.010	.050	.010
TCα	Gap	-	-	-	-	-	-	-	-
	ST. Expl.	50	.510	.050	.004	.256	$5x10^{-4}$	.437	$1.5x10^{-5}$
	Melt	50-180	.435	.442	.380	.075	.050	.015	$1.5x10^{-3}$
	Vaporiz.	240-360	.050	.050	.095	.425	.005	.025	.005
TWγ and TWγ	Gap	-	-	-	-	-	-	-	-
	Melt	1740-1860	.900	.900	.810	.150	.100	.030	.003
	Vaporiz.	1950-2070	.100	.100	.190	.850	.010	.050	.010

(a) Gap means the gap release component.
Melt means the core melt release component.
St. Expl. means the steam explosion release component.
Vaporiz. means the vaporization release component.

(b) Xe also includes Kr.
I also includes Br.
Cs also includes Rb.
Te also includes Se and Sb.
Sr also includes Ba.
Ru also includes Mo, Pd, Rh, and Tc.
La also includes Nd, Eu, Y, Ce, Pr, Pm, Sm, Np, Pu, Zr, and Nb.

TABLE 12 CONSTANTS AND PARAMETERS USED IN CORRAL-BWR RUNS

Reactor Compartment Data

Compartment	Wall Area, ft^2	Floor Area, ft^2	Height, ft	Volume, ft^3
Drywell	1.48×10^4	3.5×10^3	100	1.59×10^5
Wetwell	1.63×10^4	1.1×10^4	30	1.19×10^5
Annulus	-	-	100	2.78×10^1
Reactor Building	3.14×10^4	2.0×10^4	56	1.10×10^6
SGTS Filter	-	-	0.1	2.78×10^1

Fission Product Cleanup Specifications

Decontamination factor for suppression pool scrubbing
- 1 (noble gases and organic iodide)
- 100 (all other species)

SGTS filter efficiencies
- 99% (organic iodide)
- 99% (elemental iodine)
- 99% (particulate species)
- zero (noble gases)

Other Parameters

Organic iodide conversion ratio = 0.7%[a]

Aerosol particle diameters, μm
- Early 15
- Late 5

Time interval of aerosol particle diameter change = 4 hr

Flow rate through SGTS filters, cfm
- Minimum 2000
- Maximum 10000

Decay heat load limit for SGTS filters, watts
- HEPA units 5.4×10^4
- Charcoal units 6.4×10^4

(a) Exception for the following cases:
- ADFδ uses 0.13%
- AFα uses 0.35%

TABLE 13 (Continued)

Time hr	Cumulative Fractions of Core Inventory Released to the Atmosphere[a] Xe-Kr	Org-I	I-Br	Cs-Rb	Te	Ba-Sr	Ru	La	Event[b]
				Case AEGδ (dry) (Continued)					
				Ground Level Releases					
3.0	3×10^{-3}	2×10^{-5}	8×10^{-5}	4×10^{-4}	9×10^{-5}	6×10^{-5}	2×10^{-5}	2×10^{-6}	Start Gnd. Leak
5.0	6×10^{-2}	4×10^{-4}	9×10^{-4}	4×10^{-3}	3×10^{-3}	5×10^{-4}	3×10^{-4}	4×10^{-5}	
7.0	8×10^{-2}	5×10^{-4}	1×10^{-3}	5×10^{-3}	4×10^{-3}	6×10^{-4}	3×10^{-4}	5×10^{-5}	End Gnd. Leak
24.0	8×10^{-2}	5×10^{-4}	1×10^{-3}	5×10^{-3}	4×10^{-3}	6×10^{-4}	3×10^{-4}	5×10^{-5}	
				Case AEGδη (dry)					
1.4	2×10^{-3}	0	2×10^{-5}	3×10^{-4}	7×10^{-7}	7×10^{-9}	0	0	Just Before Melt
2.5	7×10^{-3}	2×10^{-5}	2×10^{-4}	2×10^{-3}	3×10^{-4}	2×10^{-4}	5×10^{-5}	5×10^{-6}	End Melt Rel.
3.0	2×10^{-2}	8×10^{-5}	4×10^{-4}	3×10^{-3}	5×10^{-4}	3×10^{-4}	1×10^{-4}	1×10^{-5}	
5.0	3×10^{-1}	2×10^{-3}	4×10^{-3}	2×10^{-2}	2×10^{-2}	2×10^{-3}	1×10^{-3}	2×10^{-4}	End Vap. Rel.
7.0	4×10^{-1}	3×10^{-3}	5×10^{-3}	2×10^{-2}	2×10^{-2}	3×10^{-3}	2×10^{-3}	3×10^{-4}	
24	6×10^{-1}	4×10^{-3}	6×10^{-3}	2×10^{-2}	2×10^{-2}	3×10^{-3}	2×10^{-3}	3×10^{-6}	
				Case TCα					
0.8	5×10^{-1}	0	5×10^{-2}	4×10^{-3}	3×10^{-1}	5×10^{-4}	4×10^{-1}	1×10^{-5}	Steam Expl.
3.0	9×10^{-1}	3×10^{-3}	4×10^{-1}	3×10^{-1}	3×10^{-1}	4×10^{-2}	4×10^{-1}	1×10^{-3}	End Melt Rel.
3.9	9×10^{-1}	3×10^{-3}	4×10^{-1}	3×10^{-1}	3×10^{-1}	4×10^{-2}	4×10^{-1}	1×10^{-3}	Before Vap. Rel.
4.5	1.0	3×10^{-3}	4×10^{-1}	4×10^{-1}	4×10^{-1}	5×10^{-2}	5×10^{-1}	2×10^{-3}	1/2 Vap. Rel.
6.0	1.0	3×10^{-3}	4×10^{-1}	4×10^{-1}	5×10^{-1}	5×10^{-2}	5×10^{-1}	3×10^{-3}	End Vap. Rel.
12	1.0	3×10^{-3}	4×10^{-1}	4×10^{-1}	5×10^{-1}	5×10^{-2}	5×10^{-1}	3×10^{-3}	
				Case TCγ					
3.0	0	0	0	0	0	0	0	0	Vessel Failure
3.2	9×10^{-1}	6×10^{-5}	2×10^{-2}	4×10^{-2}	2×10^{-1}	2×10^{-3}	1×10^{-2}	2×10^{-3}	Cont. Failure
4.0	9×10^{-1}	6×10^{-5}	2×10^{-2}	4×10^{-2}	2×10^{-1}	2×10^{-3}	1×10^{-2}	2×10^{-3}	
5.0	1.0	6×10^{-5}	2×10^{-2}	6×10^{-2}	3×10^{-1}	3×10^{-3}	2×10^{-2}	3×10^{-3}	End Vap. Rel.
6.2	1.0	6×10^{-5}	2×10^{-2}	6×10^{-2}	3×10^{-1}	3×10^{-3}	2×10^{-2}	3×10^{-3}	
15.0	1.0	6×10^{-5}	2×10^{-2}	7×10^{-2}	3×10^{-1}	4×10^{-3}	2×10^{-2}	4×10^{-3}	
				Case TWα					
30.0	4×10^{-1}	3×10^{-3}	5×10^{-3}	4×10^{-2}	8×10^{-3}	6×10^{-3}	2×10^{-3}	2×10^{-4}	1/2 Melt Rel.
31.0	9×10^{-1}	6×10^{-3}	1×10^{-2}	9×10^{-2}	2×10^{-2}	1×10^{-2}	3×10^{-3}	3×10^{-4}	End Melt Rel.
31.0	9×10^{-1}	6×10^{-3}	5×10^{-2}	9×10^{-2}	2×10^{-1}	1×10^{-2}	4×10^{-1}	3×10^{-4}	Steam Expl.
32.0	9×10^{-1}	6×10^{-3}	6×10^{-2}	9×10^{-2}	3×10^{-1}	1×10^{-2}	4×10^{-1}	4×10^{-4}	Vessel Melt
33.5	1.0	6×10^{-3}	7×10^{-2}	1×10^{-1}	3×10^{-1}	1×10^{-2}	4×10^{-1}	1×10^{-3}	1/2 Vap. Rel.
35.0	1.0	6×10^{-3}	8×10^{-2}	1×10^{-1}	4×10^{-1}	1×10^{-2}	4×10^{-1}	2×10^{-3}	End Vap. Rel.
42.0	1.0	6×10^{-3}	9×10^{-2}	1×10^{-1}	4×10^{-1}	1×10^{-2}	4×10^{-1}	2×10^{-3}	

TABLE 13 (Continued)

Time hr	Cumulative Fractions of Core Inventory Released to the Atmosphere[a]								
	Xe-Kr	Org-I	I-Br	Cs-Rb	Te	Ba-Sr	Ru	La	Event[b]
CM starts @ 29 hr									
				Case TWY' (Release Directly to Atmosphere)					
1 30.0	$4x10^{-1}$	$3x10^{-3}$	$4x10^{-1}$	$2x10^{-1}$	$5x10^{-2}$	$3x10^{-2}$	$9x10^{-3}$	$9x10^{-4}$	1/2 Melt Rel.
2 31.0	$9x10^{-1}$	$6x10^{-3}$	$9x10^{-1}$	$5x10^{-1}$	$9x10^{-2}$	$6x10^{-2}$	$2x10^{-2}$	$2x10^{-3}$	End Melt Rel.
32.5	$9x10^{-1}$	$6x10^{-3}$	$9x10^{-1}$	$5x10^{-1}$	$9x10^{-2}$	$6x10^{-2}$	$2x10^{-2}$	$2x10^{-3}$	Vessel Melt
33.0	$9x10^{-1}$	$6x10^{-3}$	$9x10^{-1}$	$5x10^{-1}$	$2x10^{-1}$	$6x10^{-2}$	$3x10^{-2}$	$3x10^{-3}$	1/2 Vap. Rel.
34.5	$9x10^{-1}$	$6x10^{-3}$	$9x10^{-1}$	$5x10^{-1}$	$2x10^{-1}$	$6x10^{-2}$	$3x10^{-2}$	$4x10^{-3}$	End Vap. Rel.
42.0	1.0	$6x10^{-3}$	$9x10^{-1}$	$5x10^{-1}$	$3x10^{-1}$	$6x10^{-2}$	$3x10^{-2}$	$4x10^{-3}$	
				Case TWY (Release Through Annulus to Atmosphere)					
30.0	$4x10^{-1}$	$3x10^{-3}$	$5x10^{-3}$	$4x10^{-2}$	$8x10^{-3}$	$6x10^{-3}$	$2x10^{-3}$	$2x10^{-4}$	1/2 Melt Rel.
31.0	$9x10^{-1}$	$6x10^{-3}$	$1x10^{-2}$	$9x10^{-2}$	$2x10^{-2}$	$1x10^{-2}$	$3x10^{-3}$	$3x10^{-4}$	End Melt Rel.
32.5	$9x10^{-1}$	$6x10^{-3}$	$1x10^{-2}$	$9x10^{-2}$	$2x10^{-2}$	$1x10^{-2}$	$3x10^{-3}$	$3x10^{-4}$	Vessel Melt
33.0	$9x10^{-1}$	$6x10^{-3}$	$1x10^{-2}$	$9x10^{-2}$	$4x10^{-2}$	$1x10^{-2}$	$5x10^{-3}$	$6x10^{-4}$	1/2 Vap. Rel.
34.5	$9x10^{-1}$	$6x10^{-3}$	$1x10^{-2}$	$1x10^{-1}$	$6x10^{-2}$	$1x10^{-2}$	$6x10^{-3}$	$8x10^{-4}$	End Vap. Rel.
42.0	1.0	$6x10^{-3}$	$1x10^{-2}$	$1x10^{-1}$	$7x10^{-2}$	$1x10^{-2}$	$7x10^{-3}$	$1x10^{-3}$	

(a) Te includes Se and Sb
Ru includes Mo, Pd, Rh, and Tc
La includes Nd, Eu, Y, Ce, Pr, Pm, Sm, Np, Pu, Zr, and Nb.

(b) Notations used are defined as follows:
Gap Rel. Only - Gap release only
Just Before Melt - Just before core melting begins
End Melt Rel. - Melt release is complete
End Vap. Rel. - Vaporization release is complete
After Vap. Rel. - After vaporization release has ended
Overpressure - Containment failure by overpressure
Steam Expl. - Containment failure by steam explosion
Just Before S.E. - Just before a steam explosion occurs
End Gnd. Leak - Ground level leakage complete.